

University of Southampton

Novel Cyclopentadienyl Transition Metal Complexes

By

Clifford Robert Veighey M. Chem.

A thesis submitted in partial fulfilment of the requirements for the
Degree of Doctor of Philosophy

Department of Chemistry

January 2001

UNIVERSITY OF SOUTHAMPTON

ABSTRACT

FACULTY OF SCIENCE

CHEMISTRY

Doctor of Philosophy

NOVEL CYCLOPENTADIENYL TRANSITION METAL COMPLEXES

By Clifford Robert Veighey

The preparation of chiral cyclopentadienyl transition metal complexes and their application to enantioselective synthesis was reviewed.

The synthesis of known chiral zirconocene (-)-(n-5-cyclopentadienyl)(n5-{1-[(1S, 2S, 5R)-2-isopropyl-5-methylcyclohexyl]-4,5,6,7-tetrahydroindenyl}) zirconium dichloride was repeated and the yields optimised. Application of this complex to a recently reported co-cyclisation / elimination reaction gave an e.e. of 11%.

A series of complexes were designed and synthesised, based on the structure of (-)-(n-5-cyclopentadienyl)(n5-{1-[(1S, 2S, 5R)-2-isopropyl-5-methylcyclohexyl]-4,5,6,7-tetrahydroindenyl}) zirconium dichloride. Three novel metallocenes were prepared and X-ray crystal structures obtained. However, these new complexes displayed no significant improvement over the enantioinductive properties of the parent system.

A new class of cyclopentadienyl ligand was designed comprising a tethered heteroatom held over one face by a rigid [2,2,2] bicyclic backbone. A synthesis was developed to allow the preparation of a number of ligands with differing heteroatoms and substitution around the cyclopentadienyl ring.

A new ligand with an OCH₃ group held over one face of the cyclopentadienyl ring was prepared. Complexation to CpTiCl₃ gave a mixture from which only one compound could be isolated in 40% yield. NMR and nOe experiments showed that the titanium was bound to the opposite face to the heteroatom linker. Two further complexes bearing ligands of this type were synthesised, however both were difficult to isolate.

Nevertheless, comparison of NMR data suggested that in both cases the metal selectively binds to the least sterically hindered face.

Novel complexes were tested for suitability as propene polymerisation catalysts.

Table of Contents

1	INTRODUCTION TO TRANSITION METAL CATALYSIS.....	1
1.1	TRANSITION METAL CATALYSIS.....	1
1.2	D-BLOCK METALLOCENES.....	1
1.2.1	<i>Metal centred asymmetry and facial selectivity of complexation.....</i>	<i>2</i>
1.2.2	<i>Stereocontrol in metallocene mediated reactions.....</i>	<i>6</i>
1.3	APPLICATIONS OF TRANSITION METAL COMPLEXES.....	7
1.3.1	<i>α-olefin polymerisation.....</i>	<i>7</i>
1.3.2	<i>Chiral Lewis acid catalysed reactions.....</i>	<i>13</i>
1.3.3	<i>Co-cyclization Reactions.....</i>	<i>14</i>
1.3.4	<i>Carbomagnesiation Reactions.....</i>	<i>16</i>
1.3.5	<i>Carboalumination Reactions.....</i>	<i>17</i>
1.3.6	<i>Amine Synthesis.....</i>	<i>20</i>
1.3.7	<i>Asymmetric Hydrogenations.....</i>	<i>20</i>
1.3.8	<i>Pauson-Khand Type Cyclisations.....</i>	<i>21</i>
2	SYNTHESIS AND APPLICATION OF NOVEL CHIRAL CATALYSTS BASED ON THE NEOMENTHYL INDENYL ZIRCONIUM SYSTEM.....	22
2.1	C ₁ SYMMETRIC NEOMENTHYL INDENYL MONOCYCLOPENTADIENYL ZIRCONIUM.....	22
2.1.1	<i>Improved synthesis of 13.....</i>	<i>23</i>
2.2	NEW COMPLEXES BASES ON THE MENTHYLINDENYL ZIRCONIUM SYSTEM.....	26
2.2.1	<i>Pentamethylcyclopentadienyl derivatives.....</i>	<i>27</i>
2.2.2	<i>4,7-Dimethyl-indene derivatives.....</i>	<i>29</i>
2.2.3	<i>Methyl substituted indenyl complexes.....</i>	<i>33</i>
2.3	STEREOSELECTIVE ZIRCONIUM CATALYZED CYCLISATION REACTIONS.....	36
2.3.1	<i>Asymmetric Co-cyclization reactions.....</i>	<i>37</i>
2.4	CONCLUSIONS.....	38
3	DEVELOPMENT AND UTILISATION OF NOVEL BICYCLIC CYCLOPENTADIENYL LIGANDS WITH PENDANT HETEROATOM LINKERS.....	39
3.1	HETEROATOM CONTROL OF FACIAL SELECTIVITY.....	39
3.2	DESIGN OF A RIGID LIGAND SYSTEM.....	40
3.3	SYNTHESIS OF LIGANDS OF TYPE B.....	42
3.3.1	<i>Construction of [2,2,2] bicyclic backbone.....</i>	<i>42</i>
3.3.2	<i>Cyclopentadiene ring annulation.....</i>	<i>43</i>
3.3.3	<i>Large scale development of key enone 52.....</i>	<i>44</i>
3.3.4	<i>Alkylation and elimination.....</i>	<i>47</i>
3.4	SYNTHESIS OF PHENYL SUBSTITUTED LIGANDS.....	49
3.5	PREPARATION OF DISUBSTITUTED CYCLOPENTADIENYL LIGAND.....	53
3.5.1	<i>Acid/base catalysed elimination of 62 and 63.....</i>	<i>54</i>
3.5.2	<i>Pd⁰ catalysed elimination of 62 and 63.....</i>	<i>55</i>

3.6	SYNTHESIS OF NOVEL GROUP IV COMPLEXES.....	58
3.6.1	<i>Titanium complexes</i>	58
3.6.2	<i>Zirconium complexes</i>	61
3.7	SYNTHESIS OF TRIDENTATE METHOXY LINKER LIGANDS	67
3.8	SYNTHESIS OF LIGANDS CONTAINING OTHER HETEROATOM LINKERS	69
3.9	CONCLUSIONS	73
3.10	FUTURE WORK	73
4	APPLICATION OF NOVEL METALLOCENES TO PROPENE	
	POLYMERISATION.....	74
4.1	α -OLEFIN POLYMERISATION	74
4.2	POLYMERISATION CONDITIONS.....	74
4.3	POLYMERISATION REACTIONS	76
4.4	ANALYSIS OF POLYMER PROPERTIES	79
4.4.1	<i>Catalyst activity</i>	79
4.4.2	<i>Activity vs Molecular Weight</i>	80
4.4.3	<i>Molecular Weight Distribution</i>	80
4.4.4	<i>Isotacticity</i>	82
4.4.5	<i>Conclusions</i>	83
5	EXPERIMENTAL.....	84
5.1	GENERAL EXPERIMENTAL	84
5.1.1	<i>Air sensitive materials</i>	84
5.1.2	<i>Spectroscopic techniques</i>	84
5.1.3	<i>Chromatography</i>	85
5.1.4	<i>Reagent purification</i>	85
5.2	EXPERIMENTAL FOR CHAPTER 2.....	86
5.2.1	<i>Cyclopentadienyl zirconium trichloride (14)</i>	86
5.2.2	<i>5-Trimethylsilyl cyclopenta-1,3-diene</i>	86
5.2.3	<i>Cyclopentadienyl zirconium trichloride. Tetrahydrofuran complex (14)</i>	87
5.2.4	<i>(1S,2R,5S)-2-isopropyl-5-methylcyclohexyl 4-methyl-1-benzenesulfonate (17)</i>	87
5.2.5	<i>3-[(1S,2R,5S)-2-isopropyl-5-methylcyclohexyl]-1H-indene (4)</i>	88
5.2.6	<i>Cyclopentadienyl(1-neomenthyl-4,5,6,7-tetrahydroindenyl)zirconium dichloride (13)</i>	89
5.2.7	<i>4,7-dimethyl-1H-indene (27)</i>	90
5.2.8	<i>3-[(1S,2R,5S)-2-isopropyl-5-methylcyclohexyl]-4,7-dimethyl-1H-indene (29)</i>	90
5.2.9	<i>Cyclopentadienyl (3-[(1S,2R,5S)-2-isopropyl-5-methylcyclohexyl]-4,7-dimethylindenyl) zirconium dichloride (32)</i>	91
5.2.10	<i>Cyclopentadienyl (3-[(1S,2R,5S)-2-isopropyl-5-methylcyclohexyl]-4,7-dimethyl-4,5,6,7-tetrahydroindenyl) zirconium dichloride (33)</i>	92
5.2.11	<i>3-[(1S,2R,5S)-2-isopropyl-5-methylcyclohexyl]-1-methyl-1H-indene (34)</i>	92

5.2.12	Cyclopentadienyl(3-[(1 <i>S</i> ,2 <i>R</i> ,5 <i>S</i>)-2-isopropyl-5-methylcyclohexyl]-1-methyl-4,5,6,7-tetrahydroindenyl)zirconium dichloride (35).....	93
5.2.13	1,2,3,4,5-pentamethyl-1,3-cyclopentadiene (22).....	94
5.2.14	1,2,3,4,5-pentamethyl-1,3-cyclopentadienyl-zirconium trichloride etherate (20).....	95
5.3	EXPERIMENTAL FOR CHAPTER 3.....	95
5.3.1	Methyl bicyclo[2.2.2]oct-5-ene-2-carboxylate(48).....	95
5.3.2	Bicyclo[2.2.2]oct-5-en-2-ylmethanol (49).....	96
5.3.3	5-(Methoxymethyl)bicyclo[2.2.2]oct-2-ene (50).....	96
5.3.4	Acetylene dicobalt hexacarbonyl (51).....	97
5.3.5	9-(Methoxymethyl)tricyclo[5.2.2.0 ^{2,6}]undec-4-en-3-one (52a) and 8-(Methoxymethyl)tricyclo[5.2.2.0 ^{2,6}]undec-4-en-3-one (52b).....	97
5.3.6	(3 <i>R</i>)-8-(Methoxymethyl)-3-phenyltricyclo[5.2.2.0 ^{2,6}]undec-4-en-3-ol (57) and (3 <i>R</i>)-9-(Methoxymethyl)-3-phenyltricyclo[5.2.2.0 ^{2,6}]undec-4-en-3-ol (58).....	98
5.3.7	9-(methoxymethyl)-3-phenyltricyclo[5.2.2.0 ^{2,6}]undeca-2,5-diene (59).....	99
	(3 <i>R</i>)-9-(Methoxymethyl) tricyclo[5.2.2.0 ^{2,6}]undec-4-en-3-ol (62) and (3 <i>R</i>)-8-(Methoxymethyl)-tricyclo[5.2.2.0 ^{2,6}]undec-4-en-3-ol (63).....	100
5.3.9	(3 <i>S</i>)-8-(methoxymethyl)tricyclo[5.2.2.0 ^{2,6}]undec-4-en-3-yl methyl carbonate (67a) and (3 <i>R</i>)-9-(methoxymethyl)tricyclo[5.2.2.0 ^{2,6}]undec-4-en-3-yl methyl carbonate (67b).....	101
5.3.10	8-(methoxymethyl)tricyclo[5.2.2.0 ^{2,6}]undeca-2,5-diene (64).....	102
5.3.11	Cyclopentadienyl-(8-(methoxymethyl)tricyclo[5.2.2.0 ^{2,6}]undeca-2,5-dienyl) titanium dichloride (70).....	103
5.3.12	Cyclopentadienyl-(8-(methoxymethyl)tricyclo[5.2.2.0 ^{2,6}]undeca-2,5-dienyl) zirconium dichloride (71).....	104
5.3.13	6-((Methylsulphanyl)methyl)bicyclo[2.2.2]oct-2-ene (80).....	104
5.3.14	9-((Methylsulphanyl)methyl)tricyclo[5.2.2.0 ^{2,6}]undec-4-en-3-one (81a) and 8-((Methylsulphanyl)methyl)tricyclo[5.2.2.0 ^{2,6}]undec-4-en-3-one (81b).....	105
5.3.15	4-Oxatricyclo[5.2.2.0 ^{2,6}]undec-8-ene-3,5-dione. (72).....	106
5.3.16	[3-(Hydroxymethyl)bicyclo[2.2.2]oct-5-en-2-yl]methanol (75).....	106
5.3.17	5,6-Di(methoxymethyl)bicyclo[2.2.2]oct-2-ene (73).....	107
5.3.18	8,9-Di(Methoxymethyl)tricyclo[5.2.2.0 ^{2,6}]undec-4-en-3-one (74).....	108
5.4	PROPENE POLYMERISATION (REPRESENTATIVE PROCEDURE).....	108
6	REFERENCES.....	109
7	APPENDICES.....	113

Acknowledgements

I would like to thank Prof. Richard Whitby for the opportunity to work with him at Southampton and for advice, ideas and encouragement throughout my project. I would also like to thank Dr. Ray Jones and AstraZeneca for funding the work and for regular help and consultations.

Thank you to the Whitby group members past and present for making my time in Southampton an enjoyable one. To Dan, Simon and Stevie for memorable 5-Nations weekends. To Thomas for Dublin field trips. To Nick, Kwok, Ian, Graham and Mark for being good lab mates and for Friday nights at the staff club.

Thanks to Marianne Cardno, Simon Green, Dan Brookings, Mark Garrett and Joanne Veighey for proof reading and to Dave Dossett and Steve Harrison for help with last minute data collection

I would also like to thank Joan Street for excellent NMR work and Dr. John Langley and Julie Herniman for the mass spectrometry service.

Finally, thanks to Maz, Jo and Mum for all their support and for putting up with me while I wrote this thesis.

Abbreviations

APCI	atmospheric pressure chemical ionisation
Ar.	aryl group
B.p.	boiling point
Br.	broad
<i>n</i> -Bu	<i>n</i> -butyl
<i>t</i> -Bu	<i>tert</i> -butyl
<i>n</i> -BuLi	<i>n</i> -butyl lithium
COSY	correlated spectroscopy
Cp.	cyclopentadienyl
Cp*	1,2,3,4,5-pentamethyl-cyclopentadienyl
CpTMS	1-trimethylsilylcyclopentadienyl
CSA	camphorsulfonic acid
d	doublet
dd	double-doublet
ddd	double-double-doublet
DEAD	diethyl azodicarboxylate
dec.	decomposed
DME	dimethoxyethane
DMF	dimethylformamide
DMS	dimethylsulfide
DMSO	dimethylsulfoxide
e.e.	enantiomeric excess
ebthi	ethylene-bistetrahydroindenyl
EI	electron impact (mass spectrometry)
ES	electrospray
Et	ethyl
Et ₂ O	diethyl ether
GC	gas chromatography
GCMS	gas chromatography mass spectrometry
h	hour
HPLC	high pressure liquid chromatography
HRMS	high resolution mass spectrometry
<i>i</i> -Pr	<i>iso</i> -propyl
IPA	<i>iso</i> -propyl alcohol
IR	infra-red
LRMS	low resolution mass spectrometry
M	molarity in moles per litre
m	medium (intensity in IR data)
m	multiplet
MAO	methylaluminoxane

MCPBA	<i>meta</i> -chloroperbenzoic acid
Me	methyl
min	minute
mmol	millimoles
M.p.	melting point
Ms	methanesulfonyl
MS	mass spectrometry
NMR	nuclear magnetic resonance
nOe	nuclear Overhauser effect
o	ortho
p	para
Ph	phenyl
ppm	parts per million
q	quartet
R	general aliphatic substituent
RT	retention time
s	strong (intensity in IR data)
s	singlet
t	triplet
TBAF	<i>tert</i> -butyl ammonium fluoride
TBDMS	<i>tert</i> -butyl dimethylsilyl
TFA	trifluoroacetic acid
Tf	trifluoromethanesulfonyl
THF	tetrahydrofuran
thi	tetrahydroindenti
TLC	thin layer chromatography
Ts	<i>p</i> -toluenesulfonyl
UV	ultra violet
w	weak (intensity in IR data)
<i>m/z</i>	mass / charge ratio
$[\alpha]_D^{254}$	specific optical rotation (298K, sodium D line)
λ	wavelength

1 Introduction to transition metal catalysis

1.1 Transition metal catalysis

The search for cheap, clean and efficient methods for performing organic transformations is one of the main goals of modern industrial chemistry. Both economic and environmental concerns necessitate the use of the smallest amounts possible of any reagents used. As a result of this, catalytic reactions have obvious benefits. Transition metals have found use in the field of catalysis due to their extra d-orbitals which are available for bonding to a range of organic molecules, particularly electron rich molecules such as olefins and aromatic compounds. To this end a great deal of work has centred on the use of a suitable modified d-block metal complex as a catalytic species.

1.2 D-block metallocenes

The discovery of ferrocene in 1951 prompted a resurgence in organometallic chemistry and in the following 50 years a wide variety of metallocenes have been synthesised and investigated.¹ All metallocenes consist of two cyclopentadienyl rings, η -5 bound to the metal centre to form a "sandwich" structure. The geometry is determined by the nature and oxidation state of the metal centre. Ferrocene adopts an eclipsed conformation Figure 1a, with the cyclopentadienyl centroids in an almost linear configuration.² Group IV metals form bent metallocenes, Figure 1b, with two free binding sites allowing the binding of substrates and so these complexes, when suitably activated, can catalyse a variety of reactions.^{3 4 5,6 7 8 9} The simple group IV metallocenes Cp_2ZrCl_2 , Cp_2TiCl_2 and Cp_2HfCl_2 are commercially available¹⁰ and these complexes along with their derivatives have found a variety of uses in synthetic and polymer chemistry.

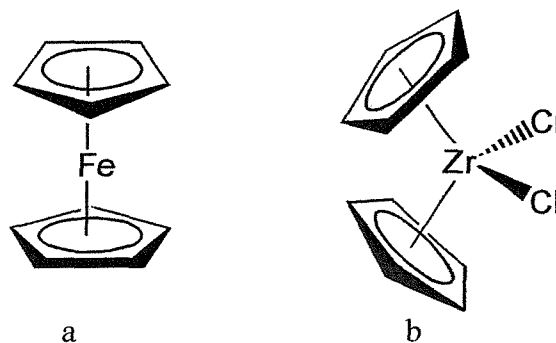


Figure 1

However as these simple metallocenes possess no inherent asymmetry, they produce only racemic products when used in reactions forming non-symmetric products. In order to achieve non-racemic products it is necessary to incorporate some asymmetry in the catalyst precursor.

One way of incorporating such asymmetry is to attach a chiral group to one or both of the cyclopentadienyl rings. This approach has certain advantages but to achieve the highest levels of enantio-induction it is necessary to get the chiral information as close as possible to the catalytic site and as close as possible to the metal centre. The complexes with the chiral information closest to the active site are those with metal-centred asymmetry.

1.2.1 Metal centred asymmetry and facial selectivity of complexation

Complexes of the form **1** and **2** are asymmetric due to the planar chirality of the cyclopentadienyl ring. Cyclopentadienyl rings with three or more different substituents have enantiotopic faces Figure 2a. Metallation therefore leads to a racemic mixture of complexes, even though the cyclopentadienyl ligand does not possess a chiral centre.

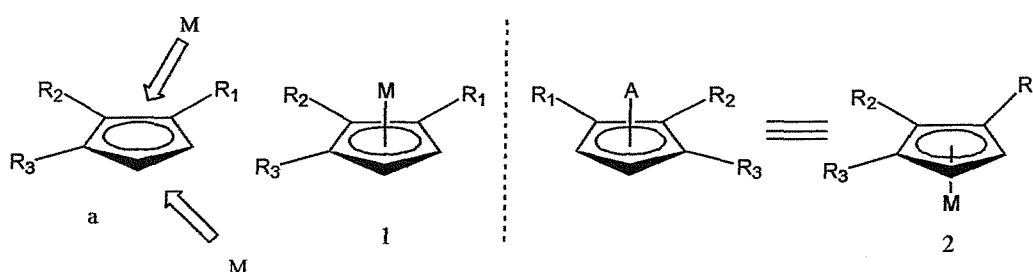
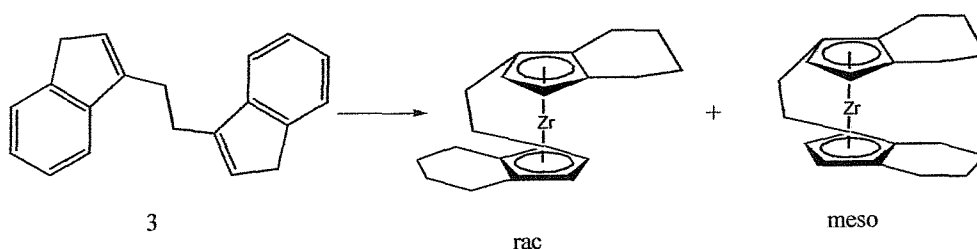


Figure 2

For example, in ligand **3** both cyclopentadienyl rings possess enantiotopically different faces so complexation affords a mixture of racemic and *meso* compounds that must be separated Scheme 1.¹¹ Preparation of an enantiomerically pure complex requires resolution of the racemic product using BINOL. This makes synthesis of such chiral complexes expensive and difficult.



Scheme 1

If one of the substituents contains further chirality, such as in ligand **4**, then the two faces are diastereotopically different. Complexation leads to a mixture of diastereoisomers and preparation of enantiomerically pure complex involves a much simpler separation of diastereoisomers. An example of this is the C_1 complex **5**.⁷

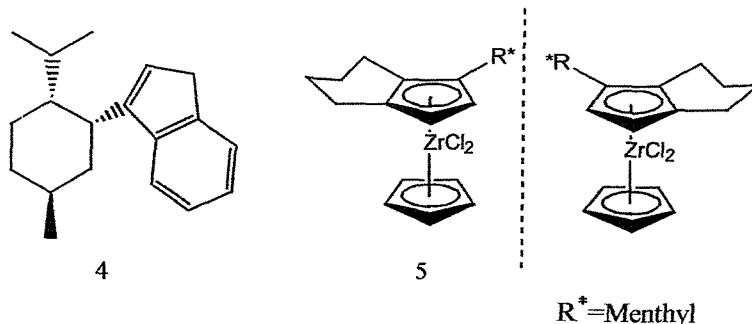


Figure 3

Complexation leads to a mixture of two diastereoisomers, which may be separated by recrystallisation. Although this greatly simplifies the preparation of an enantiomerically pure complex, a separation step is still involved. It is therefore desirable to control the selectivity of complexation in order to eliminate, or greatly simplify, the purification of the complex. There are three main methods of facial control which have been reported to date;

A) Steric control via a favoured rotomer.

Treatment of the lithium salt of **4** with $CpZrCl_3$ give a mixture of diastereoisomers in the ratio of $>6:1$.⁷ This may be rationalised by examining the conformation of the lithium salt of **4**.

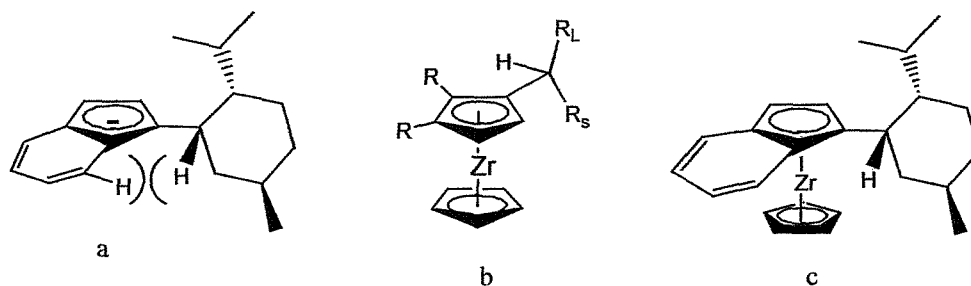


Figure 4

The lowest energy conformer of the lithium salt is adopted, placing the smallest (in this case H) group closest to the other substituents on the ring. Metallation is then directed away from the face with the largest blocking group. For example, in the neomenthyl-indene case the medium and large groups face away from the indene ring in the lowest

energy conformer Figure 4a. The large isopropyl group then blocks one face of the indene ring directing metallation to the opposite stereoface. Further evidence in support of this hypothesis comes from the observation that control in the 4,5,6,7-tetrahydroindenyl ligand is poor. This is presumably due to the change in conformer due to different steric interactions between the menthyl group and the proton(s) on the 7-carbon.

This approach has the advantage of producing good stereocontrol, however in the final complex the bulk of the menthyl group is held away from the catalytic site. Since the large group directs metallation away from that face, catalytic enantiocontrol is dependent on the medium group. A more efficient strategy would involve not only using the bulkiest group to control metallation but also to transmit chiral information to the catalytic site.

B) Steric control by bridged bicyclic systems

Steric control of metallation may be improved by a more rigid steric environment around the cyclopentadienyl anion rather than relying simply on a lowest energy conformer. Ligands such as **6**¹² and **7**¹³ based on terpene backbones with annulated cyclopentadienyl rings have been synthesised and studied by a number of workers.

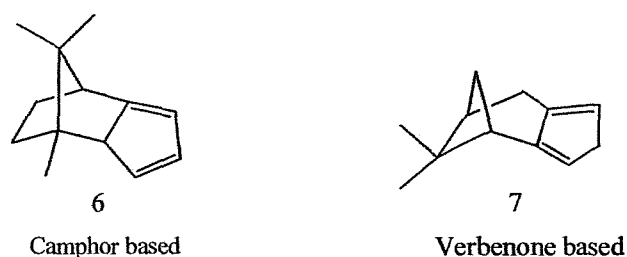


Figure 5

Facial selectivity of metallation is often excellent, such as in the camphor based ligand **6** where the gem dimethyl group blocks one face, and in some cases is even temperature dependent.¹⁴ For example, in the case of isodicyclopentadiene **8**, the lithium salt is believed to exist in two forms in solution, Figure 6. At ambient temperatures the lithium salt exists in a predominantly monomeric form and metallation proceeds by inversion from the opposite face. However, at low temperatures the lithium species form aggregates in which other molecules join to form sandwich type clusters. In this case the opposite face is blocked and metallation is forced to proceed with retention of configuration.

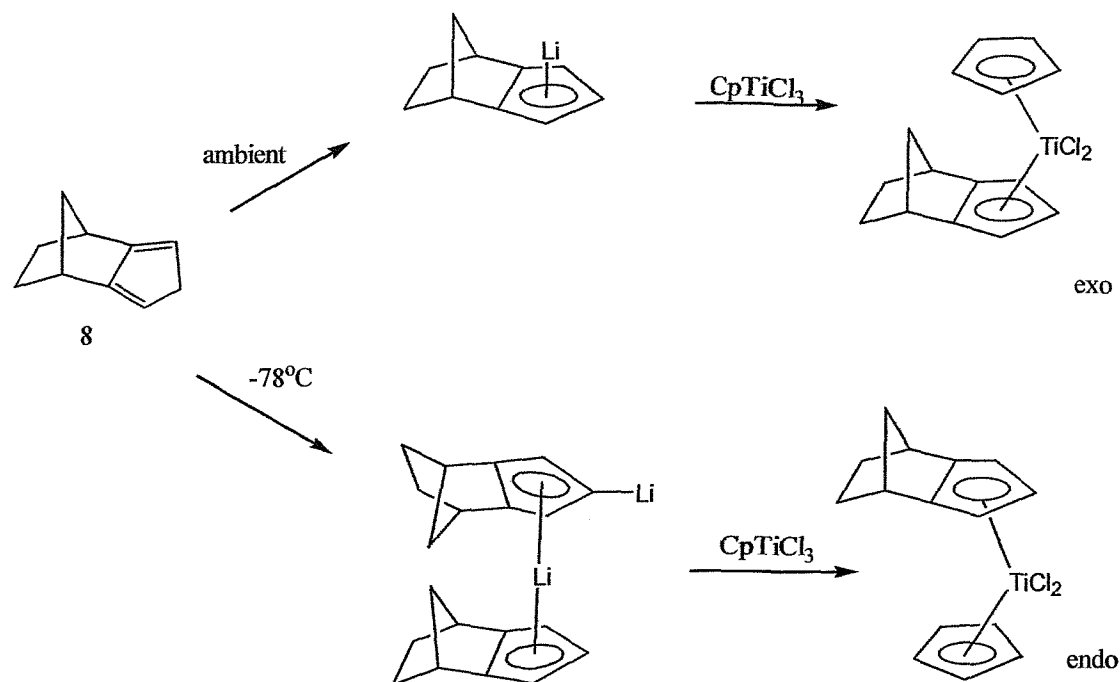
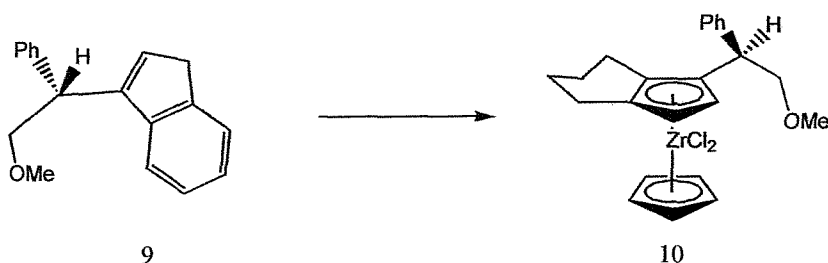


Figure 6

Stereoselectivity exhibited by complexes of this class of ligands in catalytic reactions is moderate with higher selectivity shown by examples with more highly substituted cyclopentadienyl rings.¹

C) Heteroatom control

A third approach to controlling facial selectivity is to use a pendant electron rich heteroatom to co-ordinate to the electron deficient metal centre and direct it towards one face. Brookings¹⁵ has performed work towards this in the synthesis of **10**.



This system relies on the lowest energy conformer, as discussed earlier, placing the heteroatom over one face of the cyclopentadienyl ring. Results from these experiments are inconclusive, as both steric and electronic effects could be responsible for the observed selectivity. However, results from non-heteroatom analogues seem to indicate that steric factors are dominant in this system. A better approach for the determination of the relative strengths of steric and electronic interactions would be to use a bicyclic

system to hold the pendant heteroatom fixed over one face, rather than the lowest energy conformer approach, and would have no steric block on the opposite face. Such a complex was one of the goals of this project and will be discussed in detail in later chapters.

1.2.2 Stereocontrol in metallocene mediated reactions

In most group IV metallocene mediated reactions the key intermediate is an η -2 bound alkene zirconium complex which then reacts with another alkene molecule *via* one of two possible binding sites. Regio- and stereocontrol of this binding will be dependent on the steric environment provided by the ligand structure surrounding the metal. The most successful chiral complexes reported to date have been C_2 symmetric zirconocenes such as **11**¹⁶ and **12**.³

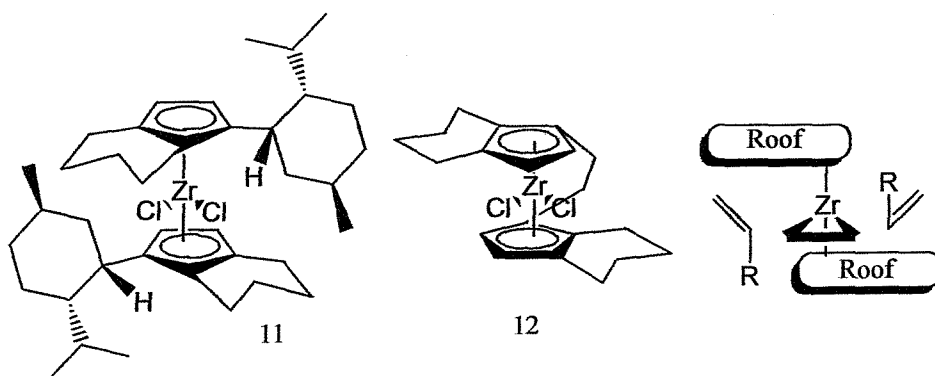


Figure 7

In these complexes regiocontrol is exerted by the bent nature of the zirconocene and stereocontrol may be envisaged as being due to steric interactions between the tetrahydroindenyl "roof" and the alkyl group on the inserting alkene molecule. The C_2 symmetry of the complex ensures that the stereochemistry of the product is the same regardless of which side the alkene inserts.

However, work by Whitby^{7 8 9} has shown that C_2 symmetry is not necessary for good stereocontrol. If one side of the complex has the "roof" structure and the other side is blocked by a steric "wall" as in complex **13**, insertion may only take place from one side. This then allows one cyclopentadienyl ring to be much less substituted and so increase the activity of the complex by general reduction of steric bulk.

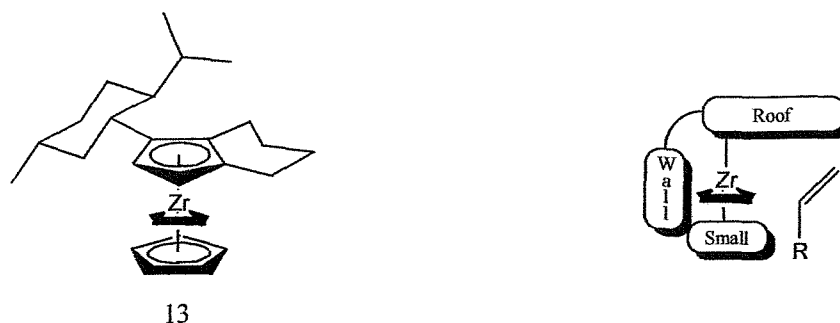


Figure 8

1.3 Applications of transition metal complexes

1.3.1 α -Olefin polymerisation

Since Ziegler's discovery in 1955 that ethylene polymerisation was catalysed by a $\text{TiCl}_4/\text{AlClEt}_2$ system,^{17,18} olefin polymerisation has been one of the major catalytic uses of transition metal complexes. Ziegler's discovery was soon followed by reports of the polymerisation of propene by Natta.^{19,20} These Ziegler catalysts are heterogeneous, with catalysis taking place at faults in the crystalline structure of the catalyst.

Heterogeneous titanium catalysts are used industrially to polymerise propene with a high degree of stereoselectivity and are used to form co-polymers with higher α -olefins to alter the properties of the resultant polymer. However, due to the range of active sites present on the crystal surface the insertion of the co-monomer is not well controlled.

After the synthesis of the first group IV metallocenes in 1953,²¹ their activity as polymerisation catalysts was explored. Mixtures of titanocene dichloride (Cp_2TiCl_2) and AlClEt_2 were found to catalyse the polymerisation of ethylene however propene was not polymerised. These soluble catalysts were prone to reduction and hydrolysis and could not compete with the existing highly active and selective heterogeneous systems. As a result they found no industrial applications.

Although these systems were sensitive to hydrolysis, it was observed that the rate of polymerisation was increased by the addition of small amounts of water.^{22,23} This suggested the partial hydrolysis of aluminium alkyls to form aluminoxanes. This idea was investigated by Sinn^{22,23} who found that zirconocene dichloride (Cp_2ZrCl_2)- AlMe_3 becomes a highly active system upon the addition of water. The effect is also apparent if the AlMe_3 is partially hydrolysed to form methylaluminoxane (MAO) before the addition of the zirconium complex. MAO is a loosely defined polymeric substance that

is soluble in organic solvents such as toluene in which it forms complex equilibria. Sinn found that MAO is a much more effective activator for metallocene dihalides than aluminium alkyl halides and even allows the polymerisation of propene with zirconocene dichloride (however without the stereoselectivity of the heterogeneous systems).

To achieve high activity, MAO must be used in large excess in Al:Zr ratios of between 1000 and 10000:1, so the cost of MAO far exceeds the cost of the zirconocene complex employed. However, despite this MAO has become the favoured activator of metallocene based catalytic systems, even on an industrial scale.

1.3.1.1 Selectivity in propene polymerisation ²⁴

Polypropylene consists of a chain of methylene groups with methyl groups on alternate groups Figure 9. As each of the centres with a methyl group is a distinct stereocentre, control of the selectivity of addition is required in order to control the properties of the resultant polymer.

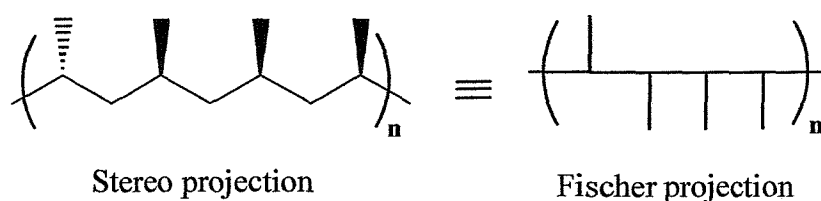


Figure 9

Polymers with all the methyl groups in the same configuration may pack closely together to form hard crystalline solids with melting points in excess of 165°C. This material is referred to as isotactic polypropylene and is the most commercially valuable form of the polymer Figure 10a.

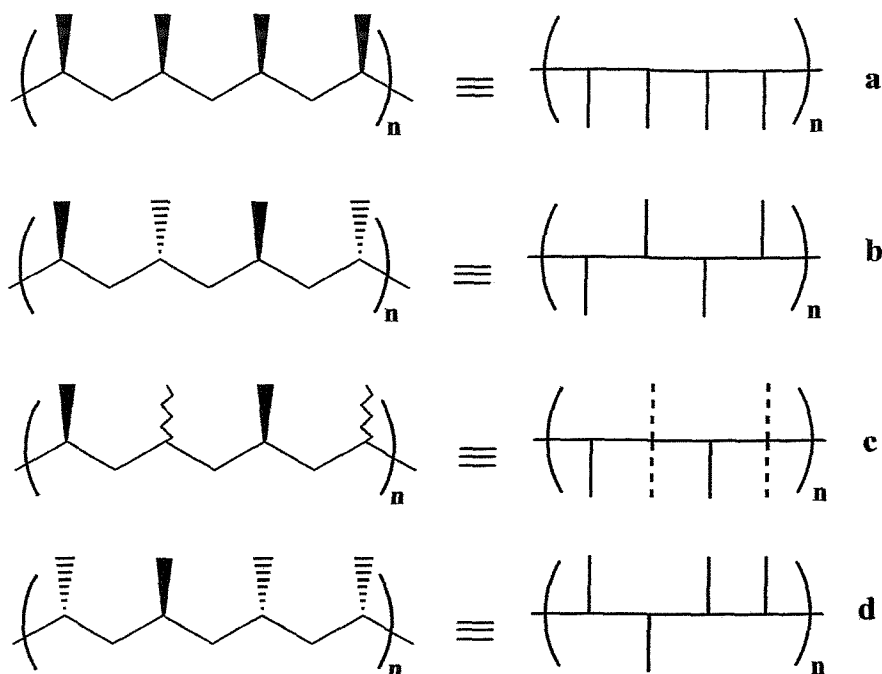


Figure 10

Polymers with a totally random arrangement of the stereocentres are referred to as atactic polypropylene. These polymers are unable to form crystalline lattices and as a result form amorphous substances with much lower melting points Figure 10d.

Two other forms of polypropylene are known with intermediate levels of stereocontrol. Syndiotactic polypropylene has every centre controlled, however the stereochemistry is reversed at every alternate centre Figure 10b. Hemiisotactic polypropylene has every other centre controlled in the same configuration with the centres in between being uncontrolled Figure 10c.

Control of the stereochemistry in the growing polymer chain is achieved via two different mechanisms, enantiomeric site control and chain end control Figure 11.

Which mechanism is in operation is dependent on the catalytic system used.

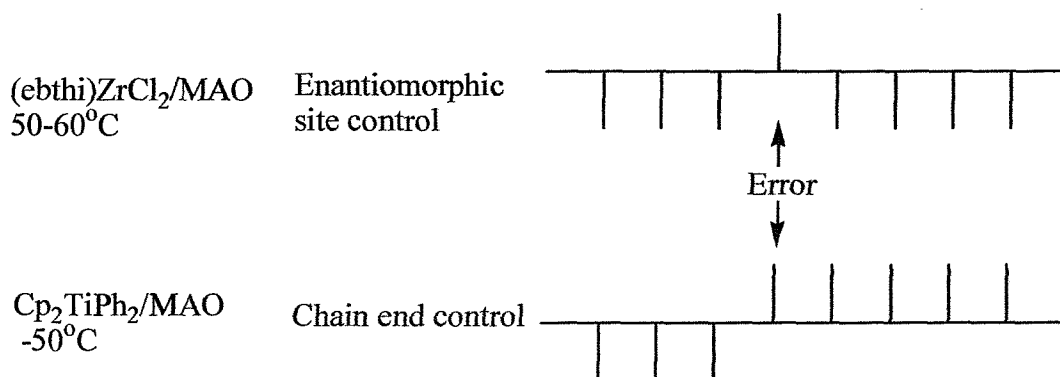


Figure 11

In heterogeneous systems and systems such as $\text{Cp}_2\text{TiPh}_2/\text{MAO}$ at low temperature, stereocontrol is achieved *via* the chain end control mechanism. In this mechanism any error occurring is perpetuated along the chain rather than being corrected. The stereochemistry at the new centre is controlled by steric interactions with the previous methyl group. For example, in heterogeneous Natta type systems the growing chain orientates itself away from the chlorine atom (marked Cl^* Figure 12) to achieve the lowest energy intermediate. The approaching propene molecule is then forced to approach from the same *si* face as the previous monomer unit by steric interactions between the two methyl groups.

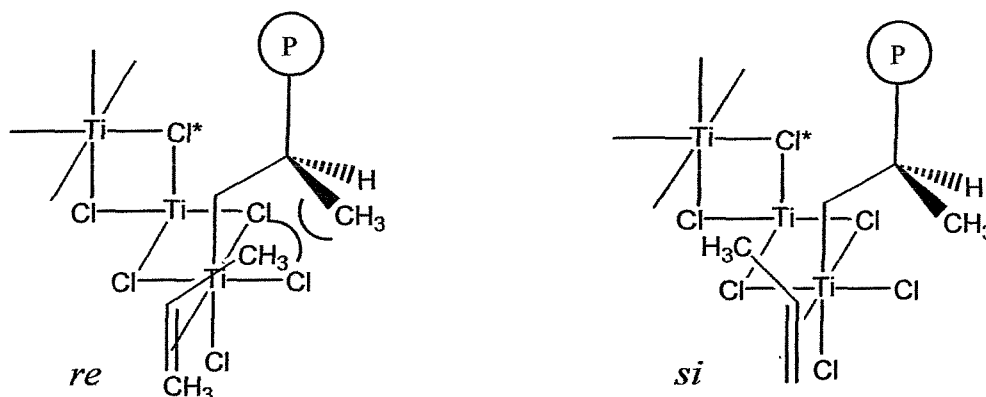


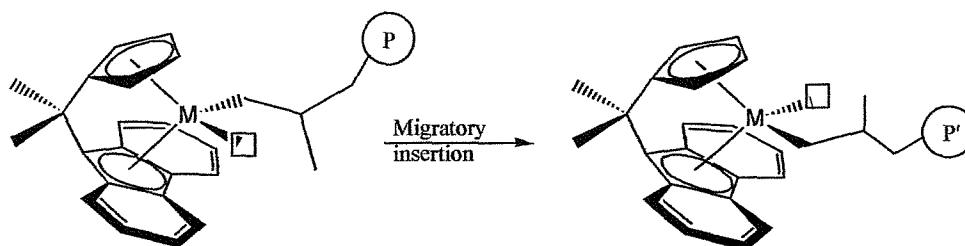
Figure 12

In contrast, C_2 symmetric zirconocenes display enantiomorphic site control where the stereochemistry of the adding monomer is controlled by the chiral environment imposed by the cyclopentadienyl ligands surrounding the catalytic metal centre. Any errors occurring in the chain are corrected in the next step and not transmitted down the chain.

1.3.1.2 Catalyst effects on polymer properties

Although achiral zirconocene catalysts may produce stereoregular block polymers by chain end control, these reactions are dependent on temperature control and it is therefore desirable to develop catalysts with enantiomorphic site control to allow reactions to proceed at elevated temperatures with the resultant increased rate advantages.

Ewen²⁵ has shown that the mechanism of polymerisation for most zirconocenes involves successive migratory insertion steps, Figure 13, and that this step is much faster than the non-insertion migration of the chain from one site to the other.

**Figure 13**

Evidence for this mechanism comes from results using a series of zirconocene catalysts with varying degrees of symmetry (Figure 14). C_2 symmetric catalysts produce highly isotactic polymers due to their ability to force addition of monomer to be from the same face by steric interactions (Figure 14, line 1). The two sides of the catalyst have inverted steric environments and this combined with the migration of the growing chain from site to site results in isotactic polymer. The C_s symmetric analogue conversely produces syndiotactic polymer (Figure 14, line 2). Both active sites have the same steric environments and the migratory insertion step causes successive monomer insertion to occur from opposite faces.

Alteration of the relative steric environments around each active site produces a resultant effect on tacticity. Placing a methyl group opposite the fluorenyl ligand (Figure 14, line 3) reduces the energy gradient between the *re* and *si* monomer coordinated transition states and thus alternate stereocentres on the chain are uncontrolled resulting in syndiotactic polypropylene. Further increase in the size of this alkyl group (Figure 14, line 4) results in the energy gradient being reversed and selectivity switches to produce isotactic polymers, similar to the C_2 symmetric case.



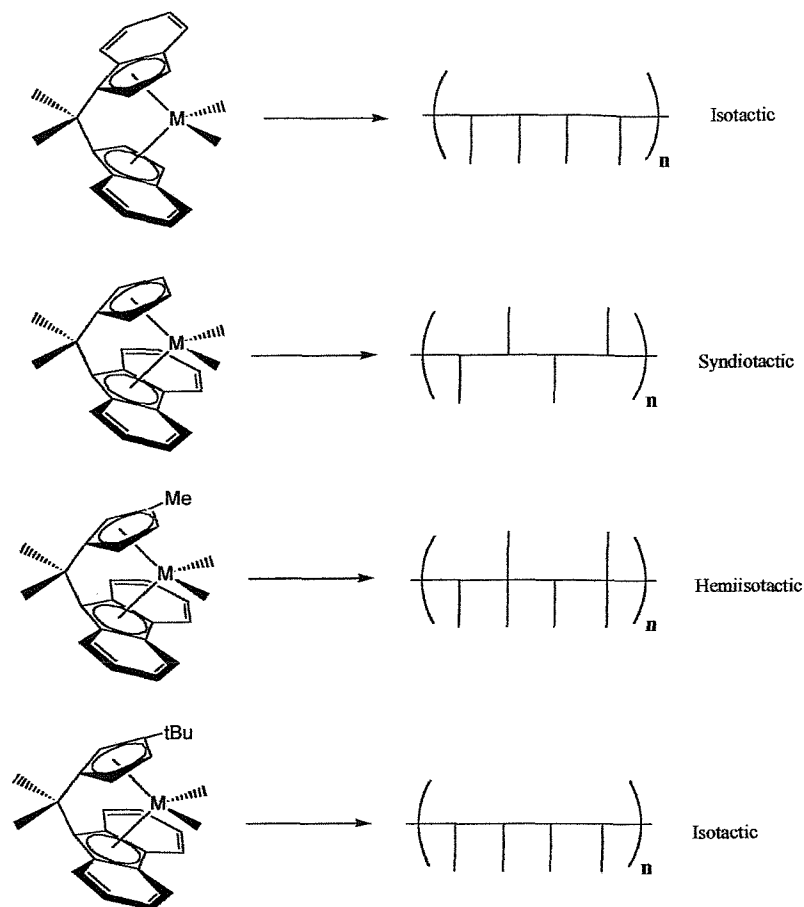


Figure 14

Although, as previously mentioned, decreased temperatures allow stereocontrol to proceed via chain end control, lower temperatures may also control the steric environment of the active site as demonstrated by Waymouth²⁶ (Figure 15).

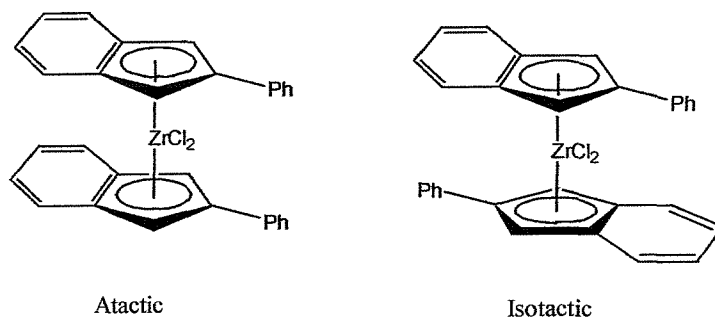


Figure 15

The catalyst may exist in two conformers, one producing isotactic polymer, the other atactic. Temperature will affect the rate at which the two interconvert and the relative populations of each, thus affecting the polymers properties. The result is a block polymer with alternating isotactic and atactic blocks having elastomeric properties.

1.3.1.3 Characterisation of polypropylene samples. ²⁷

Analysis of samples from polymerisation reactions involves the measurement of several properties. Apart from the activity, yield and melting point, the main properties being those of chain length distribution and tacticity.

The average molecular weight and molecular weight distribution may be obtained by gel permeation chromatography experiments. Tacticity is measured by analysis of high temperature NMR experiment. Melting point also gives an indication as to these properties as isotactic polypropylene will have a melting point above 165°C. Low molecular weight will also lower the melting point.

¹³C NMR experiments performed on polypropylene samples in 1,2 dichlorobenzene at 110°C show a limited number of signals. At these temperatures the chemical shift of each methyl carbon atom is influenced only by the four surrounding stereocentres - two on each side. Of the 16 (2⁴) possible pentads only 10 are non-degenerate (Figure 16). Stereochemistry of two centres resulting from consecutive insertion from the same face is classified *m* and conversely, that resulting from consecutive insertion from opposite faces is classified *r*.

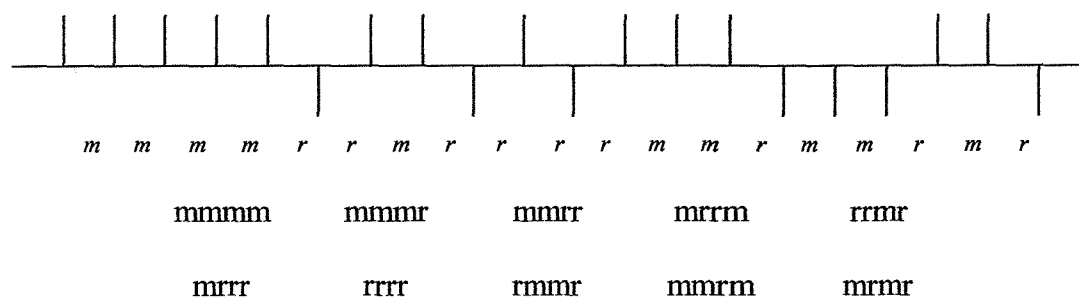


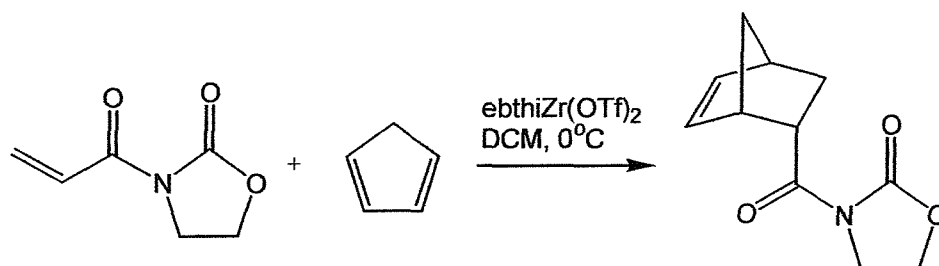
Figure 16

The tacticity may be measured by analysis of the integrals over the various pentad peaks. Isotacticity is the intensity of the *mmmm* peak expressed as a percentage of the total methyl signal integral. Hemiisotactic and syndiotactic samples will show increased levels of *r* containing pentad signals. Highly syndiotactic samples will show high levels of the *rrrr* pentad.

1.3.2 Chiral Lewis acid catalysed reactions

Collins ²⁸ has shown that Diels-Alder cyclo-addition reactions may be catalysed by (ebthi)Zr(OTf)₂ with good asymmetric induction. The effect is increased in polar or

donating solvents and is thought to proceed via a cationic zirconium species, this being stabilised by the donating solvents. The reactions between oxazolidone based dienophiles and cyclopentadiene, Scheme 2, gave e.e.s ranging from 70-95%. Reactions involving simpler dienophiles such as acrolein gave disappointing selectivity, probably due to higher conformational mobility about the Zr-O bond.

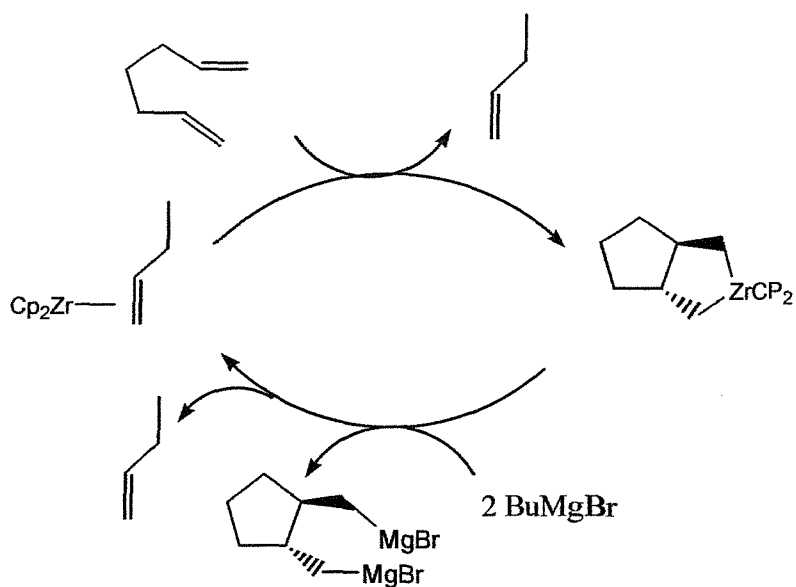


Scheme 2

1.3.3 Co-cyclization reactions

Treatment of 1,7 and 1,6 dienes with dicyclopentadienyl zirconium ethylene complex affords zirconacyclo-pentanes and hexanes^{29 30}. While relative control is good, the products are racemic. Chiral metallocenes under the same conditions have been used with some success, however due to the expense and difficulty involved in the synthesis and resolution of such complexes, a catalytic route would be required for practical applications.

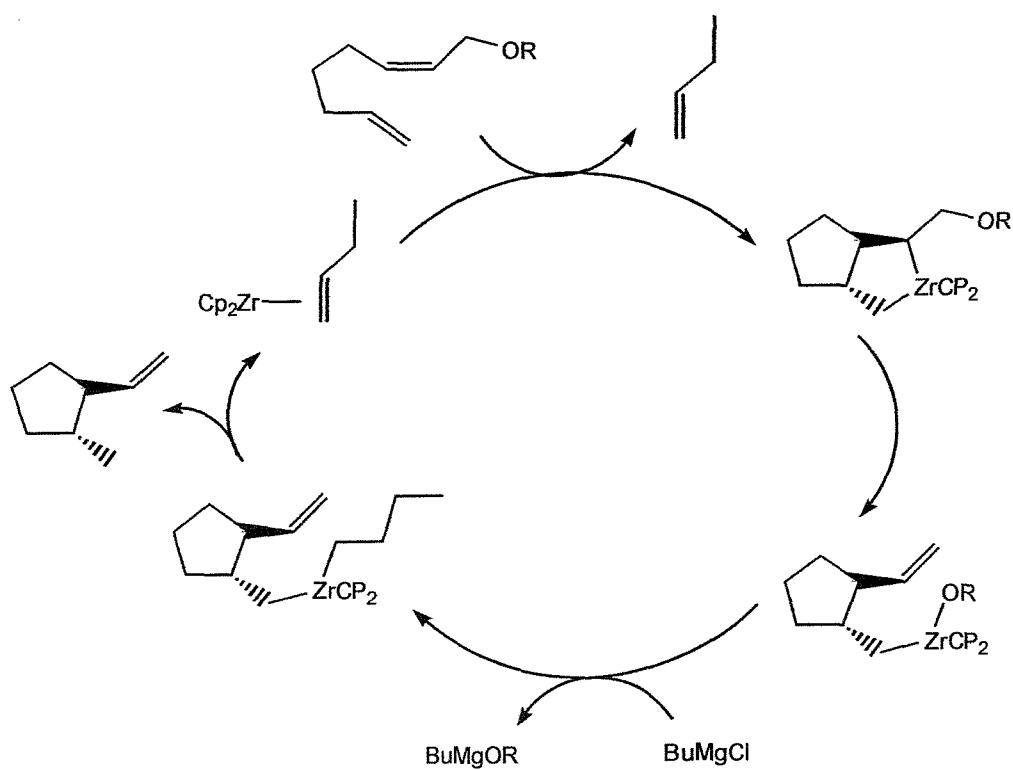
Such a method was presented by Waymouth, who showed that in the presence of an excess of BuMgCl , the cyclization reactions are catalytic in zirconium requiring as little as 2.5 mol% Scheme 3.



Scheme 3

The products are difunctionalised alkylmagnesium species, which may be quenched to afford a variety of products.

In another variant of this reaction, also reported by Waymouth,³¹ 1-methoxy-2,7-octadienes are cyclized to give exclusively *trans* methylvinylcyclopentanes.

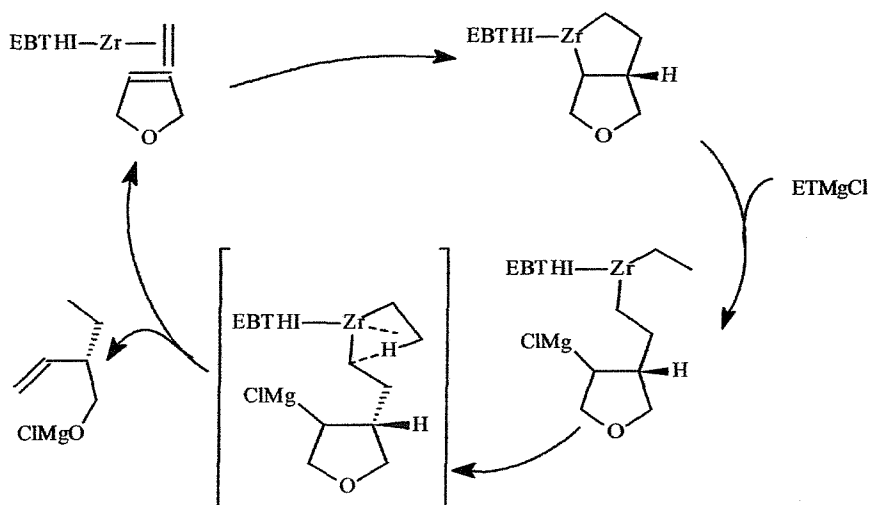


Scheme 4

In contrast to the previous example, deuteration of the reaction mixture affords no deuterium incorporation, indicating that the product contains no alkylmagnesium functional group and hence must follow a different mechanistic pathway Scheme 4.

1.3.4 Carbomagnesiation reactions

Hoveyda³² reports the catalytic ethylmagnesiation of cyclic olefins to yield 2-ethyl alkyl magnesium species with excellent enantioinduction using Brintzinger's catalyst. The olefin inserts into the Zr-ethene bond to afford a 5-membered zirconocycle which is then opened by EtMgCl to give an intermediate species which breaks down to give the product alkylmagnesium species and regenerate the Zr-ethene complex Scheme 5.



Scheme 5

Work with higher organomagnesium species was less successful due to the lack of control of the binding mode of the Grignard reagent.

It should be noted that Brintzinger's catalyst only gave good enantioinduction with cyclic alkenes such as 2,5-dihydrofurans. Work within the group has shown that with acyclic alkenes the enantioinduction is poor but the Whitby catalyst **13** gives much better results, Figure 17.⁹


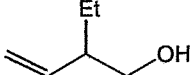
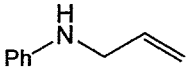
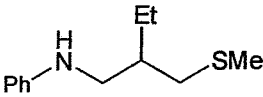
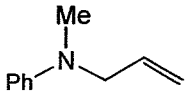
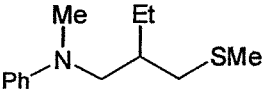
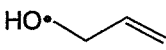
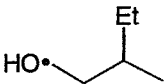
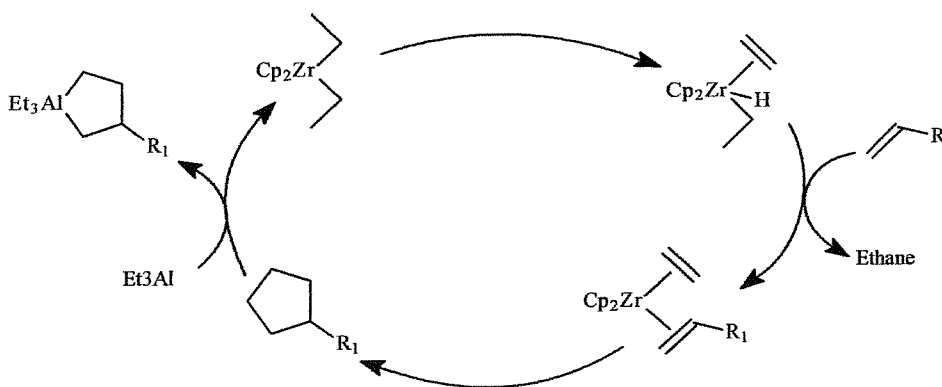
Substrate	Quench	Product	cat.	Yield(e.e%)	
				12	13
	H ₂ O			31(92)	65(98)
	(MeS) ₂			34(26)	92(62)
	(MeS) ₂			39(26)	47(46)
	H ₂ O			35(27)	75(56)

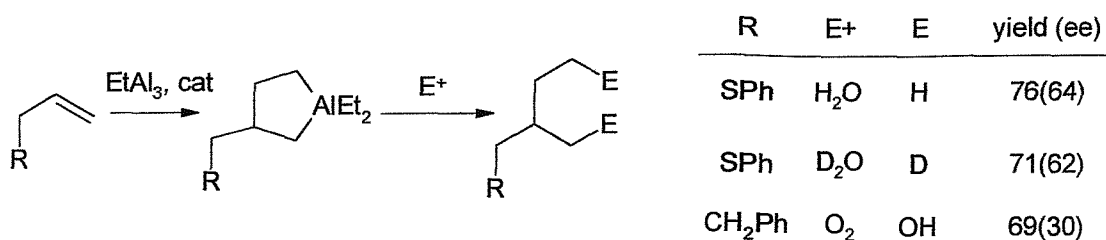
Figure 17

1.3.5 Carboalumination reactions

Dzemilev³³ reported the formation of 3- substituted aluminocyclopentanes *via* the mechanism shown below.

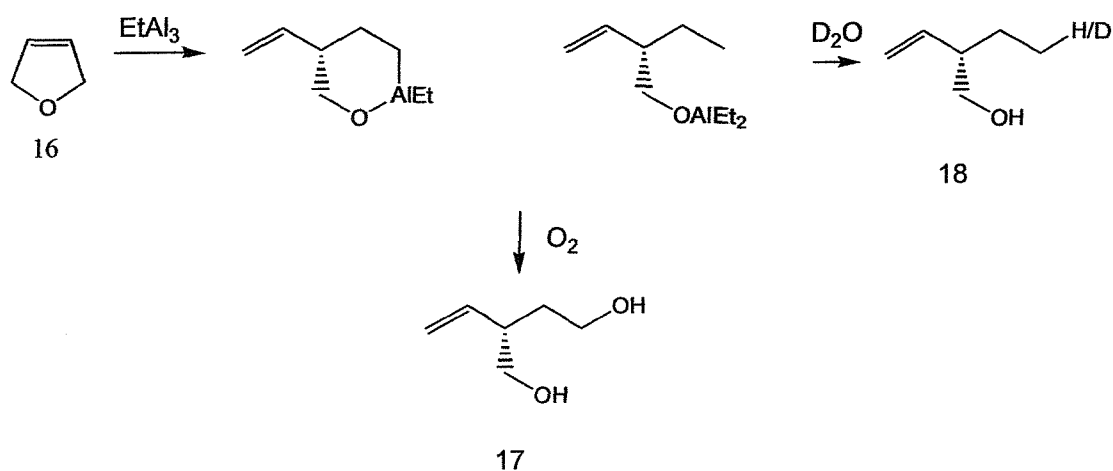


Work within the group has shown that the use of chiral zirconocenes such as **12** and **13** leads to good enantioinduction in these reactions with both cyclic and terminal alkenes.



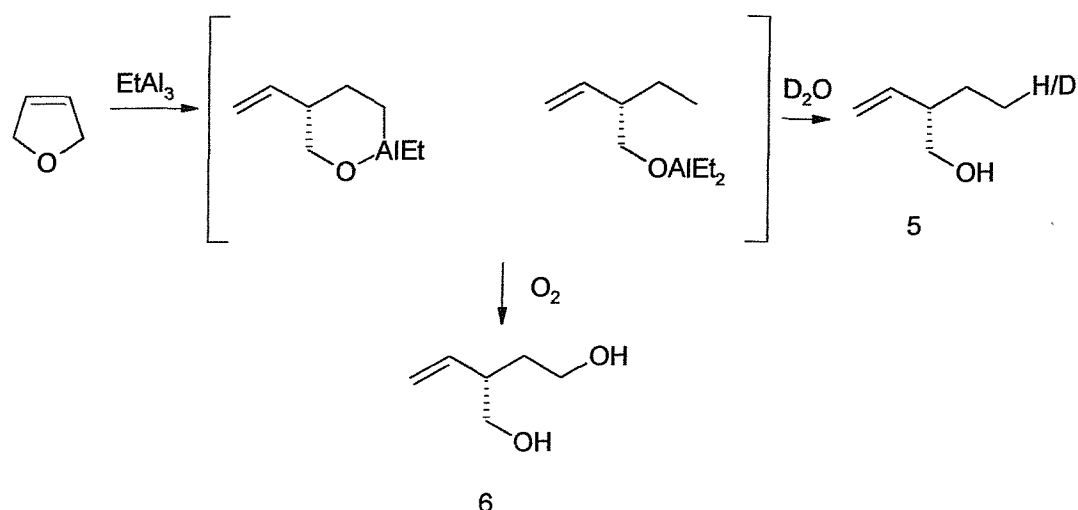
This leads to trifunctionalized products allowing more complex products to be synthesised than with the monometallated carbomagnesiation products.

In the carboalumination of 2,5-dihydrofuran **16**, complex **1** gave better enantioinduction but **13** gave a higher deuterium incorporation and so a higher yield of the diol **17**.



Quench	Product	Yield (e.e.)			
		cat. 12		cat. 13	
H ₂ O	5	90	(>99)	67	(90)
D ₂ O	5	90(67%D)	(>99)	67(94%D)	(85)
O ₂	6	45	(99)	68	(90)

Figure 18



Quench	Product	Yield (e.e.)			
		cat. 1		cat. 3	
H_2O	5	90	(>99)	67	(90)
D_2O	5	90(67%D)	(>99)	67(94%D)	(85)
O_2	6	45	(99)	68	(90)

Figure 19

Negishi³⁴ has also shown that by alteration of the conditions, this reaction may be made to proceed via a non-cyclic mechanism, to afford mono metallated 2-ethylalkylaluminium species Figure 20.

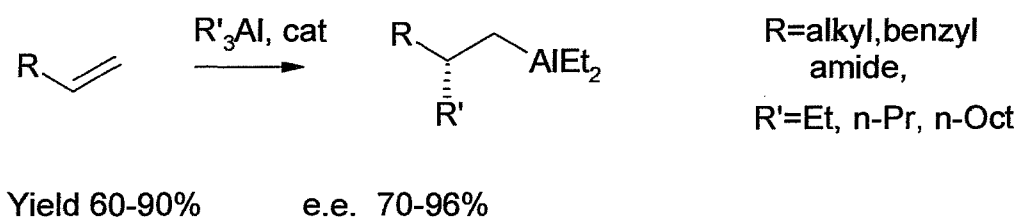
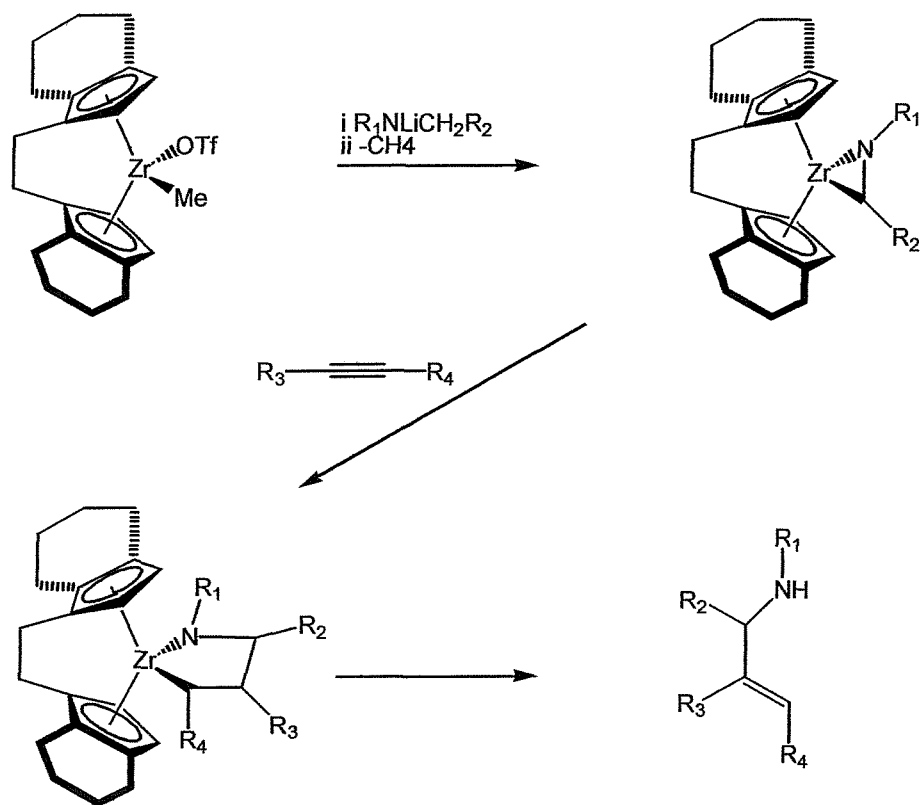


Figure 20

The incorporation of an *n*-Pr group in the aluminium species means that this does not proceed via a cyclic mechanism.

1.3.6 Amine synthesis

Buchwald and others³⁵ report the synthesis of allylic amines and other compounds via the formation of an η -2 imine zirconium complex and subsequent insertion of various alkynes, alkenes and carbonyls Scheme 6.



Scheme 6

Use of Brintzinger's complex **12** gave good to moderate yields and excellent e.e.s with a range of substrates.

1.3.7 Asymmetric hydrogenations

A variety of titanium complexes have been shown to catalyse the enantioselective reduction of alkenes,⁴ imines,⁶ and enamines⁵ Figure 21. The most successful of these has been the titanium form of the Brintzinger complex **12**.

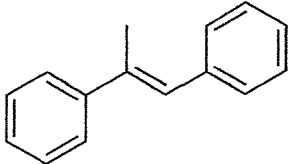
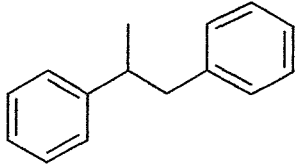
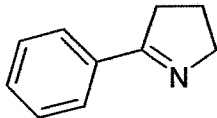
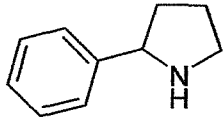
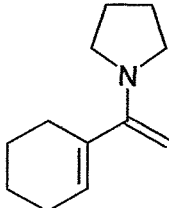
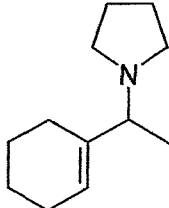
Substrate	Product	Yield(e.e.)
		91(>99)
		86(99)
		72(95)

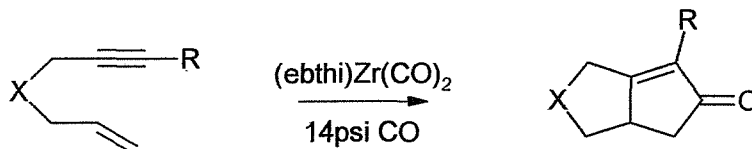
Figure 21

As can be seen from the selection of results above, a wide variety of functionalization may be tolerated and the yields and e.e.s range from good to excellent.

Zirconium complexes also catalyse these reactions but generally with lower activity and enantioinduction.

1.3.8 Pauson-Khand type cyclisations.

Buchwald has recently reported the first catalytic Pauson-Khand type cyclisation, Scheme 7, using $(\text{ebthi})\text{Zr}(\text{CO})_2$, formed *in situ*, as a catalyst.³⁶



Scheme 7

The reaction proceeds via the same mechanism as enyne co-cyclisation described earlier (see 1.3.3) to the bicyclic titanocycle, into which CO is then inserted followed by displacement of the product to regenerate the catalyst.

Various substituted enynes are converted into cyclopentanones in good yields with e.e.s ranging from 70-94%.

2 Synthesis and application of novel chiral catalysts based on the neomenthyl indenyl zirconium system

2.1 C₁ symmetric neomenthyl indenyl monocyclopentadienyl zirconium

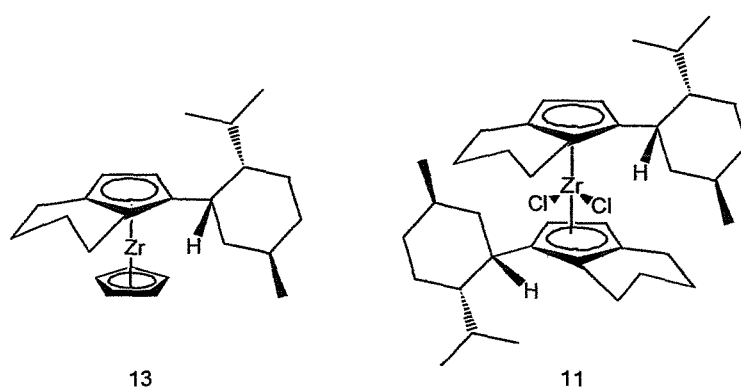


Figure 22

Previous work by Bell and Whitby^{7 8} has developed a novel C₁ symmetric zirconocene **13**, using the same neomenthylindene ligand as the C₂ symmetric complex **11** reported by Erker.¹⁶ The much smaller cyclopentadienyl ligand allows the C₁ complex to react much faster than the more sterically hindered C₂ case, Figure 22. A variety of reactions are catalysed by this complex and have been shown to proceed in moderate to good enantioselectivities.^{7 8}

However, only a few catalytic reactions have been studied to date due to the small amounts of complex available. Initial work has therefore centred on developing a more robust synthesis of **13** in order to allow more a more detailed study of its enantioinductive properties. Stoichiometric amounts of zirconocenes also mediate a range of reactions. A more readily available supply of **13** would allow investigation of the reactivity and selectivity in these reactions.

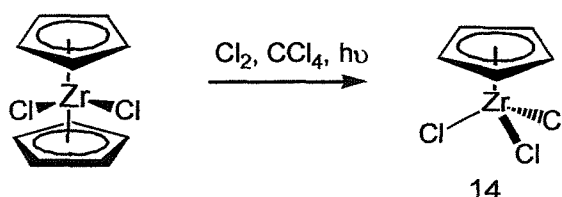
Further work was also carried out to attempt to fine-tune the properties of **13** by small structural modifications.

2.1.1 Improved synthesis of 13

Synthesis of **13** is achieved by the reaction of neomenthyl indenyl anion with cyclopentadienyl zirconium trichloride. The preparation of this organometallic reagent is discussed in the next section.

2.1.1.1 Monocyclopentadienyl Zirconium Trichloride

The original method for the synthesis of this compound was by the chlorination of zirconocene dichloride in CCl_4 using Cl_2 gas and UV light initiator, Scheme 8.³⁷



Scheme 8

Apart from the obvious problems with the toxicity of the reagents, the reaction produced an exotherm that was difficult to control. It seemed that the yield depended on the exotherm being contained within certain limits and as this proved difficult, the results were variable. This led to heat transfer problems when the reaction was scaled up. The best yield obtained via this route was 56%.

A second method, based on a method developed by Livinghouse,³⁸ has been developed within the group.³⁹ This involved the treatment of ZrCl_4 with dimethyl sulphide in DCM to afford the soluble dimethyl sulphide adduct and then subsequent treatment with CpTMS to effect single transfer of cyclopentadiene. This was then converted to the THF adduct by slow addition of THF at 0°C and subsequently purified by recrystallisation from THF/hexane.

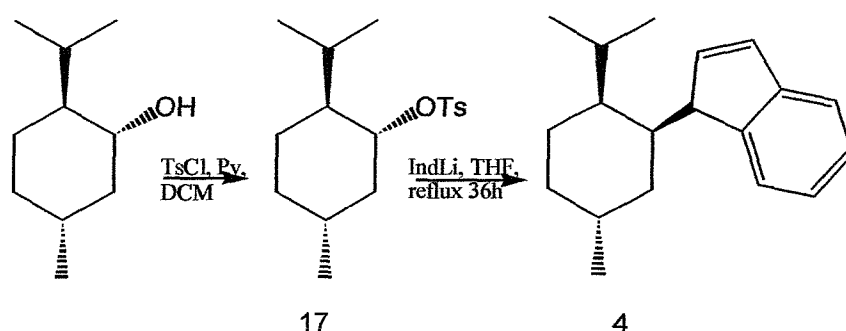
This method gave excellent results with yields ranging from 75-85%. Important in this procedure was that the CpTMS must be essentially free of THF, which complexes to ZrCl_4 , inactivating it and thus reducing the yield. Purification of CpTMS was achieved by careful fractional distillation through a vacuum jacketed Dufton column before use.

Also in the Livinghouse method,³⁸ the DME adduct is formed. It was found that the THF adduct was considerably more soluble and this was the preferred adduct for these complexation reactions.³⁹

Using this method it was possible to produce batches of $\text{CpZrCl}_3 \cdot 2\text{THF}$ **14** which were found to be >95% pure by NMR analysis with a tetramethylbenzene internal standard.

2.1.1.2 Preparation of menthylindene ligand (**4**)

Preparation of ligand **4** was achieved using a method based on that published by Erker, Scheme 9.¹⁶



Scheme 9

(-) Menthyl tosylate **17** was prepared in large quantities using standard procedures in a manner analogous to that of Erker.¹⁶ Recrystallisation from toluene yielded the product **17** as a white crystalline solid in 87% yield.

The ligand **4** had originally been prepared using various conditions and solvents.^{15 40} In the same paper¹⁶, Erker reports a method on the 76mmol scale with a 37% yield using THF as the solvent. Attempts at repeating this procedure consistently gave lower yields (~25%) so an attempt was made to optimise this reaction.

A GC analysis was attempted by simply removing a portion of the reaction mixture and comparing the response with a calibration trace run immediately beforehand.

Unfortunately the error in this procedure proved too great for any meaningful results to be gained but it was possible to increase the accuracy by removing a known volume of sample and adding a known amount of a GC standard, *n*-octadec-1-ene. The results from this analysis are given below.

Reaction time and conditions	Estimated yield from GC analysis
24h at room temperature	14%
24h at room temperature, 24h at reflux	47%
24h at room temperature, 48h at reflux	36%
recovered yield after workup	26%

The reaction was worked up immediately after the final GC analysis and the discrepancy between the recovered yield highlights one of the sources of error. The reaction is carried out for prolonged periods at reflux in a volatile solvent. The probability of solvent loss occurring during this time would be quite high and this would give a misleadingly high value for the concentration of the reaction mixture and hence for the estimated yield. This combined with loss of material during workup would account for the consistent difference of around 10% between the final estimated yields and the recovered yields.

However, even with this error it is still apparent that the concentration of product in the reaction mixture falls with prolonged reaction time. This is presumably due to some side reaction such as thermal decomposition or alkylation. It was not possible to isolate any by-products to enable such a hypothesis to be confirmed. In the light of these findings, the reaction was stopped after 48 h and the yield was found to have increased to 36%.

Purification was achieved by flash chromatography to remove excess menthyl tosylate followed by distillation. It was found that, using a vacuum of <0.1 mmHg, short path distillation was possible at around 110°C to afford the compound as a pale oil which crystallised on standing. This superseded the tricky Kugelrohr distillation of the product, which proved impractical on the larger scale.

Due to these improvements, it was possible to prepare high quality batches of around 15-20g of ligand 4.

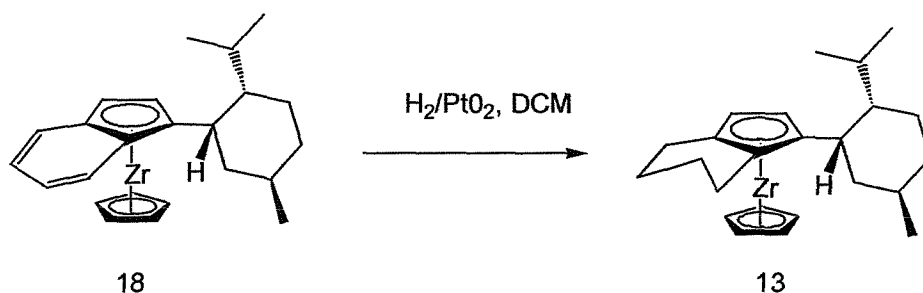
2.1.1.3 Complexation and Hydrogenation steps

The methodology is essentially the same as that used previously within the group,^{15 40} but with several experimental improvements.

The purity of the $\text{CpZrCl}_3 \cdot 2\text{THF}$ was fundamental and in order to achieve good results this needed to be in excess of 95%. Furthermore, any remaining Me_2S caused problems in the later hydrogenation step by poisoning the metal catalyst. Adequate washing of the $\text{CpZrCl}_3 \cdot 2\text{THF}$ with hexane was therefore essential.

Although it was now possible to produce suitably pure material (see 2.1.1.1), it was unstable and decomposed during storage. It proved possible to recrystallise the impure material from hot THF under argon to give the necessary level of purity.

Deprotonation of the substituted indene ligand was previously achieved by the addition of *n*-butyl lithium to a THF solution of **4** at -78°C and warming to room temperature overnight to give a dark red solution. Better results were achieved if the deprotonation was carried out in the absence of light for only two hours. This gave a greenish-yellow solution and upon complexation, the indenyl zirconium complex **18** was obtained as a pure bright yellow solid as opposed to the previously obtained orange oils which required purification. Hydrogenation of this material proceeded rapidly and cleanly to give the desired complex **13** in up to 71% yield, Scheme 10.

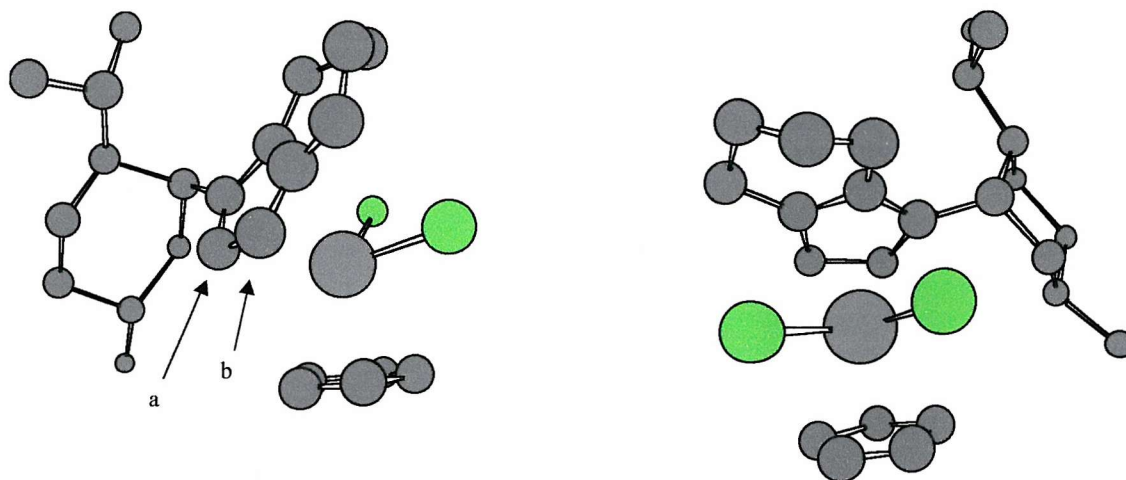


Scheme 10

By the use of $\text{CpZrCl}_3 \cdot 2\text{THF}$ instead of $\text{CpZrCl}_3 \cdot 2\text{DME}$ and indene deprotonation in the dark, overall yield of **13** (from neomenthyl tosylate) was improved from 9% to 26% and was readily carried out on a large scale.

2.2 New complexes based on the menthylindenyl zirconium system

Changing the substitution around the cyclopentadienyl rings will alter the chiral environment around the catalytic site. This can be visualised using the X-ray crystal structure of **13** shown below, Figure 23.


Figure 23

The simplest way to alter the substitution around the metal is to employ a pentamethyl cyclopentadienyl ring as the second ring. This may be achieved by using Cp^*ZrCl_3 **20** in place of CpZrCl_3 .

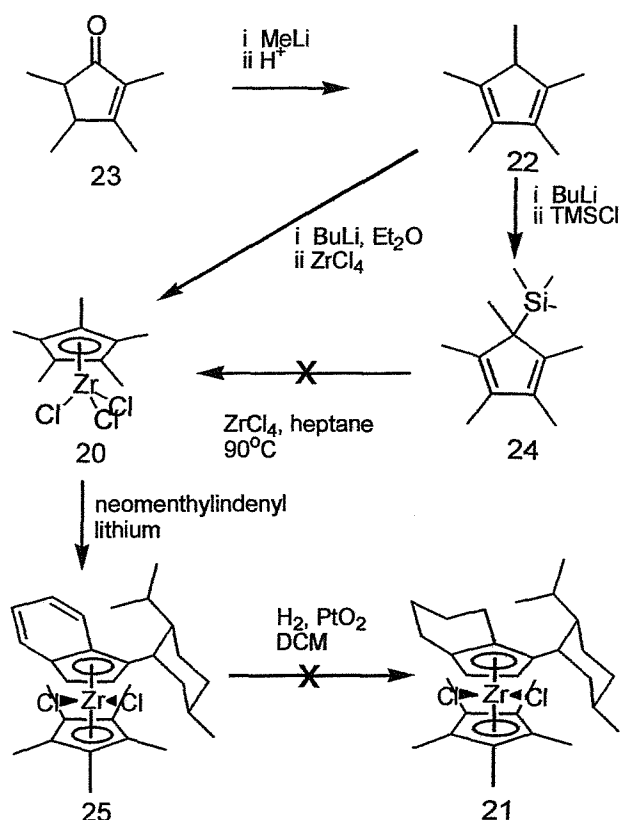
Further substitution on the trisubstituted cyclopentadienyl ring at either of the sites a or b may result in steric interactions with the unsubstituted cyclopentadienyl ring. This could cause the bite angle to be reduced and therefore increase the interaction between substrates at the active site and the chiral ligand substituents.

A third strategy envisages substitution on the tetrahydroindenyl ring over the active site in an attempt to improve the effectiveness of the "roof". (See 1.2.2)

2.2.1 Pentamethylcyclopentadienyl derivatives

Several syntheses of Cp^*ZrCl_3 **20** have been published^{41 42} and it was hoped that methodology established in Section 1.1.1.2 could be used to complex the neomenthylindene ligand to the zirconium to give the more hindered zirconocene **21**.

Cp^*H **22** was prepared by the nucleophilic addition of MeLi to the ketone **23** followed by acidic workup to give the desired product. Scheme 11⁴³



Scheme 11

The most recently reported preparation of Cp^*ZrCl_3 **20**⁴² was achieved *via* the TMS adduct of the Cp^*H , **22**, by heating with ZrCl_4 in heptane. Although in an attempted repeat of this work it proved possible to form the silane, **24** it proved impossible to isolate any of the desired zirconium complex **20** *via* this route.

In another method published by Schrock,⁴¹ the lithiated Cp^* is simply stirred with ZrCl_4 in ether to give the etherate complex. Using this method it was possible to produce the etherate, which should be as reactive as the $\text{CpZrCl}_3 \cdot 2\text{THF}$ complex used in the synthesis of the parent system.

The material obtained in this manner was treated with the lithium salt of menthyl indenyl **4** to give a yellow solution. Upon removal of solvents the yellow solution turned black and NMR revealed the presence of the reprotated ligand and a small amount of Cp^*ZrCl_3 .

In order to confirm that the zirconium source was not the problem in the complexation reactions, a small quantity of Cp^*ZrCl_3 was purchased commercially.⁴⁴ Attempts were made to assay this material by NMR in chloroform, as suggested by the literature.⁴² The material proved to be insoluble in chloroform as previously inferred, but upon

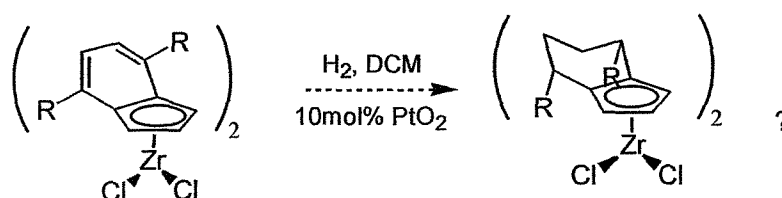
addition of a small amount of d^8 THF, full dissolution was achieved and internal standard analysis with tribromobenzene revealed purity in excess of 95%. In light of this finding, the work on the synthesis of Cp^*ZrCl_3 was inconclusive. i.e. the Cp^*ZrCl_3 may well have been formed but being insoluble in $CDCl_3$ was not detected.

Complexation of lithiated neomenthylindene **4** was carried out using analogous methods to those developed for the parent system. NMR analysis of the yellow residues revealed a mixture of compounds but doublets in the 6-7.5 ppm region were characteristic of the desired complexed indene **25**. Thus using higher quality, commercially obtained Cp^*ZrCl_3 it was possible to achieve at least partial complexation of ligand **4**.

Hydrogenation of these crude indenenes yielded colourless solids which showed no peaks at all in the 5-7 ppm region indicating that any complexed material had been destroyed. It is possible that the extra steric bulk provided by the pentamethyl cyclopentadiene group destabilised the complex to the extent that it was not possible to isolate it. It was therefore decided to discontinue this line of research.

2.2.2 4,7-Dimethyl-indene derivatives

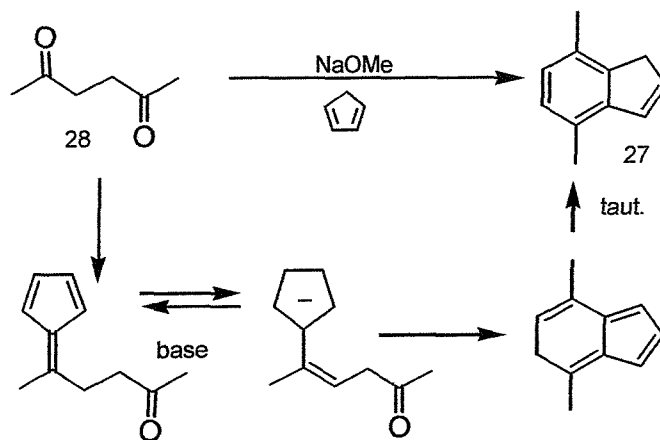
The hydrogenation of indenenes attached to zirconium is well known. Consideration of the steric environment around the indene moiety shows that one face (that with zirconium) is much more sterically hindered than the other. This difference may be enough to cause selective reduction of one face. Hydrogenation of substituted indenenes, therefore, may force the substituents downwards towards the metal centre upon reduction, Scheme 12. 4,7-Dialkyl indenenes are readily available^{45 46} and offer a simple test of this hypothesis.



Scheme 12

Coe has recently published a synthesis of 4,7-dimethyl indene **27**⁴⁶ by the treatment of cyclopentadiene and hexan 2,4-dione **28** with catalytic amounts of tert-BuOK in

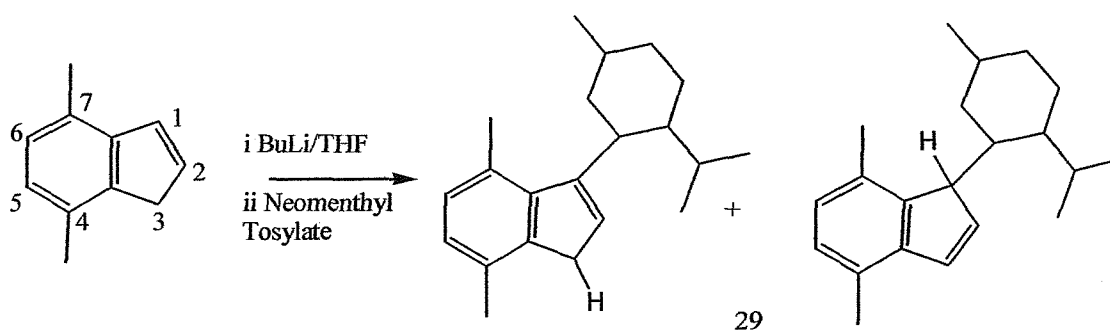
methanol. Also in a patent by Erker⁴⁵ the same transformation is carried out using cheaper NaOMe, Scheme 13.



Scheme 13

If this substituted indene were complexed to zirconium, hydrogenation would be expected to occur from the least hindered face only and so force the methyl groups down into the co-ordination sphere of the metal. These groups could be used to reinforce the "roof" and so possibly increase the stereoselectivity of reactions.

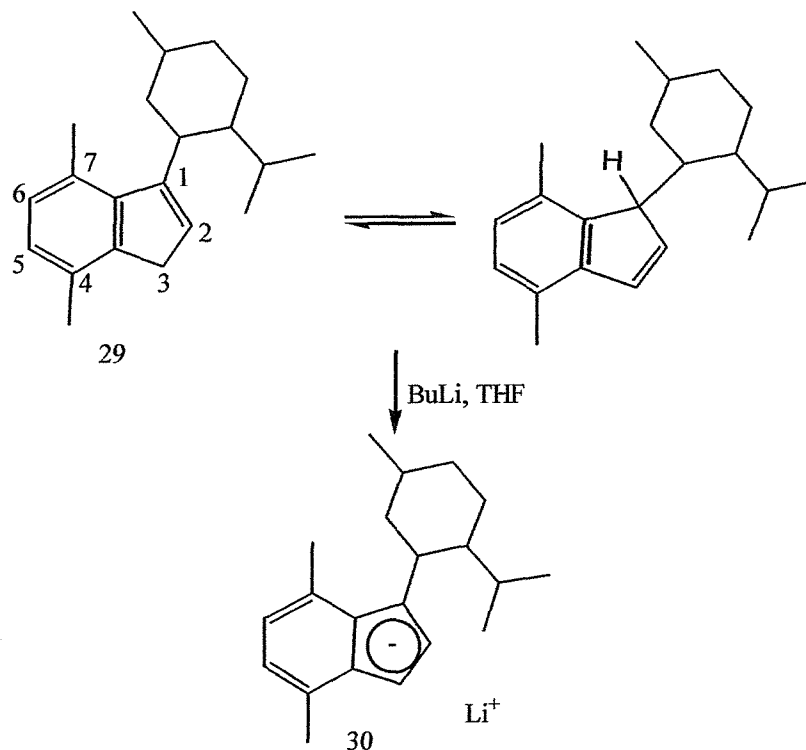
The formation of the menthyl indene **29** was achieved using the same methodology as the parent system, the extra steric crowding causing no new problems. GC analysis of the reaction using an internal standard⁴⁷ showed that maximum yield was achieved after 48 h at reflux and unlike the parent system no decomposition of product was apparent with continued refluxing, Scheme 14.



Scheme 14

The product was isolated by the same method as the parent system but interestingly was obtained as a mixture of double bond isomers on the Cp ring, - not observed in the parent system. This could be due to the destabilisation of the more substituted double

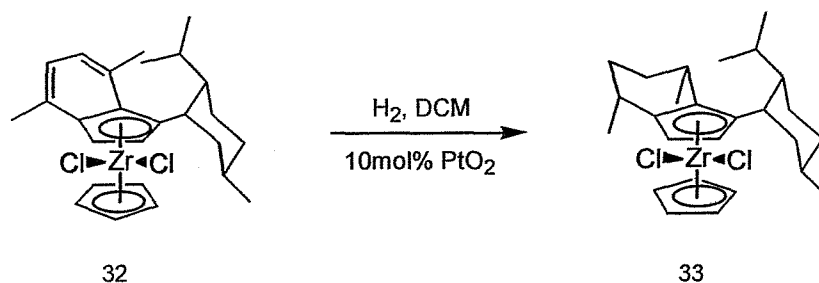
bond isomer by steric clash between the menthyl substituent and the methyl group at the 7 position, Scheme 15.



Scheme 15

Fortunately the double bond isomers have no effect upon subsequent deprotonation and metallation steps as they both give the same delocalised anion **30**.

Addition of this anion to $\text{CpZrCl}_3 \cdot 2\text{THF}$ afforded the indenyl complex **32** as a bright yellow solid, which could be recrystallised from hot hexane. X-ray analysis of these crystals gave the structure below, Figure 24. This displays the same facially selective complexation due to the favoured rotamer being that in which the 7 methyl eclipses the hydrogen rather than the menthyl ring and the isopropyl group blocks the rear face.



Hydrogenation of this complex proved more difficult than in the parent system. Due to the more substituted nature of the bonds to be reduced and possibly due to the hindered nature of the product, more forcing conditions were required. After hydrogenation under

2500 psi H_2 at $65^\circ C$ for 18 hours with Adams catalyst, complex **32** was found to have been cleanly converted to tetrahydro-indenyl complex **33** in 20% yield.

Comparison of the X-ray crystal structures of the two complexes, Figure 24, shows how the two methyl groups have been forced downwards into the coordination sphere of the zirconium.

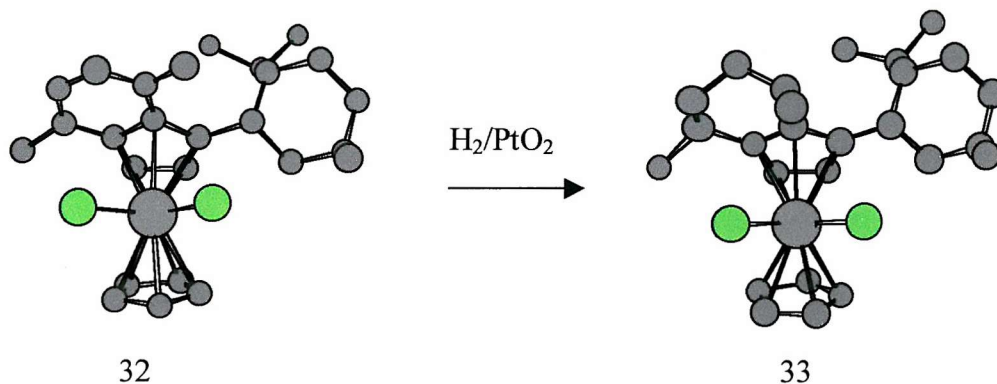


Figure 24

All attempts to catalyse terminal olefin alkylation reactions with **33** were unsuccessful giving only unreacted starting material. This was presumably due to the much more hindered nature of the active site in the complex **33** compared to complex **13**, as shown by the X-ray crystal structures Figure 25. One side of complex **33** is effectively blocked by the menthyl "wall", while the other active site sits in a pocket formed by the methyl groups on the tetrahydroindenyl ring.

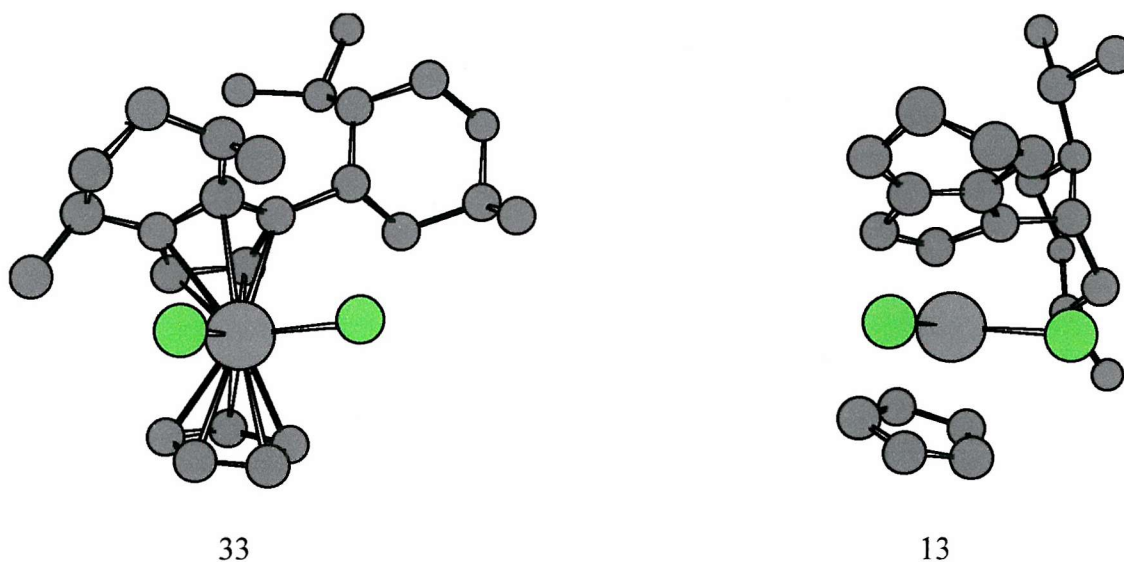


Figure 25

As a result of this excess bulk the complex seems to be inert to olefin insertion reactions. However bulky zirconocenes of this type have found utilisation as α -olefin polymerisation catalysts²⁴ and this will be discussed in chapter 5.

2.2.3 Methyl substituted indenyl complexes

Single crystal X-ray structural analysis of the metallocene **13** has shown that the two protons on the tri-substituted cyclopentadiene ring adopt the conformation in which they are closest to the other cyclopentadiene in order to reduce steric interactions between the rings to a minimum Figure 26.⁸

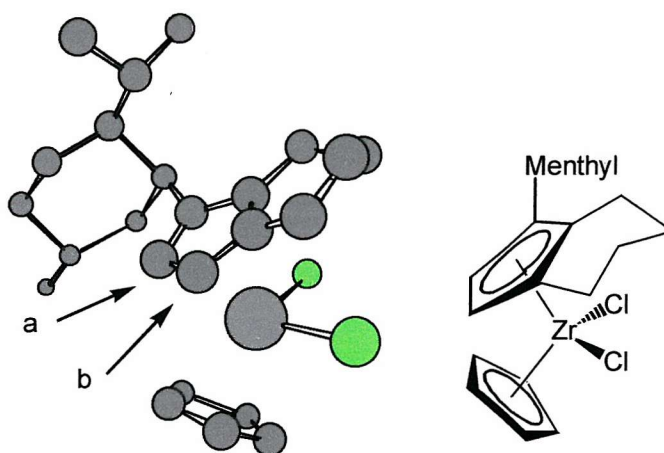
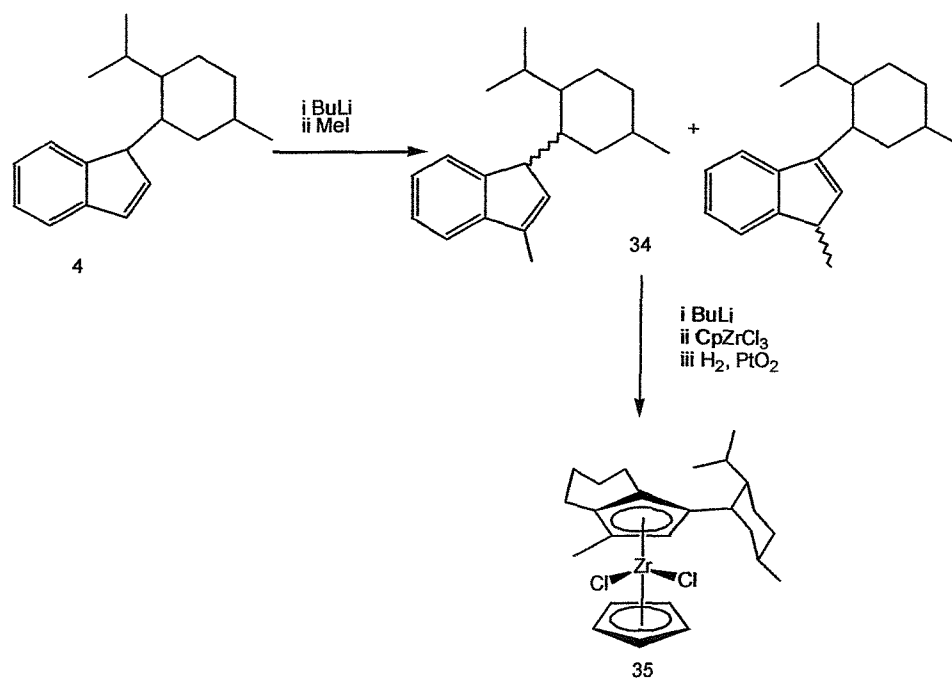


Figure 26

Substitution at one of these two positions, a and b, could cause considerable structural change by either forcing rotation around the cyclopentadiene zirconium bond or by closing the bite angle due to increased steric interactions. A convenient synthesis of such a ligand is outlined below, Scheme 16.


Scheme 16

Alkylation of indenenes occurs exclusively at the 1 and 3 positions and, as such, methylation of 1-menthyl indene **4**, Scheme 16, gave exclusive alkylation at the 3 position to yield compound **34** a mixture of double bond isomers. Treatment of this mixture with *n*-butyl lithium followed by CpZrCl₃•2THF and subsequent hydrogenation under standard conditions gave complex **35** as a white crystalline solid which proved to be a single diastereoisomer by NMR.

Utilisation of this complex to catalyse the ethyl magnesiumation reaction of *N*-allyl aniline under standard conditions in diethyl ether gave a 48% yield of the expected product in 77% e.e. When this figure is compared to the parent catalyst system **13** under the same conditions (81% e.e.) we see only a slight difference in e.e. The X-ray crystal structure of **35** is shown below with the structure of the parent neomenthylindene complex **13**, Figure 27.

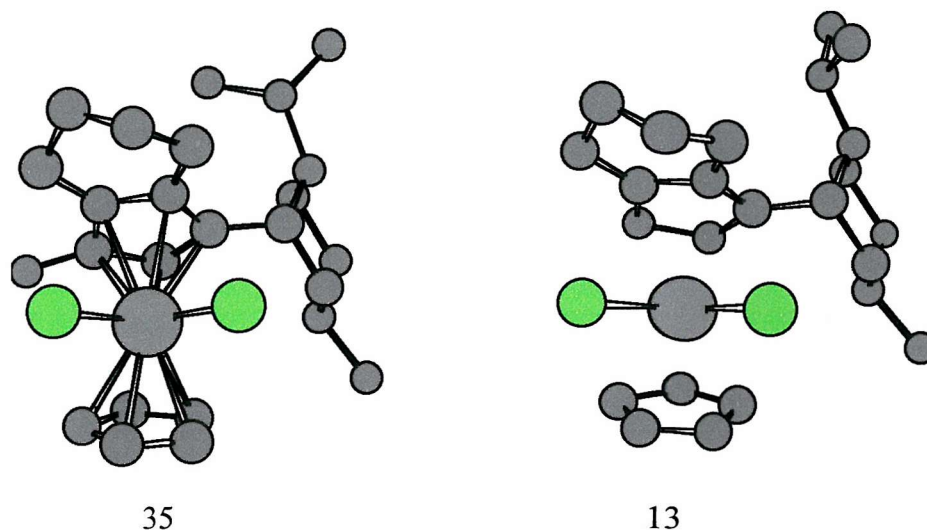


Figure 27

Comparison of the two complexes shows very few differences between the gross structures except for slight changes in the orientation of the isopropyl in the menthyl group. If we superimpose the two structures, Figure 28, we see that the addition of the methyl group has caused almost no change in the structure of the complex. (The superimposition is viewed from three different angles).

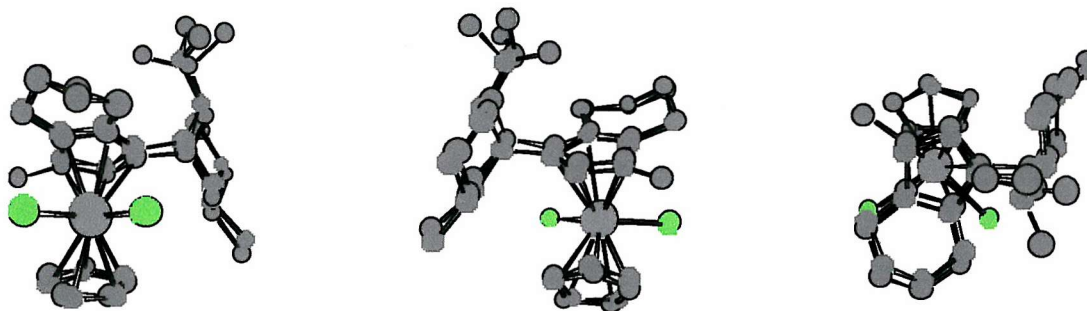
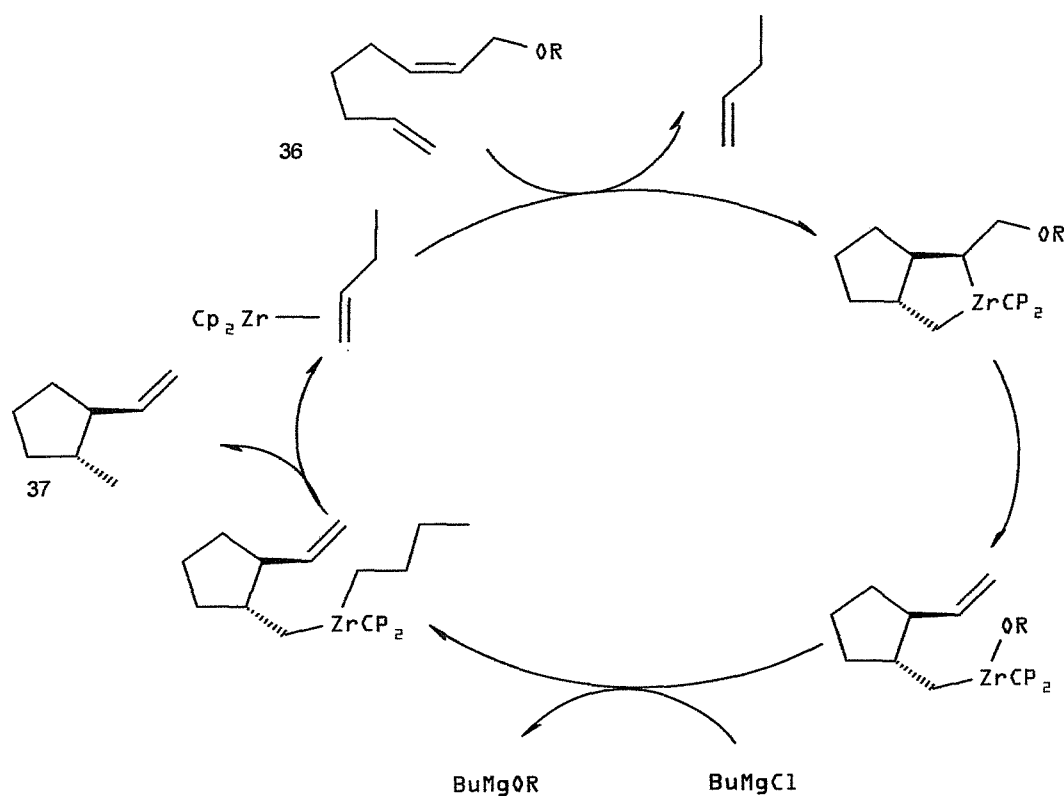


Figure 28

The only significant structural change is a change of conformation of the isopropyl group. As the isopropyl moiety lies away from the active site, there is almost no change at all in the steric environment around the catalytic centre. As a result, the enantioselectivity observed in the ethylmagnesium reaction is almost identical. From these results it is apparent that the methyl group is insufficiently bulky to force a significant conformational change to the neomenthyltetrahydroindenyl substructure. Further work in this area should centre on the use of a bulkier group, such as phenyl isopropyl, *tert*-butyl etc., to force a more significant change in the structure of the complex. However in the current work there was insufficient time to carry out such a study.

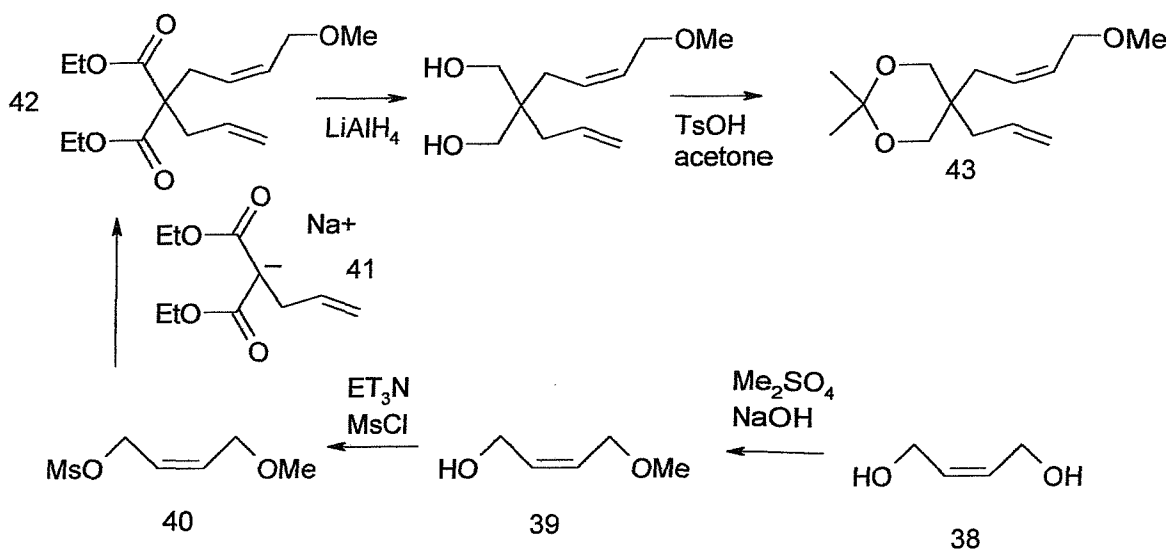
2.3 Stereoselective zirconium catalyzed cyclisation reactions

Waymouth³¹ has reported the zirconium catalyzed cyclisation/elimination of 1-methoxy-2,7-octadienes, such as **36**, in the presence of BuMgBr to give predominately the *trans* isomer **37**, Scheme 17. This work uses achiral Cp₂ZrCl₂ to achieve high diastereoselectivity via the catalytic cycle below. It is hoped that by using a chiral zirconocene such as **13**, that a degree of enantiocontrol may be achieved in these reactions.



Scheme 17

To test this application it was necessary to synthesise a suitable diene substrate. As the original Waymouth paper³¹ did not give synthetic routes to the substrates it was proposed to make the substrate **43** *via* the route shown below, as this appeared to be the simplest synthetic route, Scheme 18.



The mono methylation of the readily available diol **38** was attempted by treatment with NaH followed by MeI. This method did not yield any of the desired product so the method of Peterson⁴⁸ was employed using Me_2SO_4 and NaOH in water followed by continuous extraction with ether for 24 h. This afforded the desired monoprotected alcohol **39** in 61% yield.

The mesylation step proved more problematic. The standard conditions of Et_3N and MsCl in DCM at -40°C afforded the desired product, **40**, but in poor yield (19%). This was suspected to be due to the instability of the mesylate on silica and so this compound was not fully characterised but used in the next step without purification.

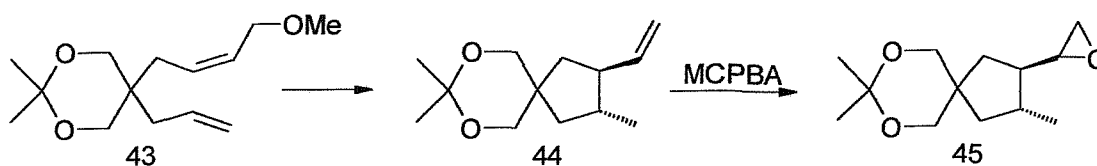
Treatment of the mesylate with sodium allyl-malonate (generated from allyl diethyl malonate and sodium ethoxide) in THF afforded the desired product **42** in 78% yield.

Treatment of this compound with LiAlH_4 in ether⁴⁹ followed by the standard workup afforded a colourless oil, which was stirred in acetone with *p*-toluene sulphonic acid overnight. Workup and column chromatography yielded the desired product **43** in 60% yield over two steps from **42**.

2.3.1 Asymmetric Co-cyclization reactions

The diene **43** was stirred in ether with zirconocene dichloride at -20°C and a four-fold excess of BuMgCl was added dropwise. The mixture was stirred at room temperature and after 36 h, workup and column chromatography yielded the alkene **44** in 83% yield.

After experimenting with a variety of columns, it proved impossible to resolve the enantiomers by chiral GC and so a small amount of the product was stirred in DCM with MCPBA and an excess of NaHCO_3 to afford the epoxide **45**. GC analysis indicated a 5:1 mixture of diastereoisomers and a chiral GC method was developed which allowed resolution of the major diastereoisomer.⁵⁰



Scheme 19

The analogous reaction was carried out using the chiral zirconocene **13**. This reaction proved much slower due to the extra steric bulk in the coordination sphere. The reaction was stopped after 7 days and the product isolated by column chromatography in 21% yield. The same analytical procedure was carried out to reveal an e.e. of 11%.

2.4 Conclusions

This chapter has described the improved synthesis of the original neomenthylindene complex **13** reported by Bell and Whitby.^{7 8} By the use of $\text{CpZrCl}_3 \cdot 2\text{THF}$ instead of $\text{CpZrCl}_3 \cdot 2\text{DME}$ and indene deprotonation in the dark, the overall yield of complex **13** (from neomenthyl tosylate) was improved from 9% to 26% and was readily carried out on a large scale. This allowed further study of this complex's enantioinductive properties.

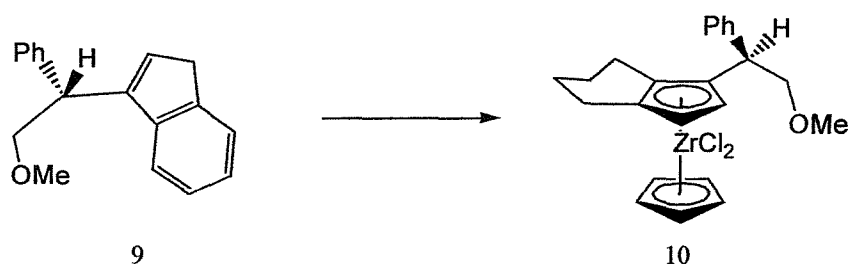
Utilisation of this complex in an asymmetric variation of a reaction reported by Waymouth³¹ gave both a poor e.e. and poor conversion. As a result of this, ways were sought to improve the properties of this complex.

To this end, three novel complexes were synthesised however the results proved less than satisfactory giving either excessively hindered inert complexes or complexes with similar properties to the parent complex. It was apparent that in order to achieve significant improvements it would be necessary to develop a new approach to ligand design and this novel approach is described in the next chapter.

3 Development and utilisation of novel bicyclic cyclopentadienyl ligands with pendant heteroatom linkers

3.1 Heteroatom control of facial selectivity

As discussed in earlier chapters, metallation of polysubstituted cyclopentadienyl rings generally gives a mixture of isomers. As such mixtures are difficult to separate by conventional means, a novel ligand design should involve a strategy for controlling the face of metallation. Recent work by Brookings and Whitby¹⁵ has centred on the use of a pendant heteroatom to achieve such control. Scheme 20



Scheme 20

This system relies on the lowest energy rotamer of the indenyl-CHPhCH₂OMe bond, placing the heteroatom over one face of the cyclopentadienyl anion. If the indenyl-CHPh bond is rotated to minimise steric interaction with the 7 proton on the indene moiety, the alkoxy group is held over one face of the indene.

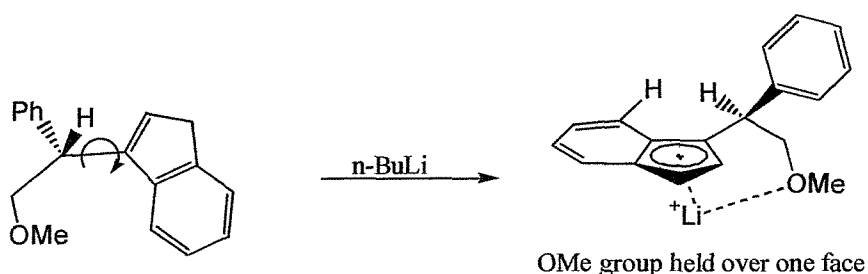
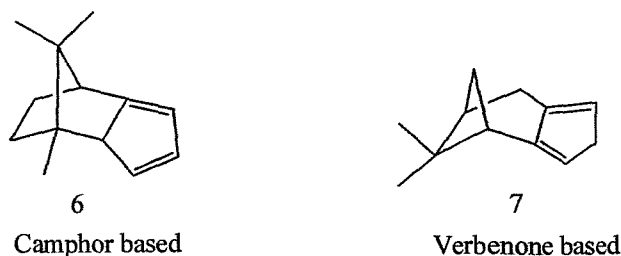


Figure 29

This may then lead to the stabilisation of the ion with the lithium on the same side as the alkoxy group, Figure 29, leading to facial selectivity in the reaction with a metal halide.

However the bulky phenyl group is also held over the upper face and steric effects would also direct metallation to the same face. Furthermore, the two rotomers would not necessarily have the same reactivity towards the metal halide. Results from this system are therefore clouded by a combination of effects and a better system for the study of electronic effects is needed.

Selectivity has been shown to be good in ligands with rigid bicyclic structures such as **6**¹² and **7**¹³ based on terpene backbones.



A new system using a fused bicyclic backbone to hold a heteroatom linker over one face of the cyclopentadienyl ring may solve the problem of conflicting steric and electronic effects.

3.2 Design of a rigid ligand system

The backbone of a suitable bicyclic system should be totally symmetric apart from the heteroatom linker so that any observed selectivity will be entirely due to this functional group.

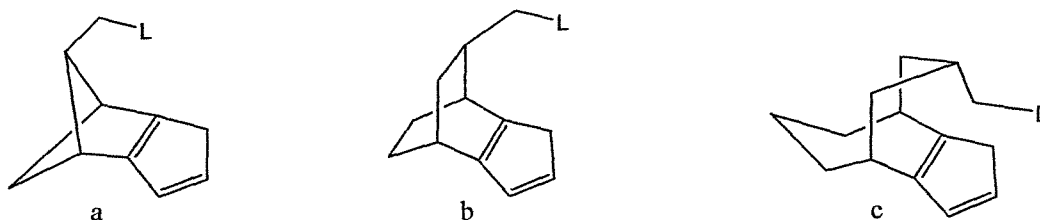
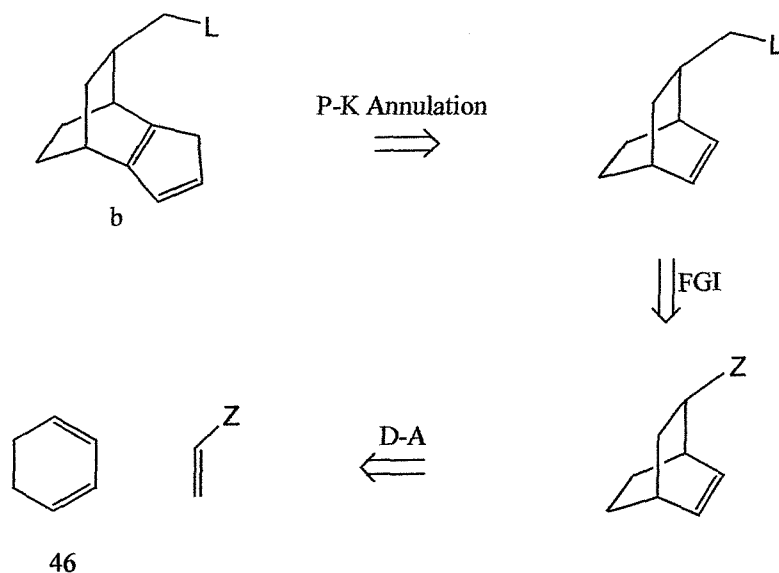
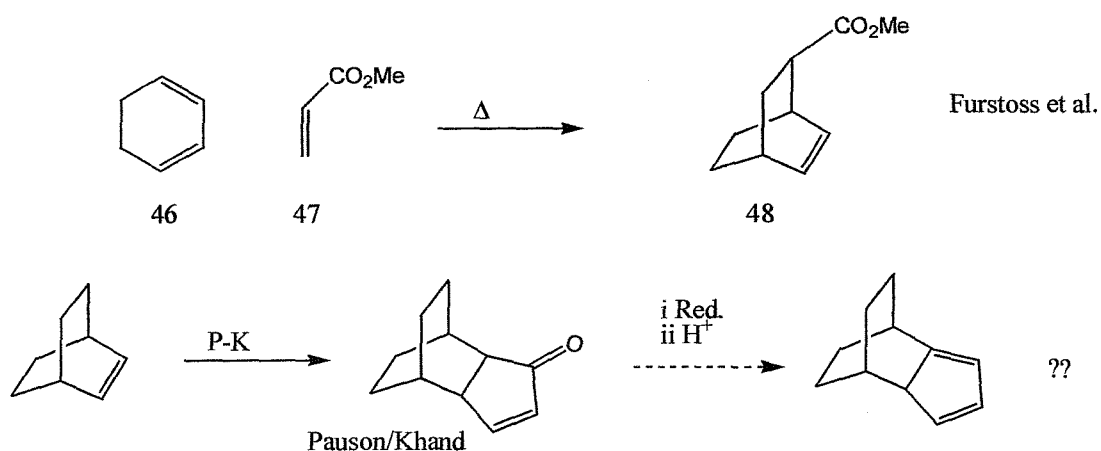


Figure 30

A number of potentially suitable symmetric bicyclic backbone systems suggest themselves, Figure 30, however only **a** and **b** would have the required structural rigidity. Example **a** contains a highly strained 4-membered ring and only **b** has a simple disconnection to a Diels-Alder type cyclisation as shown in Scheme 21.


Scheme 21

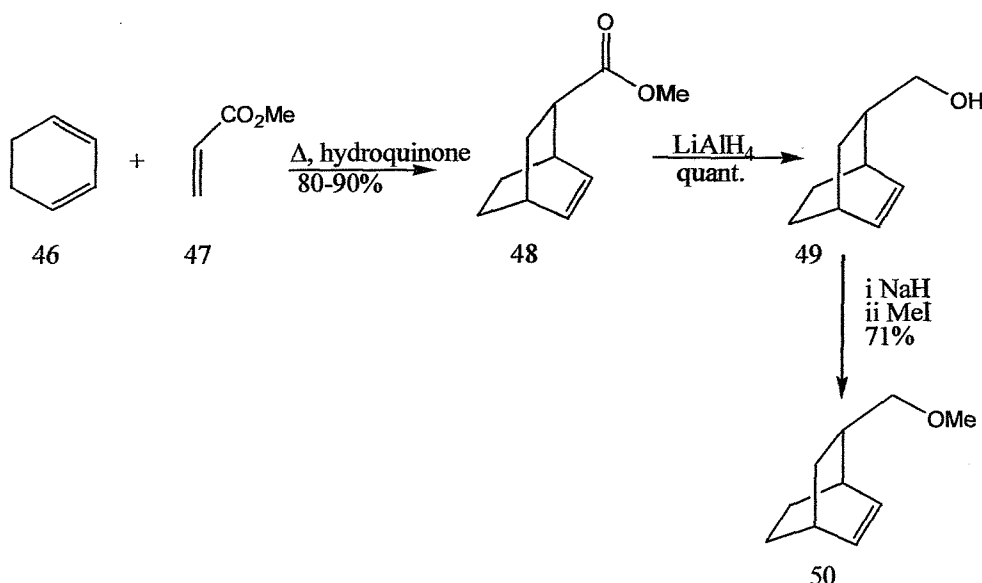
The electron-withdrawing group needed for the Diels-Alder cyclisation may be converted to the heteroatom containing group, then the cyclopentadienyl ring may be fused to the remaining double bond *via* a Pauson-Khand type annulation, Scheme 22. Diels-Alder cyclisations between 1,3-cyclohexadiene **46** and a variety of nucleophiles are well known. The cyclisation of this diene with methyl acrylate **47** has been reported⁵¹. Fusion of a cyclopentenone to a [2,2,2] bicyclic backbone has also been reported by Pauson and Khand.⁵² 1,2 Reduction followed by elimination should yield the desired compound.


Scheme 22

3.3 Synthesis of ligands of type b.

3.3.1 Construction of [2,2,2] bicyclic backbone

Initial work on the synthesis of this ligand was carried out following the method of Furstoss.⁵¹ Methyl acrylate **47** and 1,3-cyclohexadiene **46** were placed in a sealed glass tube with hydroquinone as an inhibitor. The tube was then heated in an oil bath to 150°C for 18 h. The tube was then cooled and opened before the residue was subjected to short path distillation to give the desired ester **48** in 80-90% yield. Although this method was high yielding, it was limited in scale up potential due to the limited size of Schlenk tubes available in the lab.



Scheme 23

Reduction of this ester was achieved under standard conditions without difficulty. Treatment of a solution of ester **48** in ether with lithium aluminium hydride ⁴⁹ followed by acidic workup gave the desired alcohol **49** in 99% yield.

The choice of protecting group for the pendant oxygen was large.⁵³ However, a small, stable group was required which would not cleave under reaction conditions or sterically block co-ordination of the oxygen. Silicon groups were considered too bulky and possibly too labile. A simple methyl group was decided upon as the best option.

Methylation of this alcohol with a biphasic system of aqueous sodium hydroxide and dimethyl sulphate with *tert*-butyl ammonium chloride as phase transfer catalyst⁵⁴ gave only very low yields of the desired methyl ether **50**. However treatment with sodium

hydride in ether followed by addition of methyl iodide⁵⁵ and refluxing overnight afforded **50** cleanly in 71% yield.

3.3.2 Cyclopentadiene ring annulation

Although the chemistry up to this point had been relatively straightforward, the annulation of the cyclopentadienyl ring proved much more challenging.

Treatment of alkene **50** with dicobalt acetylene hexacarbonyl in toluene at 80°C (as per the method of Khand⁵²) followed by removal of solvent *in vacuo* gave a dark red oil, still contaminated with cobalt residues. Purification was achieved by column chromatography on a neutral alumina column to give a colourless oil in 35% yield. NMR and IR analysis of this oil revealed a mixture of two compounds. Appearance of a carbonyl stretch at 1699cm⁻¹ indicated the inclusion of the enone into the molecule. Also ¹H resonances at 7.7 and 6.3 ppm were observed, characteristic of the two *sp*² protons of the enone moiety. Integration over the OCH₃ singlets (3.35, 3.32 ppm) showed the mixture to be in a 1:1 ratio. It was not however possible to separate these two compounds so the mixture was used in subsequent steps without further purification.

Theoretical consideration shows that due to the substituent on the bicyclic ring system, it is possible to form four different isomers upon reaction of **50** with dicobalt acetylene hexacarbonyl complex **51**, as shown in Figure 31.

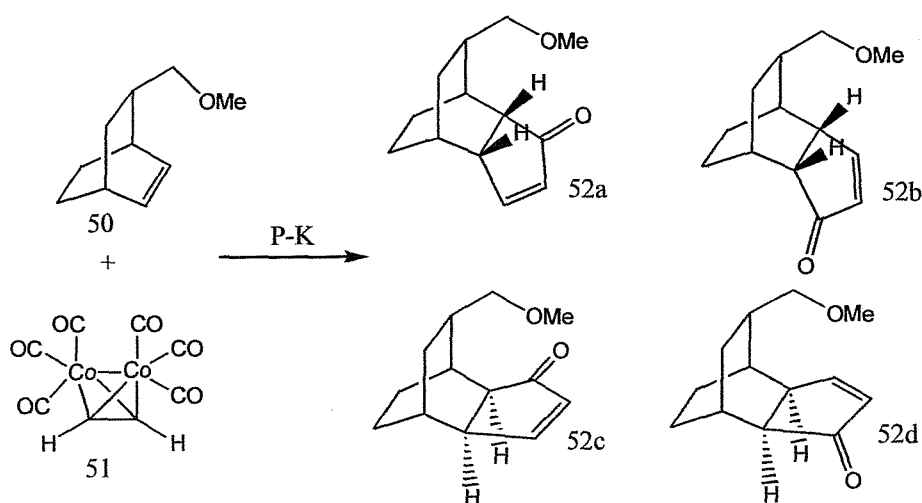


Figure 31

Analysis of the NMR spectrum of this oil showed that it comprised of a 1:1 mixture of only two components, not the four possible isomers expected. Furthermore, the chemical shifts of the two compounds, particularly for the methyl and methylene protons adjacent to the ether oxygen were very similar. This suggests that the chemical environments around the ether group were similar in the two compounds. The chemical shifts of the ether group in **52c** would be highly influenced by the proximity of the enone group. It is thus highly unlikely that **52c** was one of the observed products.

Of the three remaining isomers, **52a** and **52b** would have similar shifts for the protons around the ether group due to the *exo* orientation of the enone. Furthermore it would be difficult to explain the formation of either **52a** or **52b** without the formation of the other because of their similar energies. This evidence would suggest that **52a** and **52b** were the two isomers formed.

Due to the fact that the ether group is on the opposite face, it plays no part in controlling the orientation of attack of the cobalt species so a 1:1 mixture of **52a** and **52b** was the result.

The low yield in this reaction, although expected (Khand⁵² reported only 50% yield for the unsubstituted case), proved to be something of a problem. As well as the low yield, upon scale up the alumina column proved less and less efficient at removing cobalt residues from the product. It proved possible to oxidise the excess cobalt by heating to 80°C in toluene in air overnight. This allowed purification of the material but at the expense of a slightly reduced yield.

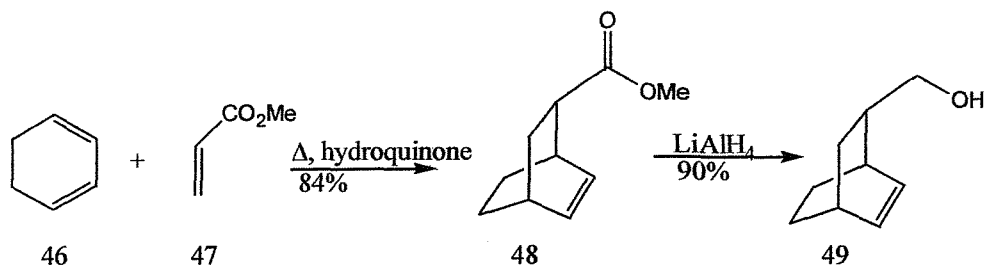
Due to these problems, only small quantities of the key enone **52** were available and this greatly affected work on the later stages of the synthesis. It was thus decided that a larger scale up project was necessary and this was undertaken using the larger scale equipment available during a placement at Zeneca PSG, Huddersfield.

3.3.3 Large scale development of key enone **52**

Scale up of the Diels Alder step was carried out in a Parr pressure reactor. A mixture of 1,3-cyclohexadiene **46**, methyl acrylate **47** and hydroquinone was placed in the reactor and degassed by three freeze pump thaw cycles. The vessel was heated to 150°C during which time the pressure rose to approx. 80 psi.

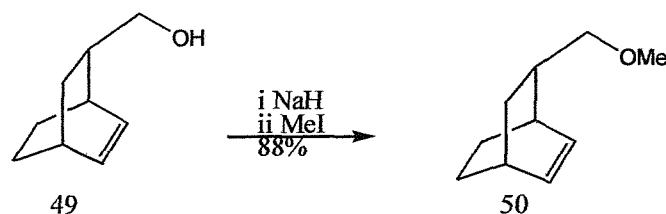
In the pressure reactor, it was possible to monitor pressure variation and as the reaction proceeded, the pressure fell as expected. The reaction was deemed to have finished when the pressure had reached a stable level (approx. 18h).

The reaction mixture was distilled under reduced pressure to give the desired ester **48** in 84% yield.



Scale up of the LiAlH_4 reduction was achieved with no new problems being encountered, however the yield was slightly reduced. This allowed the production of 75g of alcohol **49** for the study of different heteroatoms in the system.

Methyl protection of alcohol **49** was achieved as before by deprotonation with sodium hydride followed alkylation with methyl iodide. Both of these steps are surprisingly slow for a primary alcohol. This may be due to the rigid nature of the molecule causing the oxygen atom to be more sterically hindered than in an acyclic case.



Full deprotonation was estimated to have occurred when hydrogen gas was no longer generated. This being somewhat inaccurate meant that sometimes a small amount of unreacted starting material was recovered (8-10%). However mass recovery was always >95% and the desired bicyclic ether **50** was recovered in 88% yield.

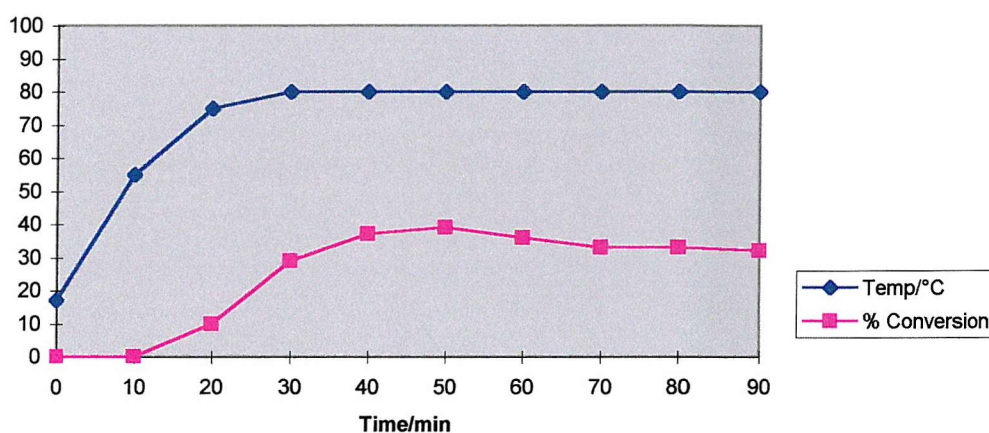
3.3.3.1 Pauson Khand Reaction

The Pauson Khand step has previously only proceeded in low yield with starting material being recovered. However, this material was not recyclable due to

contamination with unknown cobalt compounds. The product was also contaminated with unknown cobalt compounds that required repeated chromatography for removal.

Analysis of the reaction profile was attempted by GC analysis using an external standard however the results were not useful due to large errors. These were thought to be due to undissolved solids in the reaction mixture and inaccuracies in the sample volume measurement. It was possible to estimate conversion by comparison of product and starting material peaks in the chromatogram and assumption of 100% efficiency.

Pauson Khand Reaction Profile



From these results, it may be seen that the reaction does not begin until the temperature rises to above approx. 70°C. A colour change was observed at this point from dark red to almost black. Conversion was seen to proceed rapidly to about 30-40% before slowing. From this observation it may be inferred that one of the starting materials may be decomposing faster than it is reacting. It was thus decided to try addition of the less stable cobalt compound slowly to a hot solution of the alkene. In this way the recovered yield was increased from 35% to 48%. Increased dilution and elevated temperature were also tried as a method of altering reaction and decomposition rates but were shown to have no effect.

The other problematic aspect of this reaction was the purification of the product. Chromatography (Neutral Alumina, 50% ether/hexane) removed unreacted starting materials and inorganic impurities but a small amount of highly coloured cobalt impurities were left. The previous method of removal of these impurities was to heat a solution of the compound in toluene to 80°C overnight. This decomposed the cobalt

residues which were then easily removed by chromatography on alumina. This however had the disadvantage of lowering the yield.

As organocobalt complexes are known to be susceptible to oxidation and the previous technique appears to be essentially an air oxidation, a series of chemical oxidants were tried in an attempt to avoid this loss in yield. Oxygen gas, hydrogen peroxide, N-methyl morpholine N-oxide and ceric ammonium nitrate were all tried but with no success.

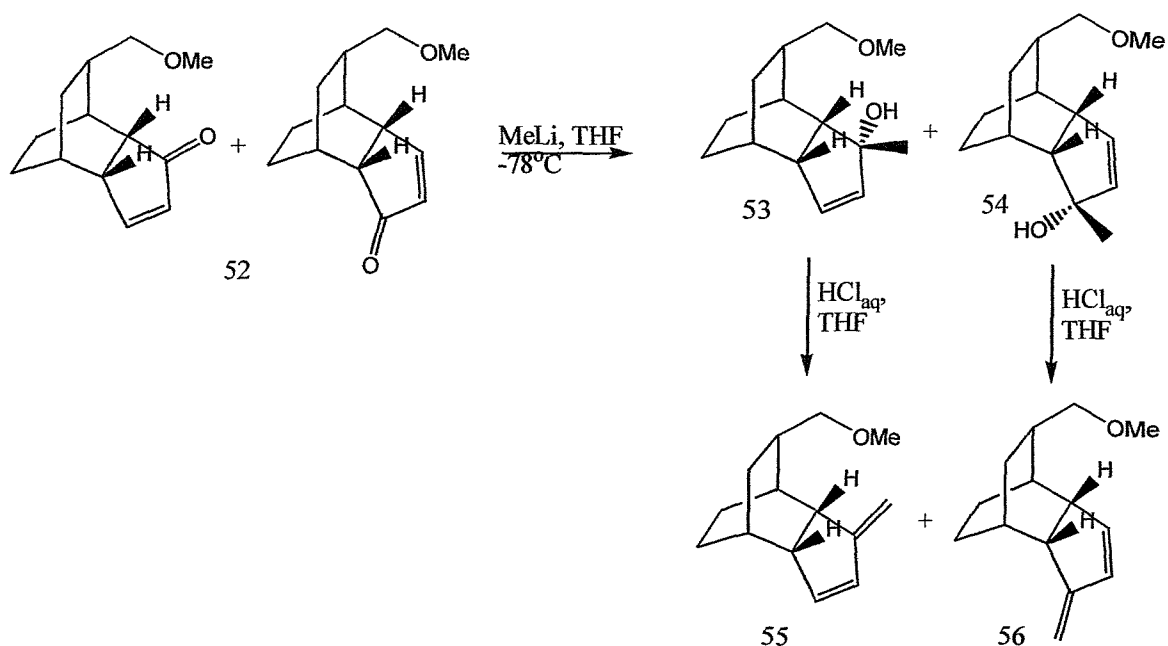
In light of this failure, some attempts were made to use a solvent to extract the cobalt residues. After many attempts, it was discovered that the enone **52** was soluble in 50% methanol/water whereas a significant portion of the coloured cobalt impurities was not. Extraction into this solvent system followed by filtration and removal of solvents *in vacuo* removed most of the coloured impurities. Kugelrohr distillation of material purified in this way gave the desired product as a colourless oil with negligible loss in yield.

With a significant quantity of both key intermediates, enone **52** and alcohol **49** now available it was possible to continue with the synthesis.

3.3.4 Alkylation and elimination

The simplest way to form a cyclopentadienyl ring from an enone would be to alkylate the carbonyl group in a 1,2 fashion and then eliminate the resultant tertiary alcohol. The elimination of tertiary allylic alcohols is well known⁵⁶ and proceeds rapidly due to the stabilised tertiary cation formed in the mechanism. The alkyl group would also be of benefit in the ligand design, as it would form a roof type structure as discussed in chapter 1 and may improve any selectivity displayed by the final complex. Provided the alkyl group had no inherent asymmetry, the planar symmetry of the cyclopentadienyl ring would remain unaltered. However, it would cause added problems with diastereoisomers.

Treatment of the mixture of enones **52** with methyl lithium in THF at -78°C gave only two isomers cleanly in 63% yield as shown by the loss of enone resonances in the ¹H NMR. It was possible to separate the two alcohols by chromatography on basic alumina to give a 2:1 ratio of isolated products. **53** and **54** are proposed structures for these compounds, the ethano bridge effectively blocking the rear face of the ketone and forcing attack to come exclusively from the front face.



Scheme 24

Elimination of these alcohols was achieved with aqueous HCl in THF. Both isomers gave mixtures of compounds with signals in the ^1H NMR spectrum characteristic of terminal alkenes. This observation was consistent with the fact that the cyclopentadiene had not been formed but the elimination had proceeded to give the exocyclic double bond compounds **55** and **56**.

Molecular modelling of these compounds⁵⁷ showed that the exocyclic compounds had similar energy to the cyclopentadiene compounds so an attempt was made to isomerise them, in the hope that the exocyclic compound was only the kinetic product.

Unfortunately attempts to cause isomerisation of the double bond into the ring with acid catalysis all failed. No change in the ^1H NMR spectrum was observed even after extended heating. From these results, it must be assumed that the relief in ring strain gained by the exocyclic compound has made this the favoured product.

This factor severely limits the choice of nucleophile for addition to the ring. All nucleophiles with α -protons could potentially give the exocyclic double bond upon acid catalysed elimination so our choice was effectively limited to phenyl and *tert*-butyl groups.

In order to avoid encountering further problems of this nature it was decided to follow two paths.

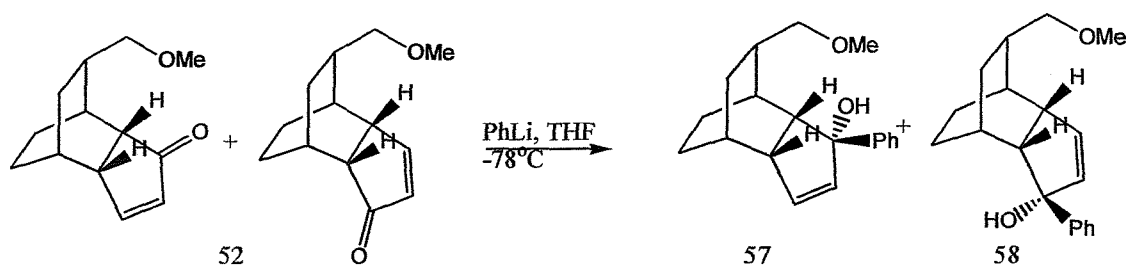
- 1 To attempt the alkylation/elimination route with a nucleophile bearing no α -proton i.e. phenyl.

- 2 To simply reduce the enone to the secondary alcohol before elimination, thus avoiding problems with both exocyclic eliminations and separation of diastereoisomers.

3.4 Synthesis of Phenyl Substituted Ligands

In light of the previous results, the most suitable group for alkylation appeared to be a phenyl group. Not only does a phenyl group eliminate the problems associated with exocyclic elimination, the extra stabilisation afforded by the phenyl to the tertiary cation should make the subsequent elimination more facile.

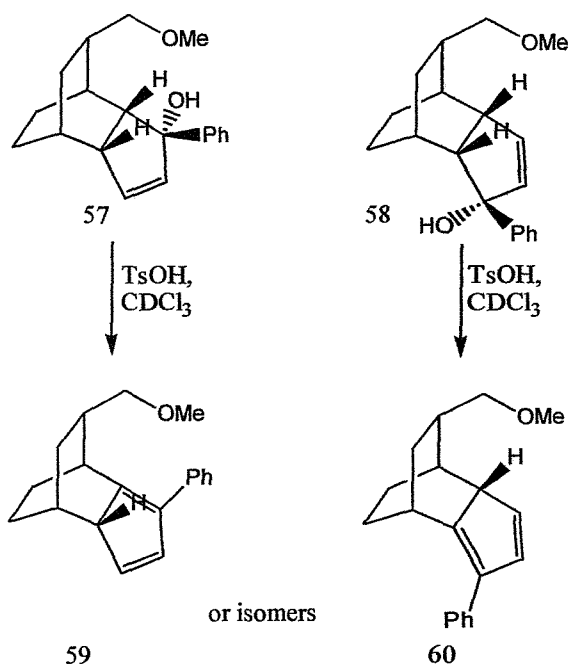
Treatment of a mixture of enones **52** with phenyl lithium in THF at -78°C followed by protic workup gave a mixture of two alcohols **57** and **58** as a colourless oil. These tertiary allylic benzylic alcohols were expected to be considerably less stable than their secondary alcohol analogues, due to the stability of the tertiary carbocation formed on elimination of water, and so were handled in base washed glassware.



Separation of the isomers was achieved by careful chromatography on basic alumina in 83% overall yield. When separated, it was discovered that both compounds were in fact white crystalline solids. Single crystal X-ray analysis (see Appendix 4) revealed the relative stereochemistry of **58**, in agreement with the expected structure of these compounds.

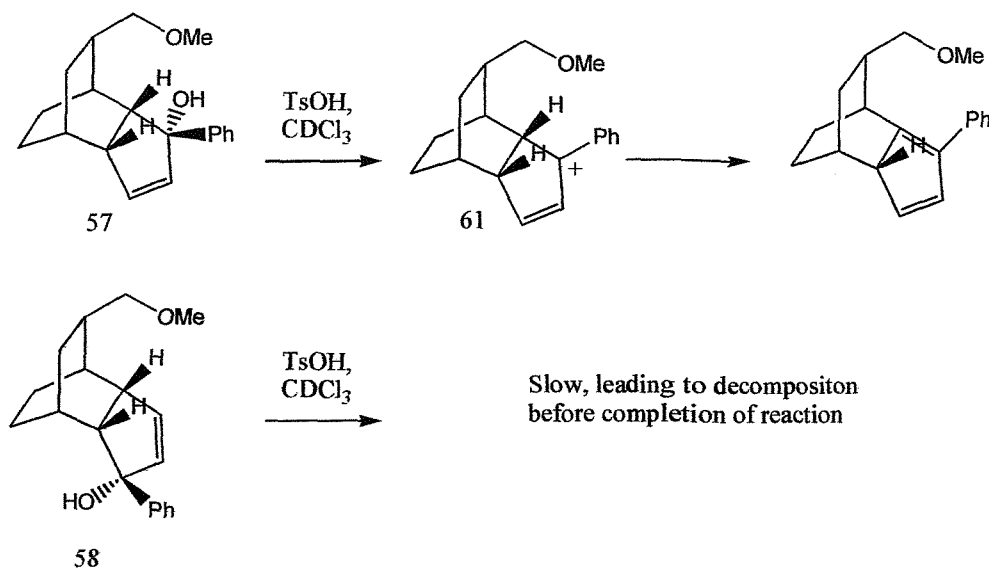
However, despite expectations, in practice these alcohols proved to be rather more stable. Treatment of ethereal solutions of these alcohols with silica, alumina or even acidic ion exchange resin caused no change even after stirring for up to 48 h. In light of this discovery it was possible to improve the purification step by changing the solid phase used for chromatography from basic alumina to flash silica. The improved resolution using this solid phase allowed much faster preparation of alcohols **57** and **58**.

Treatment of either of the two alcohols with a catalytic amount (~5 mg) of solid *p*-toluene sulphonic acid in ether did indeed cause elimination to take place, as revealed by TLC and ^1H NMR, but the reaction times and conversions were variable. This was thought to be due to the low solubility of the acid in ether as during the reaction a brown sludge was formed at the bottom of the vessel. Yields were also extremely low, possibly due to the fact that the product cyclopentadiene would be expected to be unstable to acidic conditions. As the reaction time could not be accurately judged, considerable decomposition of the product was observed.



Changing the solvent from ether to chloroform improved the reproducibility of the reaction, presumably due to all the acid being in solution.

In order to shed some light on this problem a study of the reaction profile of this elimination was carried out by NMR analysis, the reaction being performed in deuterio chloroform. A surprising difference in reactivity was observed between the two alcohols, Scheme 25.



Scheme 25

When treated with *p*-toluene sulphonic acid, alcohol **57** was rapidly (< 5 min) transformed to a new compound with two ^1H signals in the 5.0-6.0 ppm region of the ^1H NMR spectrum. Flushing the reaction mixture through basic alumina to remove acid at this stage and removal of solvent afforded a different material but one with ^1H signals consistent with an isomer of the initially formed cyclopentadiene. Longer treatment (~4 h) of the solution saw gradual conversion of the first product to the final product. Prolonged treatment (~24 h) resulted in conversion to a material with aromatic signals but no signals in the cyclopentadiene region. Figure 32

Treatment of **58** in the same manner afforded a similar elimination product however the rate was greatly reduced. After 1 h, there was still remaining starting material. Further reaction time showed that decomposition of the product began before the complete consumption of starting material. Consequently, yields in this reaction were low and the purity of the product poor.

This remarkable difference in reactivity may be explained by the orientation of the methyl ether group. Since the reaction must follow an $\text{S}_{\text{N}}1$ mechanism, the rate-determining step is the elimination of H_2O to afford the cyclopentadienyl cation **61**. In **59** the proximity of the oxygen may stabilise the cation and thus accelerate this step.

Complexation reactions to titanium or zirconium using material obtained in this way gave no desired complexes. Due to the difficulties involved in this elimination reaction, it was decided to discontinue this line of research.

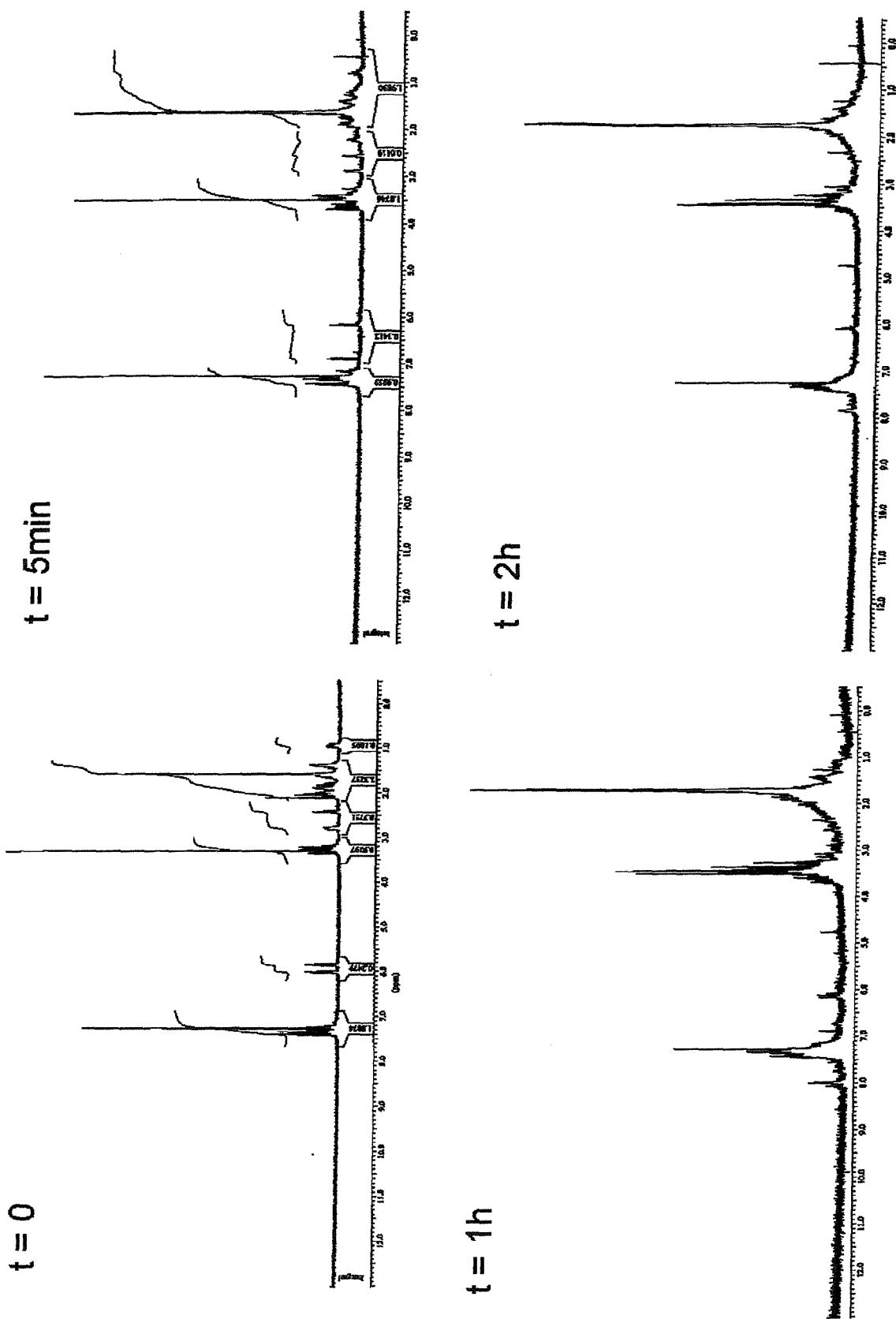
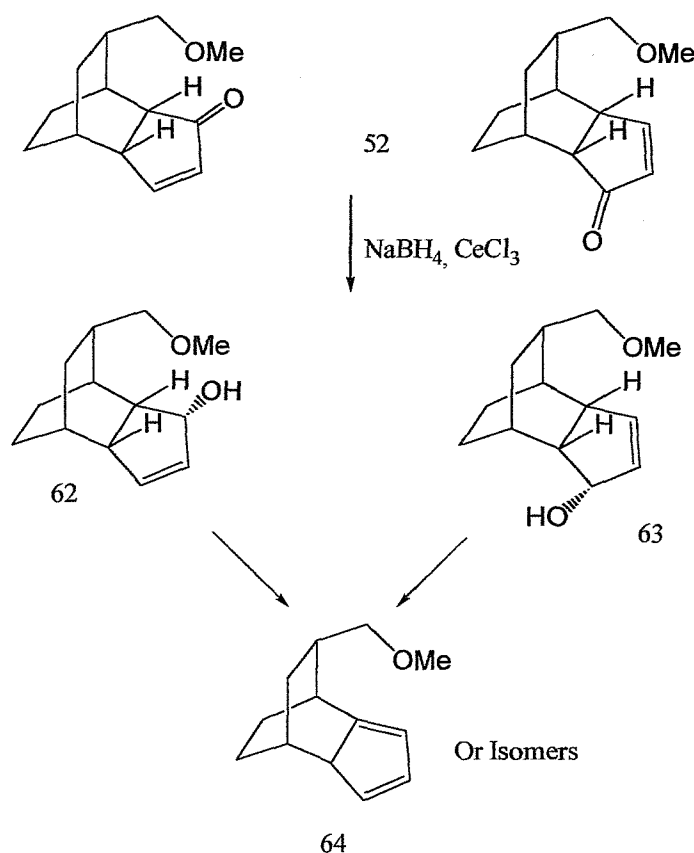


Figure 32

3.5 Preparation of disubstituted cyclopentadienyl ligand.

The second solution to the exocyclic elimination problem is the avoidance of any alkyl group at this position. Conversion of enone **52** to the disubstituted cyclopentadiene was envisaged by the reduction to the secondary allylic alcohols **62** and **63** followed by elimination.

Preparation of alcohols **62** and **63** was performed following the methods developed by Luche.^{58,59} Reduction was achieved by the treatment of a mixture of enones **52** with sodium borohydride in the presence of cerium chloride heptahydrate to effect almost exclusively 1,2 reduction. A 2:1 mixture of the desired alcohols **62** and **63** was obtained in 80-90% yield, however it was not easy to separate the mixture by chromatography. This was not a problem as both the isomers, when eliminated, would be expected to give the same product, Scheme 26.



Scheme 26

3.5.1 Acid/base catalysed elimination of **62** and **63**

Elimination of secondary allylic alcohols **62** and **63** however, proved difficult.

Treatment of a solution of **62** and **63** in ether with *p*-toluene sulphonic acid monohydrate afforded a complex mixture from which it was impossible to isolate any of the desired product.

Excellent yields have been reported for the elimination of similar systems using *p*-toluene sulphonic acid monohydrate in toluene.⁶⁰ However, use of this method within the group on secondary alcohols of this type has given variable and irreproducible results. NMR experiments on **63** and **64** in *d*-8 toluene using 10 mol% of *p*-toluene sulphonic acid monohydrate showed the appearance of signals in the 5-6 ppm region and the appearance of a second OMe peak, consistent with the partial formation of **64**. The product was not clean and the acid did not fully dissolve, forming a brown sludge on the wall of the NMR tube and reducing the resolution of the spectrum. Repetition of this procedure on a large scale again resulted in the formation of brown sludge and following aqueous work up NMR showed the same signals contaminated with unidentified impurities. It proved impossible to purify this material by chromatography and attempted metallation under standard conditions (see Chapter 2) gave no desired complex.

Biphasic conditions using aqueous HCl and hexane with tetra-butyl ammonium chloride as phase transfer catalysts gave a complex mixture.

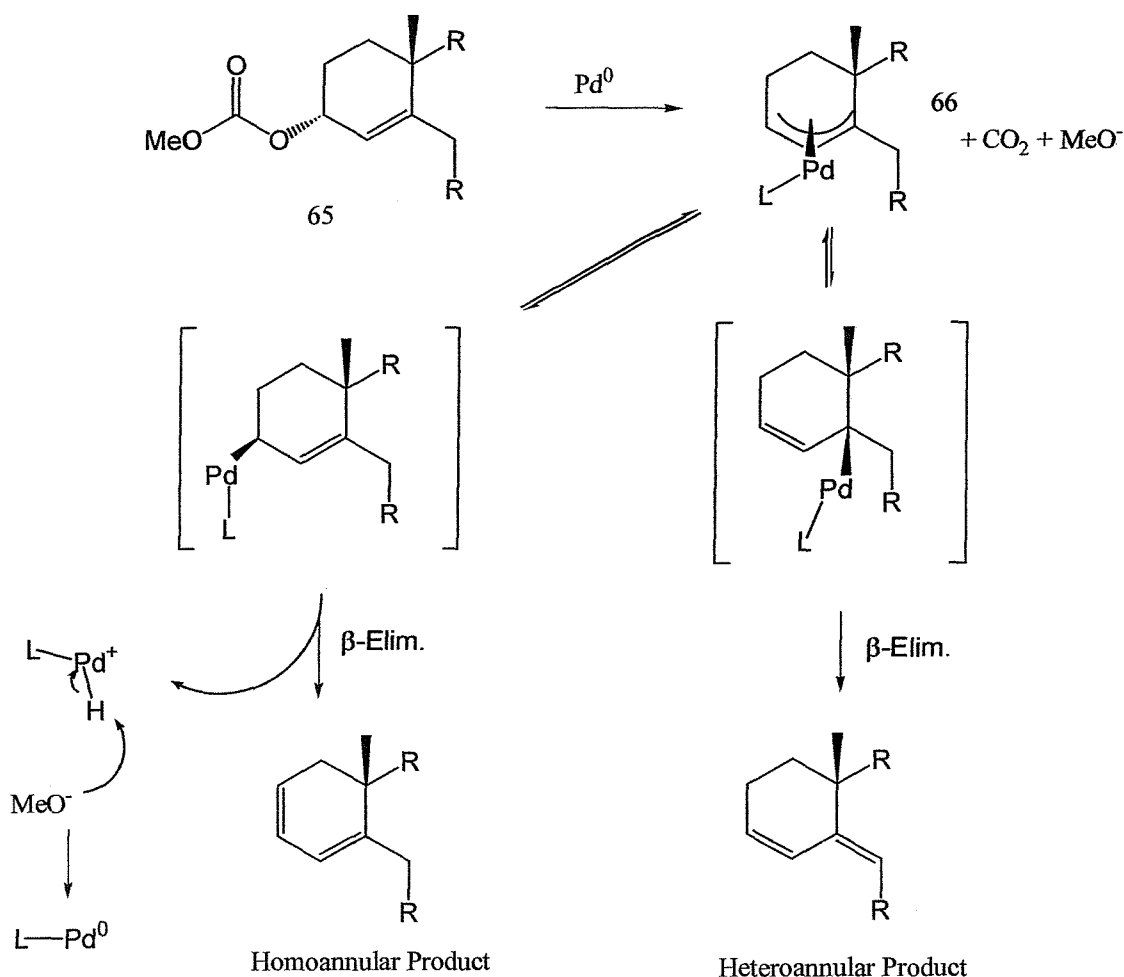
Treatment of **63** with methane sulphonyl chloride and triethylamine in DCM at 0° gave a mixture of two compounds, suspected to be the mesylate and the chloride. Treatment of this mixture with excess triethylamine caused no change. Treatment of the same mixture with neat DBU gave a black tar, which was impossible to purify.

In conclusion, both the acid and base catalysed elimination of secondary allylic alcohols to form cyclopentadienes has proved very difficult. Although success has been achieved within the group in the acid catalysed elimination of tertiary allylic alcohols, secondary alcohols have always given irreproducible results. It is thus desirable to develop neutral conditions for this reaction, which may allow the elimination to proceed in tolerable yields.

3.5.2 Pd⁰ catalysed elimination of 62 and 63

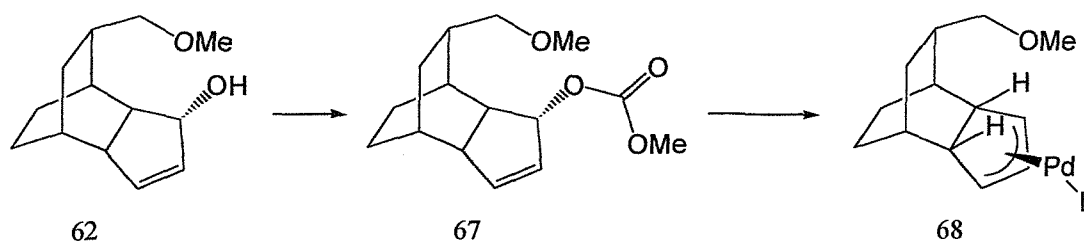
As a consequence of the poor results reported above for the elimination of secondary alcohols a search for a better method was instigated. A literature search revealed that a palladium catalysed elimination of allylic carbonates in decalin and steroid systems has been reported.^{61,62} This methodology gives both homoannular and heteroannular dienes. Notably 1,3 cyclohexadienes may be formed in this manner, under neutral conditions. If this reagent could work to form 1,3-cyclopentadienes then a novel and useful method for the preparation of potential ligand systems would result.

The proposed mechanism was the conversion of the carbonate **65** to a π -allyl palladium species **66** with inversion, followed by β -hydride elimination to afford the relevant diene, Scheme 27. The methoxide anion formed in the first step acts as a base to regenerate the Pd⁰ catalyst.



Scheme 27

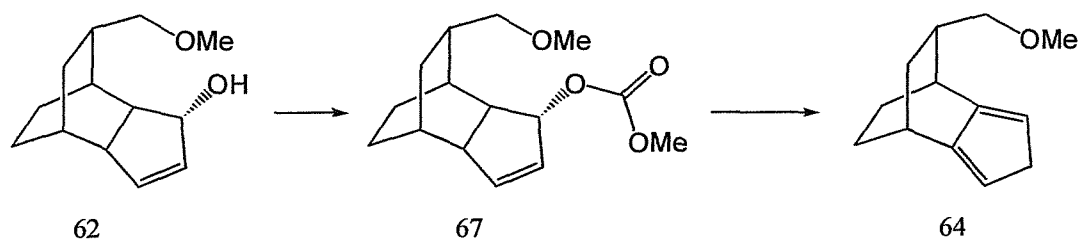
Conversion of alcohol **62** or **64** to the carbonate **67** followed by treatment with palladium should give a complex **68** in which the palladium is syn to the hydrogen which must be removed and is thus perfectly set up for the elimination.



Scheme 28

In this case there is no possibility of the elimination occurring to form an exocyclic double bond as the only substituents in the ring would lead to highly strained bridgehead alkene compounds.

Treatment of **62** and **63** with pyridine and methyl chloroformate in DCM at 0° gave the desired product **67** in 77% yield. Treatment of this compound with 10 mol% palladium (1:1 Pd(OAc)₂/*n*-Bu₃P⁶²) in THF at reflux overnight gave the desired product **64** in 90% yield.



Analysis of the complex NMR spectra proved difficult however GCMS analysis revealed the product of this reaction to be a mixture of two compounds in a 73:26 ratio, both with a molecular ion at $m/z = 190$ (M^+).⁶³ This evidence strongly suggests that the product was a mixture of double bond isomers of compound **64**, Figure 33.

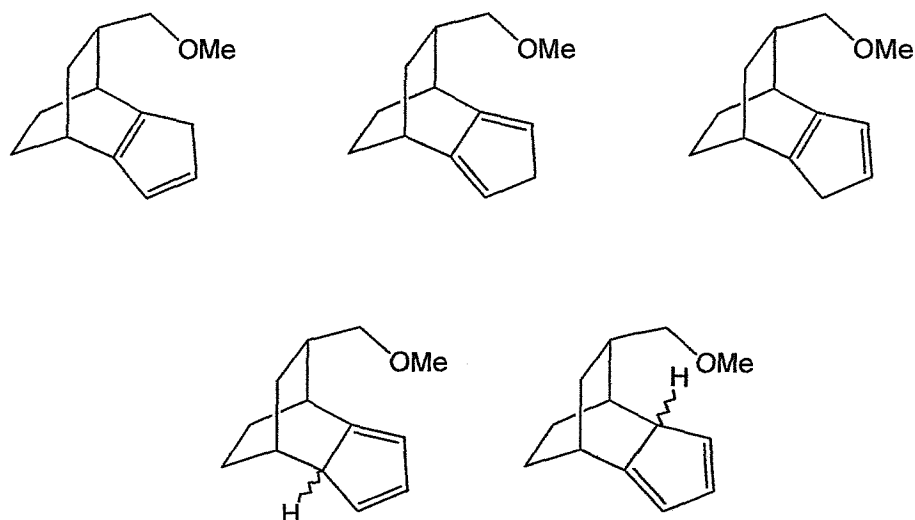
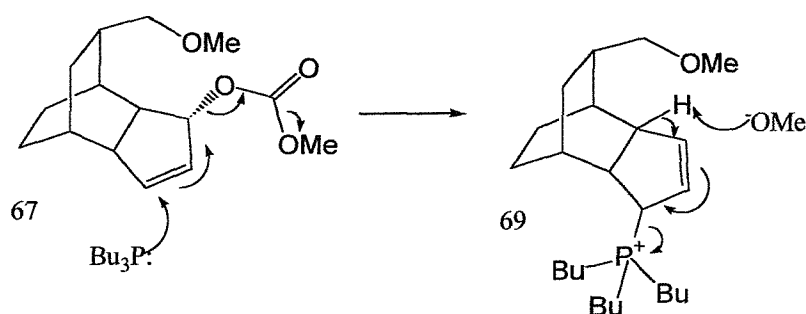


Figure 33

Separation of these isomers did not prove possible but as deprotonation of all isomers would generate the same anion, the product was used without further purification.

It was possible that the reaction may be catalysed by tributyl phosphine alone, *via* the phosphorus compound **69**, Scheme 29.



Scheme 29

Experiments under the same reaction conditions only without the presence of palladium were carried out to test this hypothesis. Without palladium it was not possible to detect any conversion of the starting material either by TLC or HPLC. It is thus clear that palladium must play a catalytic role in the reaction mechanism.

With this new and powerful method of forming cyclopentadienes from secondary 2-hydroxycyclopentanes under mild conditions, it was possible to generate significant quantities of ligand **64**. As this compound was believed to be unstable towards cycloaddition to itself, it was stored frozen in a benzene solution at -5°C .

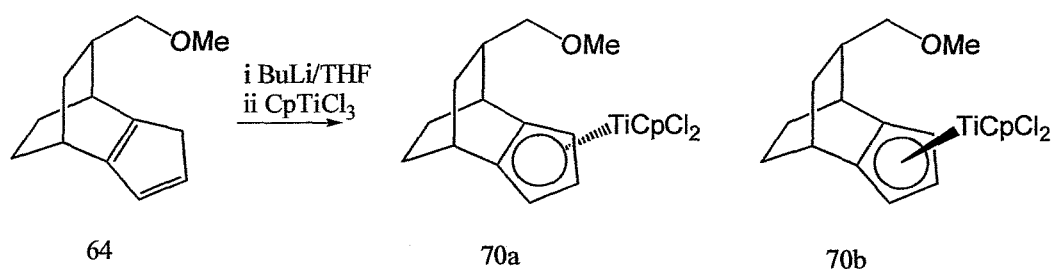
3.6 Synthesis of novel group IV complexes

With the ligand synthesis developed to such an extent that reasonable quantities of ligand **64** were available, attention was focused on the preparation of novel complexes utilising this ligand. The metals chosen for the first attempts at complexation were titanium zirconium and rhodium.

3.6.1 Titanium complexes

The standard conditions were employed for the formation of C₁ titanocene complexes.^{15 39} The anion of the cyclopentadienyl ligand was formed by treatment with *n*-butyl lithium in THF at low temperature. This anion was then added to a solution of the cyclopentadienyl metal halide.

Treatment of cyclopentadiene **64** with *n*-butyl lithium in THF at -78°C with exclusion of light gave a pale yellow solution that was allowed to warm to room temperature. Upon addition of this anion to a THF solution of CpTiCl₃ at -78°C, a deep red colour was developed. The mixture was stirred overnight after which time the solvent was removed *in vacuo*. ¹H NMR performed on a small sample showed signals in the regions expected for the desired products **70** however due to other impurities and overlapping signals the ratio of diastereoisomers could not be determined from the crude mixture, Scheme 30.



Scheme 30

Column chromatography on neutral alumina caused decomposition of the product and concurrent loss of the red colour.

Extraction into 1:1 toluene / hexane and cooling to -5°C precipitated a red solid which was shown by NMR spectroscopy to be one of the desired complexes **70**, as a single isomer.

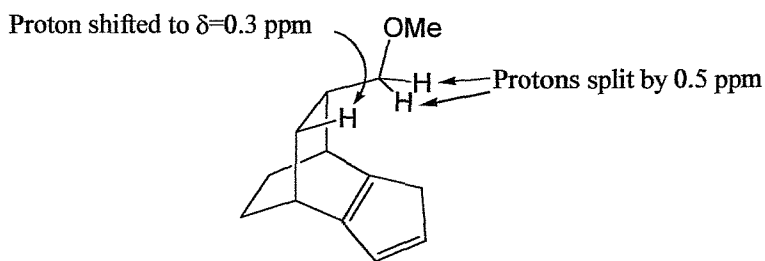
When the experiment was repeated with the addition carried out at room temperature, identical results were obtained.

3.6.1.1 Facial selectivity in titanium complexation

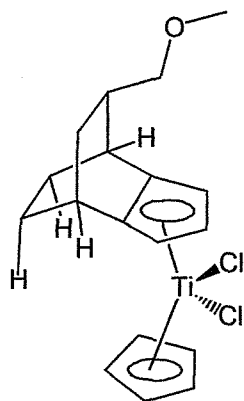
It was not possible to determine a ratio of diastereoisomers from this result as the purification procedure could selectively precipitate one isomer over the other. As the yield was low, it is only possible to say that this complex was formed, not if it was formed exclusively or even only in preference to the other isomer.

A number of NMR experiments were carried out in order to ascertain to which face of the cyclopentadienyl ring the titanium moiety was bound. ⁶⁴

Upon consideration of the ¹H results a number of signals stand out. Firstly, there is a ddt at 0.3 ppm. This signal arises from one of the protons on the ligand (usually at around $\delta=2$) being shifted downfield by an extremely shielding environment. This does not reveal much in itself as an unusually shielded region may arise either from the ring current on the reverse side of a cyclopentadienyl ring or an electron rich orbital on the metal centre. In addition, the two CH_2OCH_3 protons are split by almost 0.5 ppm. (The CH_2 protons were assigned by 2D C-H correlation). This was in agreement with the previous data, in that there is an area of anomalous shielding on the same face as the OMe group.



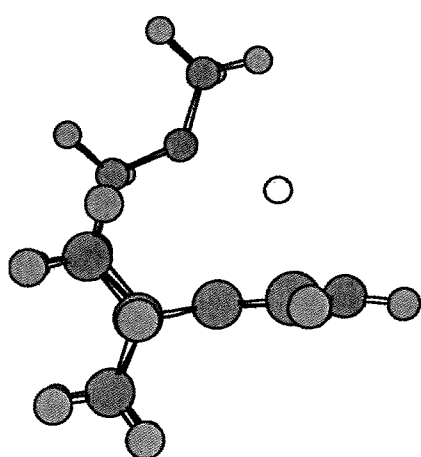
Irradiation at the frequency corresponding to the C_5H_5 singlet caused a nuclear Overhauser enhancement in four proton signals at shift 3.2, 2.8, 1.8 and 1.6 ppm. None of these signals corresponds to either the CH_2OCH_3 protons or the 0.3 ppm proton. Consequently, the CH_2OCH_3 group must be on the opposite face to the metal, the anomalous shift being due to the ring current present on the opposite face of the cyclopentadienyl ring. The four protons displaying an nOe must correspond to the four protons indicated below, Figure 34.



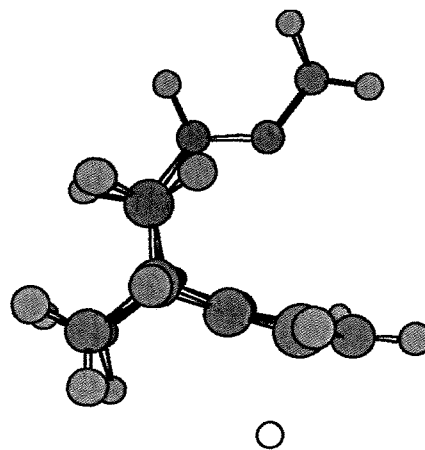
C_5H_5 shows nOe to marked protons

Figure 34

The results show that regardless of temperature, the metal became attached to the face of the cyclopentadienyl ligand opposite to the pendant oxygen linker. This result may be rationalised by considering the lithium anion species. Molecular modelling⁶⁵ shows that the anion with lithium attached to the same face as the oxygen is stabilised by 38.11 kJ mol⁻¹ relative to the opposite face.



$\Delta H_f^\ddagger = -27.99$ kcal/mol



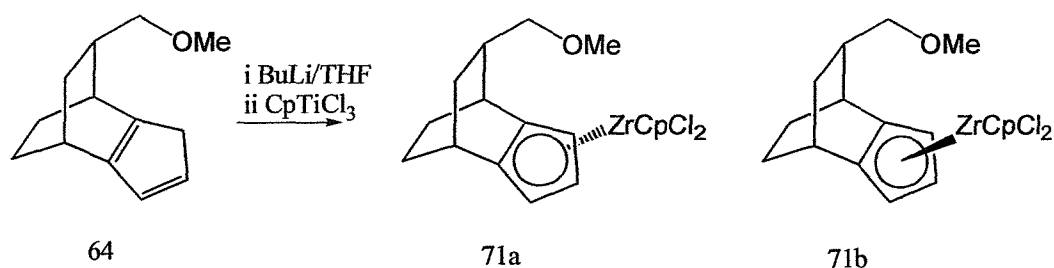
$\Delta H_f^\ddagger = 10.12$ kcal/mol

Thus, the majority of the anion will exist in this conformation. Reaction of this anion may occur with either inversion or retention¹⁴ but as the OMe linker provides a steric block on the lithiated face, this transition state may be destabilised enough to cause the inversion pathway to dominate.

However as Paquette has shown¹⁴, the relationship between the stability of anions and facial control of metallation with group IV metal halides is complex. Composition is dependent on a number of factors such as temperature and concentration with aggregates often being formed. Therefore, further work on the structure of this anion is necessary to confirm this theory.

3.6.2 Zirconium complexes

Attempts to form the zirconium analogue were performed using standard conditions for the formation of zirconocenes. The anion of **64** was formed under the same conditions as before. Treatment of the cyclopentadiene with *n*-butyl lithium in THF at -78°C with exclusion of light gave a pale yellow solution that was allowed to warm to room temperature. Upon addition of this anion to a solution of $\text{CpZrCl}_3 \cdot 2\text{THF}$ at -78°C a pale greenish-yellow solution was obtained that was stirred overnight. ^1H NMR showed signals in the 5.5 -6 ppm region, characteristic of the desired products **71** however, as in the titanium case, the spectrum was messy and a ratio of isomers could not be determined, Scheme 31.



Scheme 31

This compound proved much more difficult to handle than the titanium analogue. Purification to a single compound was not possible due to rapid decomposition both in air and in light. Extraction into 1:1 toluene / hexane followed by removal of solvent gave a greenish solid which ^1H and ^{13}C NMR revealed to be mainly one of the desired compounds, contaminated with unidentified impurities, possibly other isomers.

Due to its instability it was not possible to determine which face the zirconium was attached to by direct means. However, comparison of the ^{13}C spectra showed that the main product from the zirconium reaction had an almost identical pattern of resonances as the titanium compound. Previous experience within the group has shown that analogous zircono- and titanocenes display almost identical ^{13}C spectra.^{40 15 7}

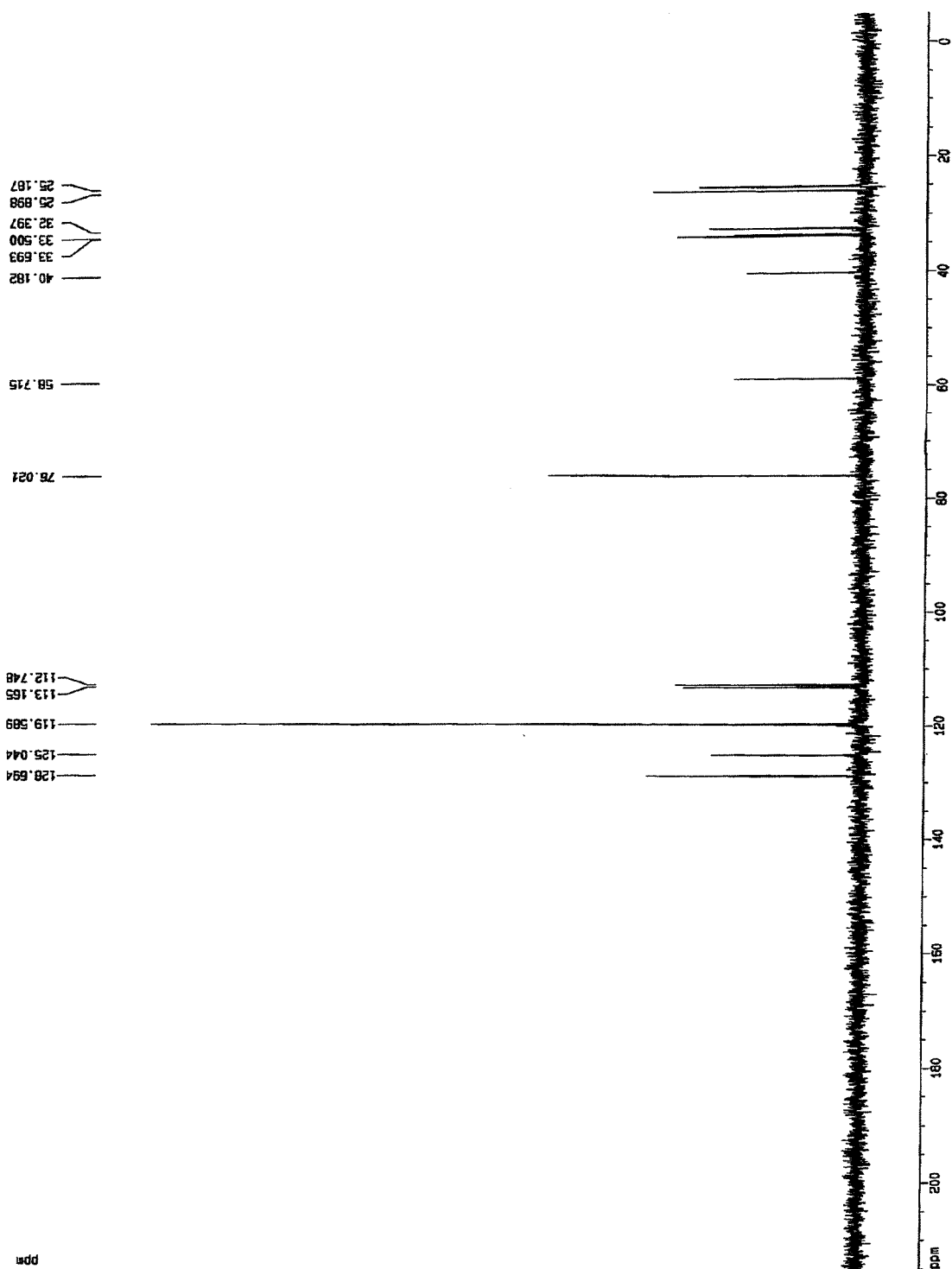


Figure 35 ^{13}C NMR spectrum of 70

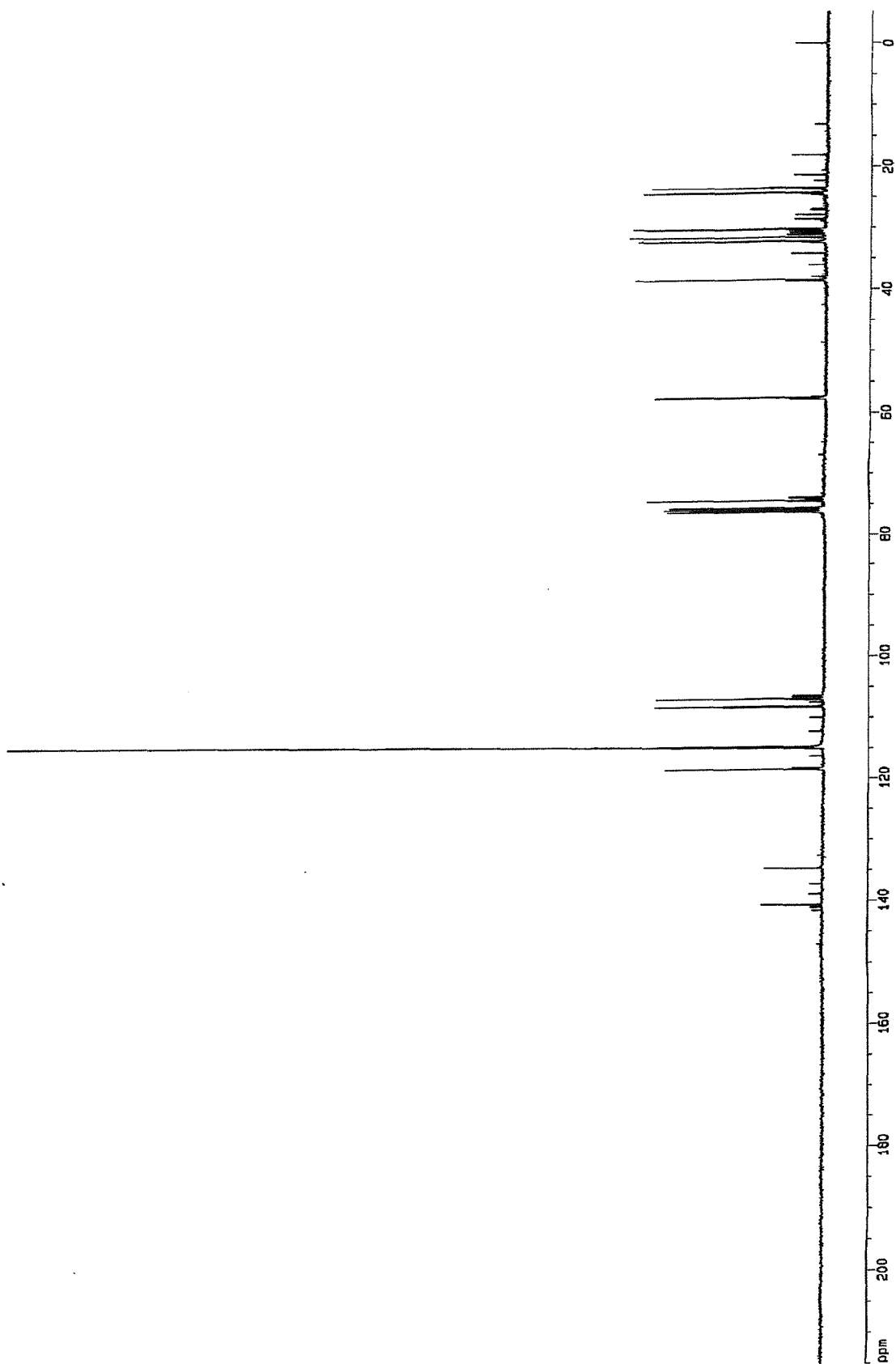


Figure 36 ^{13}C NMR spectrum of 71

Furthermore analysis of the somewhat messy ^1H spectrum showed a 1-H multiplet at 0.3 ppm, again almost identical to the titanium analogue and presumably due to the shielding effect of the electron density on the reverse of the cyclopentadienyl ring, Figure 37. From this evidence, it may be inferred that the zirconium was bound to the same face of the cyclopentadienyl ring as the titanium analogue.

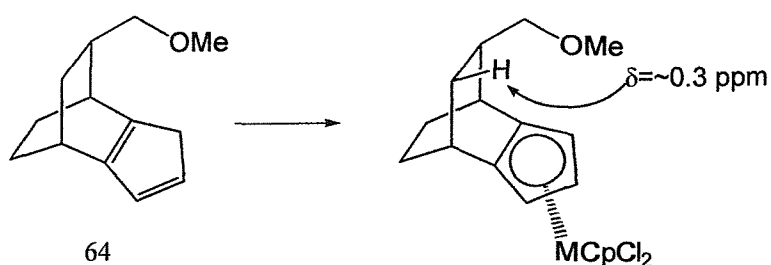


Figure 37

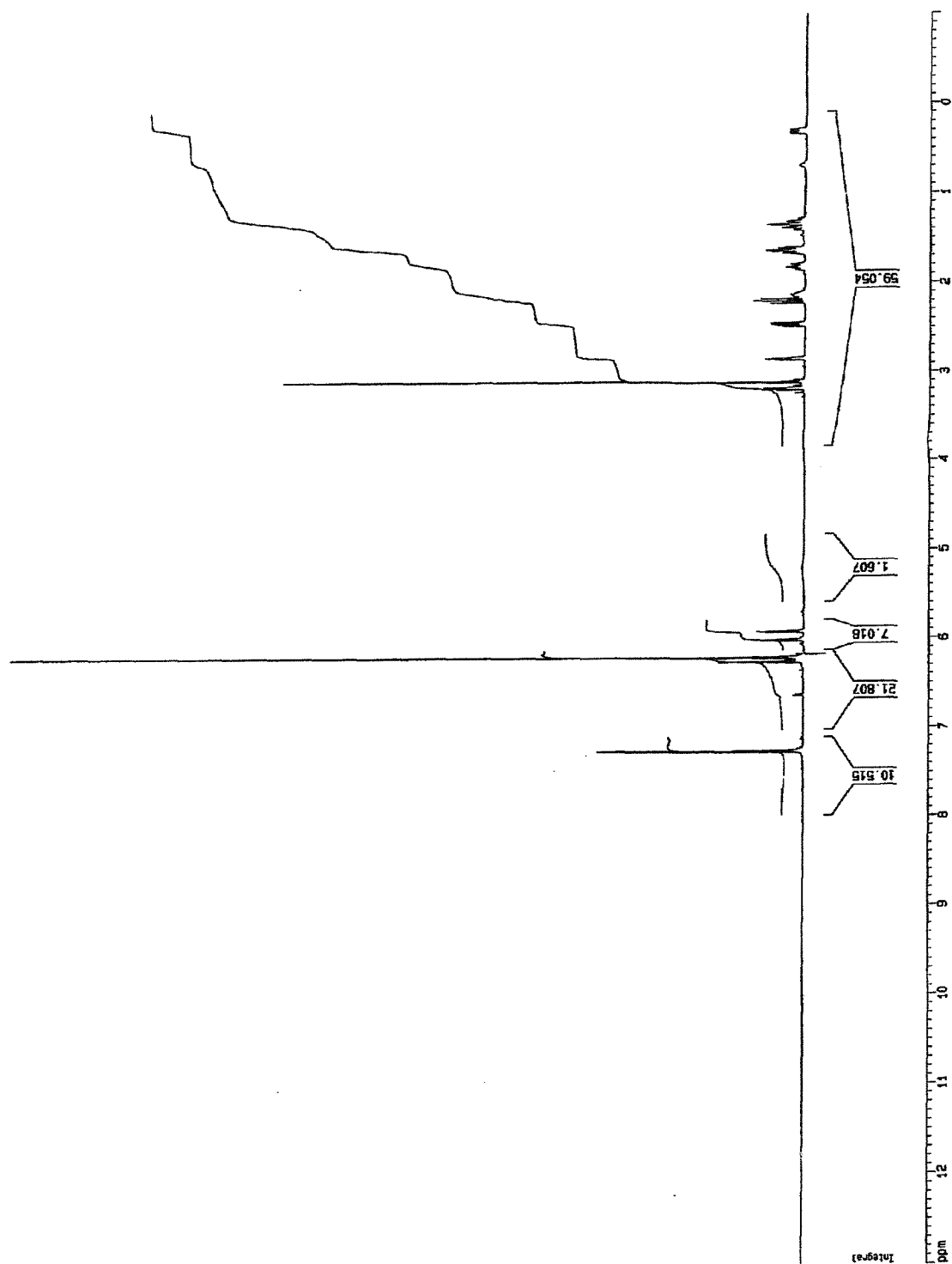


Figure 38 ^1H NMR spectrum of 70

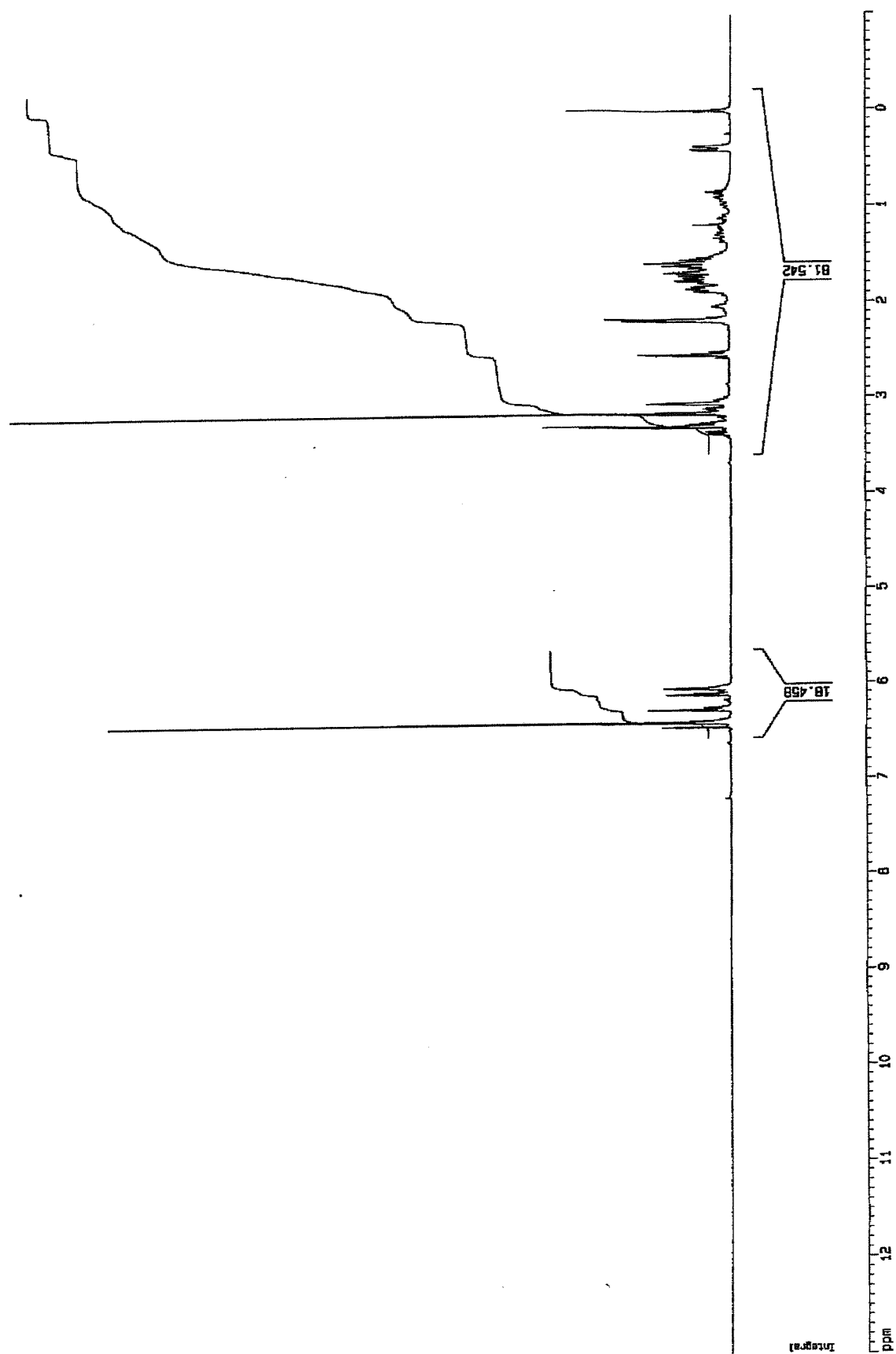


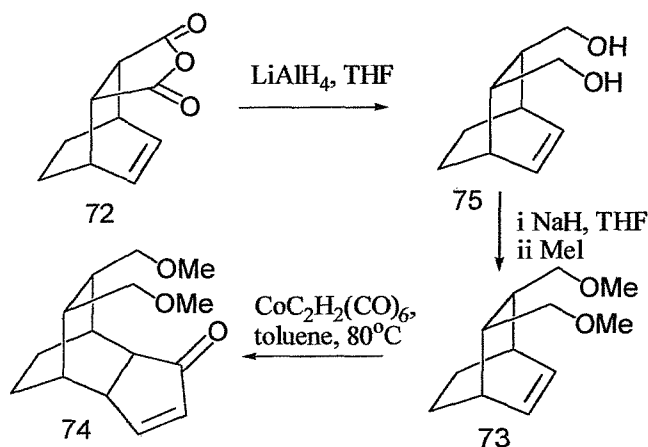
Figure 39 ^1H NMR spectrum of 71

3.7 Synthesis of tridentate methoxy linker ligands

It is a simple matter to extend the methodology of the previous sections to the synthesis of a tridentate dimethoxy cyclopentadienyl species. If two identical heteroatom linkers were suspended from the [2,2,2] bicyclic backbone then the resultant symmetry would greatly simplify the synthesis of such compounds.

Preparation of dimethoxy substituted ligands was envisaged by the scheme outlined below. Diels Alder cycloaddition of 1,3-cyclohexadiene to maleic anhydride affords bicyclic product **72**.⁶⁶ Subsequent reduction with lithium aluminium hydride⁶⁷ and methyl protection should give bicyclic alkene **73** which should undergo thermal Pauson Khand reaction with acetylene dicobalt hexacarbonyl to give enone **74** which may be elaborated to various cyclopentadienes.

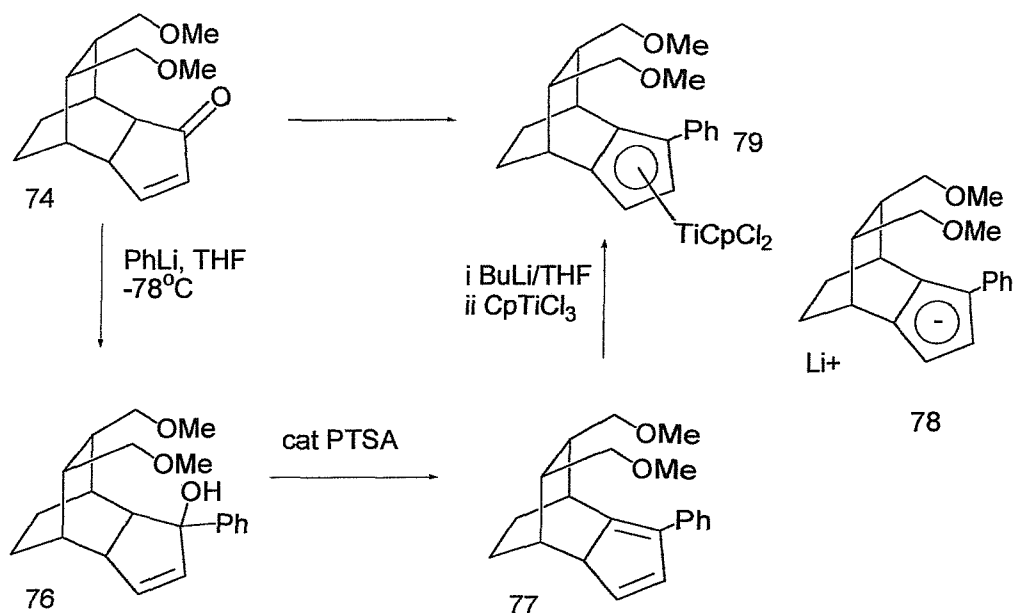
Bicyclic diol **75** was prepared in a two step procedure according to the methods of Avenati and Stockman.^{67,66} Treatment of diol **75** with sodium hydride in THF overnight followed by addition of methyl iodide gave dimethoxy compound **73** in 74% yield.



Treatment of **73** with dicobalt acetylene hexacarbonyl in toluene at 80°C for 18 h gave the tricyclic enone **74** in 32% yield. As the [2,2,2] backbone contains no asymmetry, only a single racemic compound was produced.

Conversion of enone **74** to a cyclopentadienyl ligand was achieved by alkylation followed by acid catalysed elimination.

Treatment of enone **74** with phenyl lithium at -78°C afforded tertiary alcohol **76** in 98% yield. Due to the potential acid sensitivity of this compound and the next one in the synthesis, they were used without further purification.

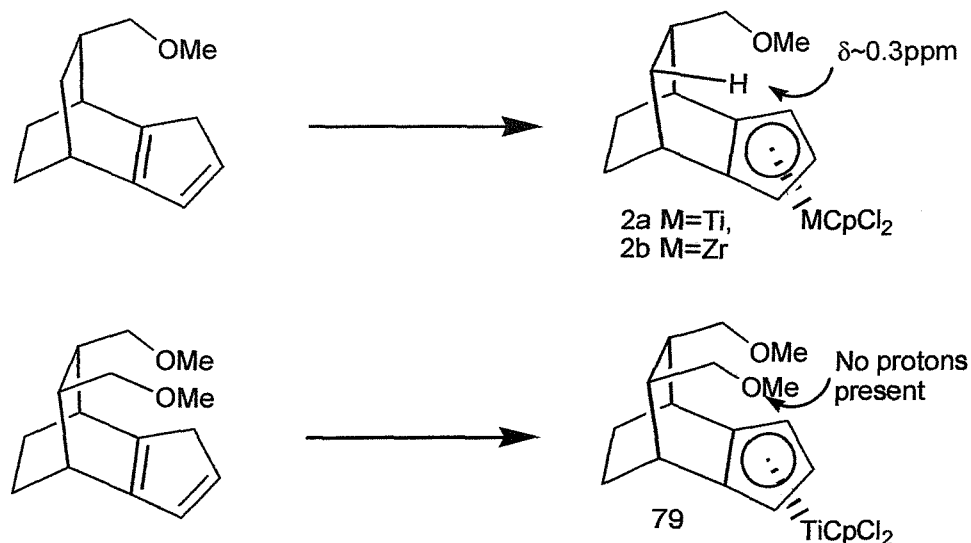

Scheme 32

Treatment with a catalytic quantity of *p*-toluene sulphonic acid in ether for 7 h caused elimination of alcohol **76** to give cyclopentadiene **77**. The product was purified by passing through a pad of basic alumina to remove any acid before the solvent was removed *in vacuo*. The residue was dissolved in THF and treated with *n*-butyl lithium to afford the lithium salt **78**.

Upon addition of this anion to a solution of CpTiCl₃ at -78°C, a deep red colour was formed. NMR analysis of a small sample of the mixture showed a number of signals consistent with formation of the desired titanocene **79**. However, due to broad and overlapping signals it was not possible to obtain a ratio of diastereoisomers.

Removal of solvent *in vacuo* afforded a dark red residue, which was subjected to column chromatography. A dark red substance was obtained which was shown to be a single compound by NMR.

It was not possible to obtain conclusive evidence for which face the titanium was attached to. However by analogy with previous examples it was possible to derive some information. Any protons on the reverse face of the cyclopentadienyl ring have previously had an anomalous low shift value due to the electron density found there. The ¹H NMR spectrum of complex **79** shows no such signal and so it may be tentatively inferred that as in previous examples, metallation occurred on the least sterically hindered face, Scheme 33.



Scheme 33

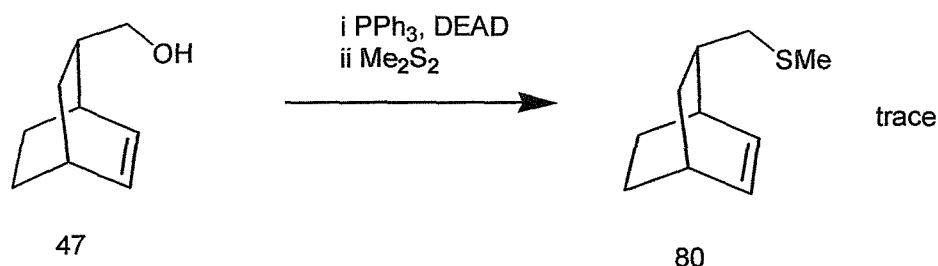
3.8 Synthesis of Ligands containing other heteroatom linkers

In order to study the effect of different heteroatoms on the selectivity of complexation it was decided to prepare analogues of **64**, namely the sulphur, nitrogen and phosphorus derivatives. Nitrogen linked cyclopentadienyl ligands are well preceded in group IV transition metal chemistry and a pendant nitrogen could be expected to play a role in the transition state of any catalytic process if the metal was on the same face as the metal.

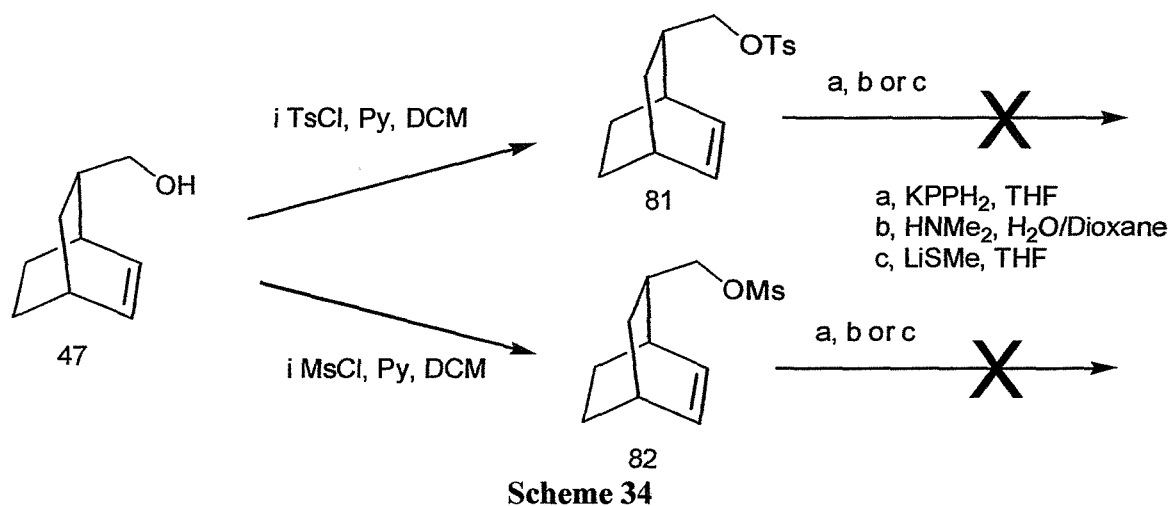
Phosphine groups on the linker chain would open up areas of late transition metal chemistry, such as rhodium and ruthenium complexes.

Pendant thioethers have been shown to direct the intermolecular Pauson Khand reaction in some cases ⁶⁸ and in light of this, sulphur would also make a good choice of heteroatom.

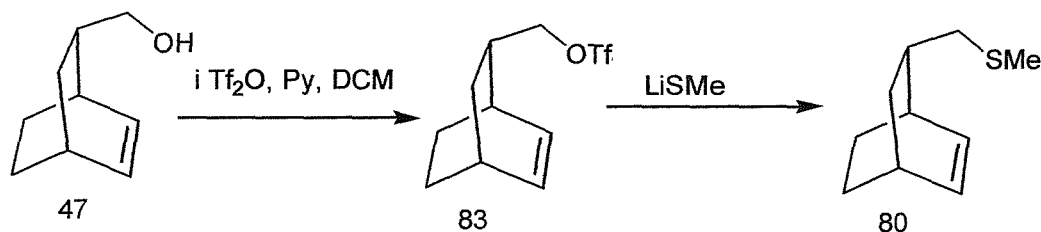
Initial attempts to synthesise thioether **80** via Mitsunobu type chemistry afforded only a small amount of material which appeared to be the desired product, and also a quantity of unidentified material which as revealed by NMR, possessed both a phosphorus group and the [2,2,2] bicyclic backbone.



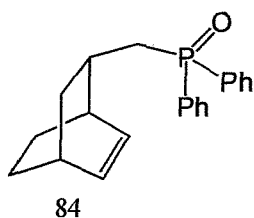
Treatment of alcohol **47** with *p*-toluene sulphonyl chloride and pyridine in DCM at 0°C afforded the tosylate **81** in 75% yield. However the *p*-toluene sulphonyl ester proved to be inert to nucleophilic substitution, probably due to the steric hindrance caused by the branching at the β position. The methane sulphonyl ester **82** was also formed easily under standard conditions but again proved to be inert to substitution by nitrogen sulphur or phosphorus nucleophiles, presumably for the same reason.



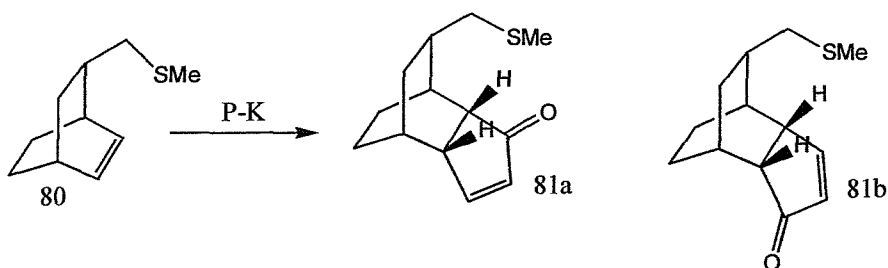
Fortunately, the trifluoromethane sulphonyl ester of **47** was much more reactive. Treatment of alcohol **47** with pyridine and trifluoromethane sulphonyl in DCM at -78°C gave triflate **83** which was filtered through silica and used immediately without further purification. Treatment of this compound with LiSMe (formed by the treatment of Me_2S_2 with *n*-butyl lithium in THF at -78°C) in THF at -78°C gave mercaptan **80** in 78% yield from alcohol **47**.



Treatment of triflate **83** with HNMe_2 in H_2O /dioxane only caused hydrolysis of the ester. Treatment of triflate **83** with KPPH_2 in THF at -78°C gave a colourless solution, which upon workup was shown to contain phosphine compounds. Mass spectrometry showed a single peak corresponding to the phosphine oxide **84**, however the material was not pure and attempts to purify this air sensitive material by chromatography have so far been unsuccessful.



Treatment of thioether **80** with dicobalt acetylene hexacarbonyl in toluene at 80°C afforded enone **81** as expected in 25% yield, Scheme 35.



Scheme 35

GC analysis of the reaction profile (Figure 40) shows similar profiling to the oxygen analogue, maximum yield of around 35-40% being achieved after several hours reaction time and then falling off.

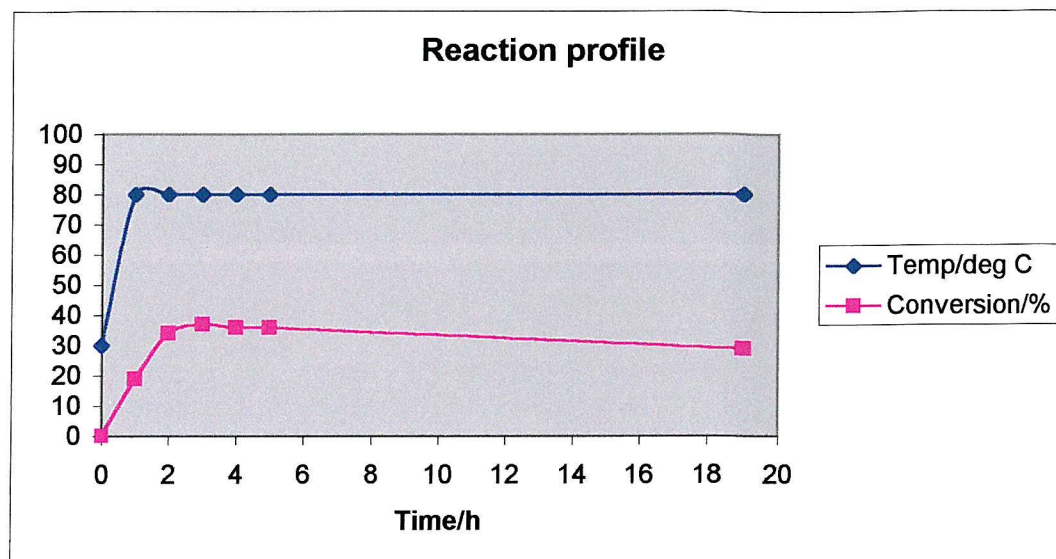
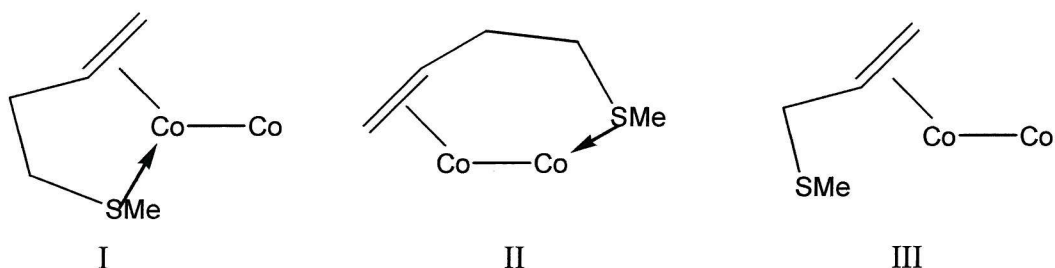


Figure 40

Unfortunately GC analysis also showed that the products were formed in a 1:1 ratio of isomers. This result may be rationalised by looking at the effect of chain length on the intermediate. Kraaft envisages three modes of binding of the substrate to the binuclear cobalt complex.⁶⁸



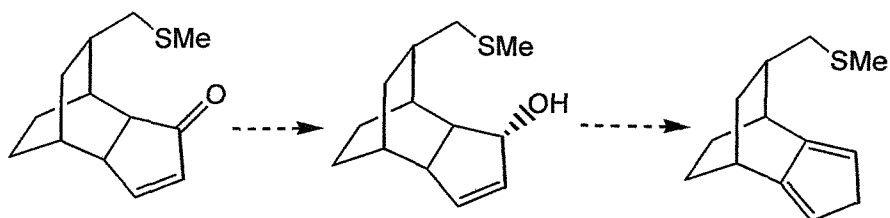
Transition states in which the linker is too short can only bind in a monodentate fashion (III) and thus selectivity is poor. Substrates with a longer chain bind across the two metal centres (II). This binding mode leads to the CO moiety being introduced on the opposite side from the sulphur group. The optimum distance for co-ordination of this type seems to be for alkenes with the sulphur group at the homo allylic position.

A third mode involves binding of both alkene and sulphur to the same cobalt atom. This leads to introduction of the CO moiety on the same side as the sulphur linker.

In the case of thioether **80**, the linking chain is restricted by the rigid bicyclic structure and this may make it conformationally unfavourable to adopt binding mode (I) or (II). It is also possible that the polycyclic nature of a bidentate intermediate would sufficiently

destabilise it to only allow binding through mode (III) affording a 1:1 mixture of products.

Reduction and elimination of enone **81** should allow the preparation of a sulphur analogue of ligand **64**, however there was insufficient time to explore the rest of this route.



3.9 Conclusions

A variety of novel rigid bicyclic cyclopentadienyl ligands have been synthesised and used in complexation reactions with early transition metals.

Three novel complexes were synthesised from ligands bearing tethered oxygen linkers complexed to titanium and/or zirconium. In all cases the only compound that it was possible to isolate was the isomer with the metal attached to the opposite face of the cyclopentadienyl ring from the oxygen linker. From this it may be seen, that for oxygen linker systems with group IV metals, steric factors seem to play the dominant role in the determination of facial selectivity.

3.10 Future Work

There is obviously great scope for the synthesis of a variety of ligands based on this system. However, as stereo control relies on having an asymmetric environment around the catalytic site, the oxygen-based systems seem to be less than satisfactory. The most promising area of work in this field would therefore seem to lie in the development of phosphorus, nitrogen and sulphur analogues of the ligands described here and their application to late transition metal catalysis.

4 Application of novel metallocenes to propene polymerisation

4.1 α -Olefin polymerisation

As discussed in previous chapters, one of the major practical uses of metallocenes is the homogenous polymerisation of α -olefins, particularly propene. Indeed, a zirconocene developed by Brintzinger is now used in the industrial preparation of highly isotactic polypropylene.²⁴ With a large number of potentially suitable metallocenes available from within the group it seemed prudent to test these complexes in polymerisation reactions. Asymmetric zirconium complexes are mainly used to influence tacticity in propylene polymerisation using enantiomeric site control.

4.2 Polymerisation conditions

A search of the literature on propene polymerisation reveals a huge array of different catalysts and conditions. This would be expected for such a commercially valuable product, however, there are some constant factors.

All metallocenes require a co-catalyst in order to take part in the reaction. Although many co-catalysts have been reported, by far the most widely used is MAO (methylaluminoxane). MAO is a poorly defined polymeric substance formed by the partial hydrolysis of trimethyl aluminium.⁶⁹ This material appears to have several functions in the catalytic mixture. The formation of the cationic active species is achieved by first methylation of the metal chloride, followed by loss of CH_4 to give a cationic zirconium centre. This cationic centre is stabilised by a "crown aluminoxane" complex. The highly reactive aluminoxane also scavenges harmful impurities such as water and oxygen, which could quench the catalytic species. By far the majority of conditions also use toluene as the reaction solvent.

The main variables in the reaction conditions are as follows.⁷⁰

Temperature

Polymerisation of propene has been reported at temperature ranging from -80 to +80°C. Lower temperatures give lower activity but also increased selectivity.

Concentration of metallocene and aluminoxane

A wide range of concentrations has been reported; metallocene concentration ranging from 1.7 - 318 μM , aluminium concentration ranging from 16 - 810 mM, ratios of $[\text{M}]/[\text{Al}]$ in the range 800-10000

Pressure

Reported partial pressures of propene range from atmospheric to 18 bar. Some reaction conditions involve condensing liquid propene into the reaction vessel.

Obviously with such wide-ranging variables, it was necessary to find a set of standard conditions that would be easily reproducible in the laboratory. The following conditions were decided upon.

- i) In keeping with the majority of the literature precedents and due to the ready availability of reagents, toluene solvent and MAO co-catalyst were chosen.
- ii) To avoid the need for specialist equipment, dried and deoxygenated propene was used at atmospheric pressure. Drying was achieved by simply bubbling the gas through neat tri *n*-butyl aluminium.
- iii) Intermediate values of concentrations were chosen. $[\text{Al}]/[\text{M}] = 4000$, $[\text{M}] = 25 \mu\text{M}$, $[\text{Al}] = 100 \text{ mM}$.
- iv) In order to ensure reproducibility, a sufficiently large reaction volume was required to minimise the effects of any water/oxygen present. 150 mL was adequate.
- v) Ambient temperature was chosen for convenience.

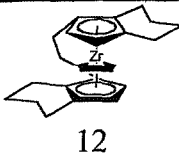
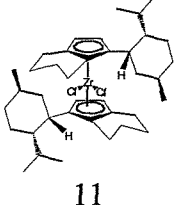
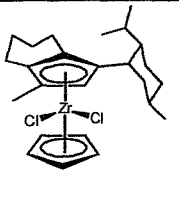
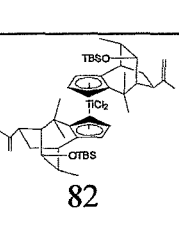
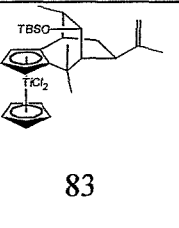
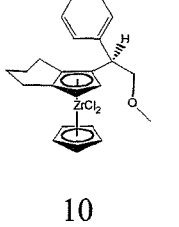
Using these standardised conditions, a series of metallocenes were tested.

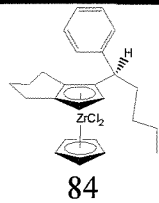
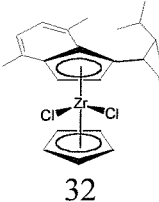
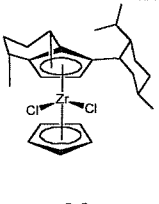
4.3 Polymerisation reactions

Due to the other projects, past and present, carried out within the research group, a variety of metallocenes were readily available for testing. These are shown in the table below.

All reactions were carried out under identical conditions with reaction times of 1.5 h. The reactions were quenched with acidic methanol and washed with water to remove inorganic salts before removal of toluene *in vacuo* to give the product which was dried under vacuum to constant mass. Activities were obtained from the mass yield of polymer produced. Isotacticity data were obtained from high temperature ^{13}C NMR experiments in 1,2-dichlorobenzene solvent.²⁷ Molecular weight distribution data were determined by RAPRA by gel permeation chromatography.

Application of novel metallocenes to propene polymerisation.

No	Complex	Mass of polymer	Activity kg(pol)/[M][Pr]h	Mn	Dispersity	Form	Tacticity
1	 12	1.64g	606	2600	2.1	White Solid	>99%
2	 11	0.442g	163	1445	3.1	White Solid	23%
3	 35	1.02g	377	1600	2.9	White Solid	49%
4	 82	0.136g	50	1255	5.5	White Solid	22%
5	 83	0.154g	57	440	4.9	Oil	<2%
6	 10	0.044g	16	1320	8.3	Oil	see text

No	Complex	Mass of polymer	Activity kg(pol)/ [M][Pr]h	Mn	Dispersity	Form	Tacticity
7	 84	0.419g	155	320	3.1	Oil	13%
8	 32	0.702g	259	1970	3.5	Oil	see text
9	 33	0.265	98	325	3.3	Oil	see text

Notes

- Samples 2 and 4 - Poor signal/noise ratio gave inaccurate results for tacticity
- Samples 4 and 6 - Bimodal molecular weight distributions.
- Sample 6 - No signals observed in correct region of NMR
- Samples 8 and 9 - No mmmm (isotactic) peak in NMR

Complex references.

- Samples 1⁷¹ and 2¹⁶ - Literature compounds
- Samples 3, 8 and 9 - See Chapter 2
- Samples 4 and 5 - S.M. Green³⁹
- Samples 6 and 7 - D.C. Brookings¹⁵

4.4 Analysis of polymer properties

As the reaction conditions varied widely in the reported literature, it was necessary to obtain reference samples to allow a comparison between our data and literature values. Also, GPC results can vary over time and so need to be compared with samples run at the same time under the same conditions⁷². Two reference samples were available from previous work within the group.

Lines 1 and 2 show results for complexes **11** and **12**, developed by Erker¹⁶ and Brintzinger⁷¹ respectively. The activity values should be reasonably consistent with literature values as they are calculated with allowances for catalyst concentration, propene concentration and time. The only other significant factor affecting activity is temperature so results for polymerisations carried out at the same temperature should be similar. Comparison of these results with literature values^{73 16} gives good correlation, indicating that comparable results may be obtained using this method. Isotacticity and molecular weight distributions are more closely related to these factors and so can only be reliably compared between similarly obtained samples.

4.4.1 Catalyst activity

Activity of the catalyst is likely to be affected by the steric and electronic effects around the catalytic centre. This relationship is likely to be complex and it will be difficult to show any definite relationships between activity and catalyst structure.

Analysis of the activity data does not show any global trend in relation to catalyst features. However, one notable trend is observed in complexes **82**, **83** and **10** (Lines 4,5 and 6) which appear to display a much lower activity in comparison to the others. Indeed, **10** and **84** are almost identical complexes except for the heteroatom and they display a 10-fold difference in activity.

These three complexes differ from the rest in that they contain oxygen heteroatoms, a feature that is quite uncommon in propene polymerisation catalysts.⁷⁰ It is possible that the oxygen somehow deactivates the cationic intermediate, probably by the lone pairs stabilising the positively charged zirconium centre.

4.4.2 Activity vs Molecular Weight

Although increased steric crowding around the catalytic centre decreases the activity of the catalyst, the extra bulk may be expected to lower the rate of β -hydride elimination in the catalytic cycle. As this is a chain-terminating step, a decreased rate of β -hydride elimination should lead to an increased average chain length. Figure 41 shows that there is a direct correlation between activity and average chain length. These data seem to provide evidence that this theory is not sophisticated enough to explain the characteristics of the polymers produced by the catalysts concerned.

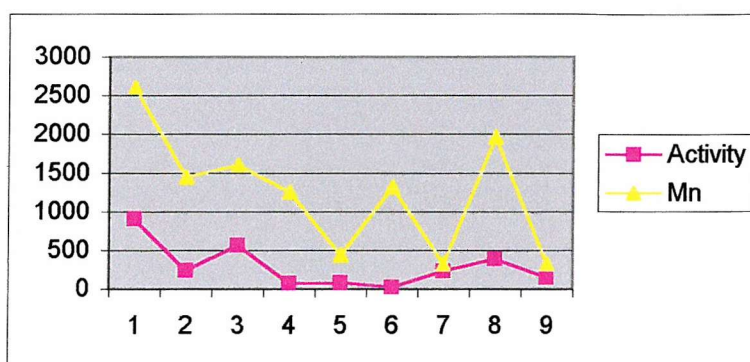


Figure 41

4.4.3 Molecular Weight Distribution

The molecular weight distributions of the polymer samples display some distinct differences. There are three main groups. Although all the samples had a relatively low molecular weight, there was a group with high molecular weight, one with low molecular weight and a group with a bimodal distribution.

Samples 5,7 and 9 all had low molecular weight distributions with polydispersity of around 4. Figure 42

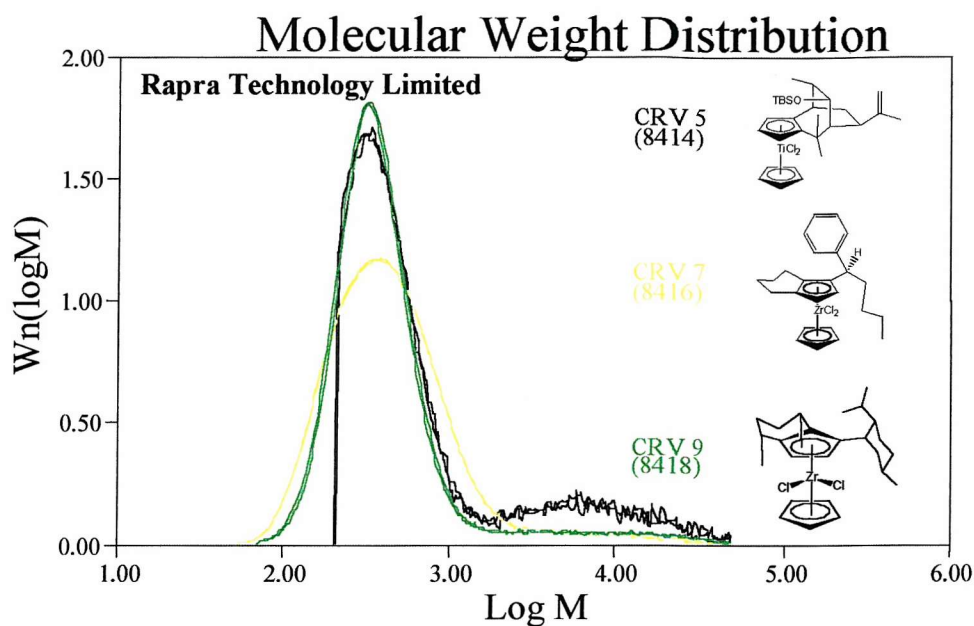


Figure 42

Samples 1,2,3 and 8 had high molecular weight distributions ($1500 < M_n < 2600$) with polydispersity of 2-3. Figure 43

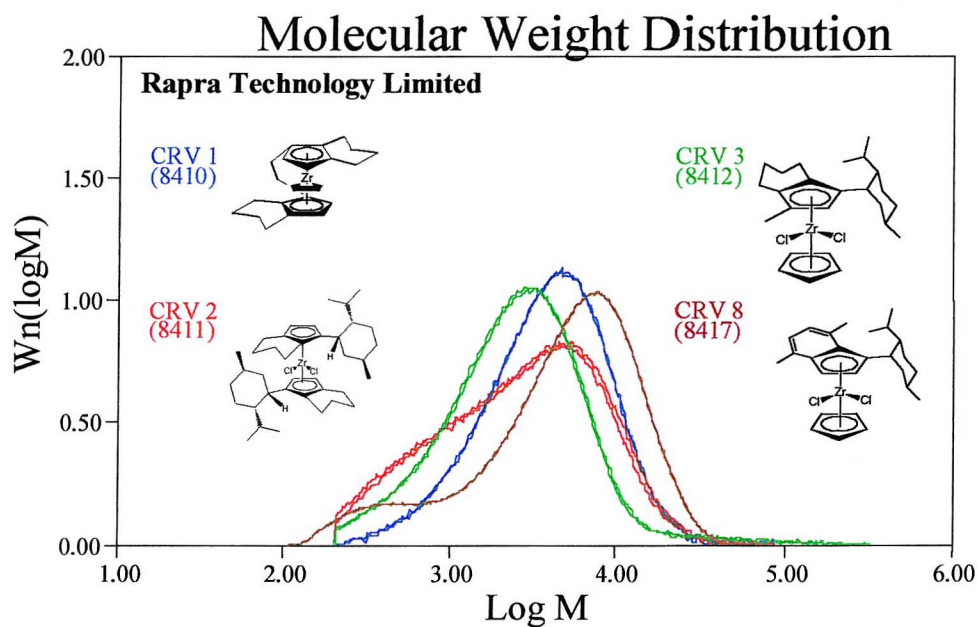


Figure 43

Samples 4 and 6 had bimodal weight distributions. Figure 44

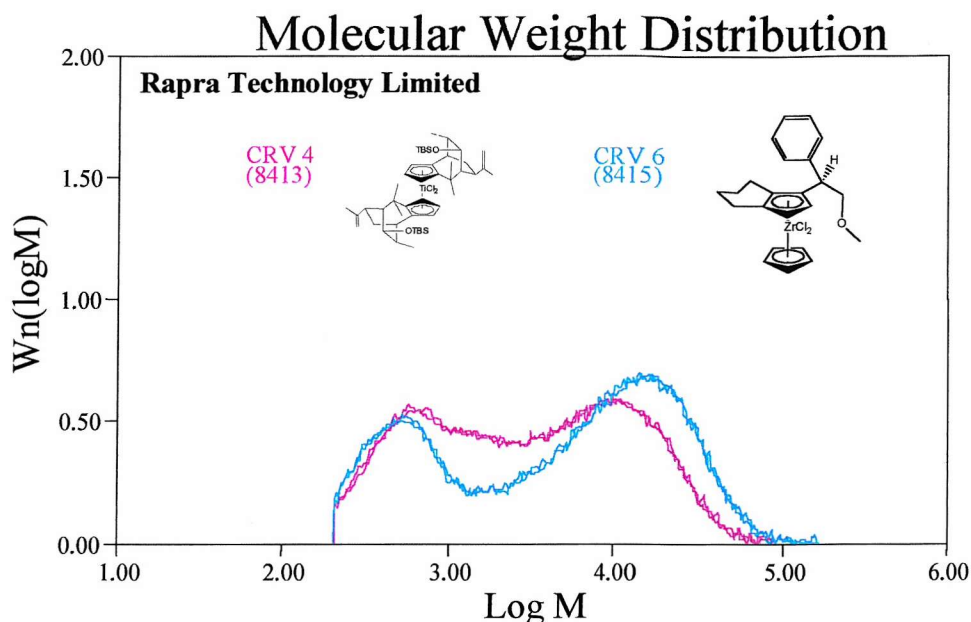


Figure 44

This bimodal weight distribution would tend to suggest that there are two active species present in the reaction mixture, one producing each molecular weight band. Behaviour of this kind has been reported²⁶, where the catalyst may switch from one form to another (see 1.3.1.2). As both these complexes have pendant oxygen linkers, it is possible that the two active species are one with oxygen co-ordinated to the metal and one without. However, it is uncertain whether the interconversion between these species would be slow enough to produce this effect.

4.4.4 Isotacticity

Isotacticity is determined by ^{13}C NMR as discussed earlier. However, this is dependent on the polymer having a sufficiently long chain, so that on average most of the carbons are in more or less the same environment. As a result of this, samples with a low molecular weight, or those with a significant low molecular weight proportion give very poor results. Even "isotactic" oligomers would give signals which are non characteristic of long chain isotactic polypropylene. This may explain some of the poor tacticity results.

4.4.5 Conclusions

This polymerisation work has developed a method for testing the polymerisation properties of various metallocenes. While **35** performed better than the Erker complex **11**, none of those tested performed better than the best literature compound **12** for the production of long chain, isotactic, crystalline polypropylene. However most complexes formed polymers of quite short chain length, and this type of polymer may find uses in other applications.

One interesting observation is that inclusion of an oxygen heteroatom in the ligand system greatly decreases the activity of the complex as a polymerisation catalyst. This may have application in attempts to control the properties of polymers produced in this manner, however polymer properties are dependent on a wide range of factors and any development would need to take these into account.

5 Experimental

5.1 General experimental

5.1.1 Air sensitive materials

All experiments involving organometallic or air sensitive reagents were carried out under argon using standard Schlenk, syringe and vacuum line techniques. Flasks were flame-dried and allowed to cool under vacuum (<0.1 mmHg). Syringes, needles and cannulas were dried in an oven (>150°C) overnight before use.

5.1.2 Spectroscopic techniques

Proton and phosphorus NMR spectra were recorded on a Bruker AM400 spectrometer at 400 MHz, a Bruker AM300 or AC300 at 300 MHz, or a JEOL GX270 at 270 MHz. Carbon NMR spectra were recorded on a Bruker AM400 spectrometer at 100 MHz, a Bruker AM300 or AC300 at 75 MHz or a JEOL GX270 at 68 MHz. NMR solvents were dried over 4Å molecular sieves. Unless otherwise stated, spectra were referenced to the residual proton peak in the relevant deuterated solvent. Chemical shifts are quoted in ppm on the δ scale and coupling constants are quoted in Hz.

Optical rotations were measured on an AA-100 Polarimeter and are uncorrected.

Infra-red spectra were recorded on a Perkin-Elmer 1600-series FT-IR spectrometer or a Nicolet Impact-400 spectrometer fitted with an Advanced Total Reflectance cell (ATR)

Gas Chromatography Mass Spectrometry (GCMS) was carried out on a VG 70 -SE normal geometry double focusing mass spectrometer with capillary column GC.

Electron Impact (EI) mass spectra were recorded on a VG 70 -SE normal geometry double focusing mass spectrometer. Electrospray (ES) and Atmospheric Pressure Chemical Ionisation (APCI) mass spectra were recorded on a VG platform single quadrupole mass spectrometer.

5.1.3 Chromatography

Thin layer chromatography was carried out on aluminium backed silica gel plates with UV₂₅₄ phosphor and visualised by UV light (at 254 and 365 nm), phosphomolybdinic acid and heating, I₂ vapour or treatment with K₂MnO₄ solution. Column chromatography was carried out using silica 60 (230-400 mesh) or Brockmann grade III alumina.

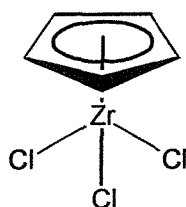
HPLC was carried out using a HP 1050 instrument with single wavelength UV detector. GC was performed on a HP 6900 using helium carrier gas and a flame ionisation detector. Peak analysis for both techniques was carried out using HP Chemstation software.

5.1.4 Reagent purification

Unless otherwise stated materials were used as supplied from commercial sources, without further purification. Cyclopentadiene was prepared by cracking of the dimer and was distilled before use. THF, toluene, benzene and diethyl ether were freshly distilled from Na/benzophenone. DCM was distilled from calcium hydride. Petroleum ether refers to the petroleum fraction B.p. 40-60°C and was distilled prior to use. Acetylene was purified by condensing residual acetone at -78°C followed by bubbling through concentrated H₂SO₄ and passing through NaOH pellets.

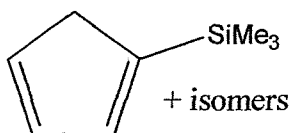
5.2 Experimental for Chapter 2

5.2.1 Cyclopentadienyl zirconium trichloride (14) ³⁷



Cp₂ZrCl₂ (10 g, 34.24 mmol) was dissolved in CCl₄ (120 mL) under argon atmosphere. The flask was purged with Cl₂ gas and a steady flow of gas established. The flask was irradiated with UV radiation for 1 min before shielding from light was maintained. The temperature rise due to exothermic reaction was controlled by cooling in an ice bath and the temperature kept between 15° and 40°C. After 1 h the exotherm had ceased and the solids were removed via filtration under argon. The residue was washed with CHCl₃ (4 x 20mL) and hexane (4 x 20mL) before drying under vacuum to yield the title compound (5.07 g, 56%) as a grey solid. NMR data were collected for the THF adduct which was formed by dissolving a small amount in THF at 0°C and stirring for 1 h before removing the solvent *in vacuo*. δ_H (300 MHz, CDCl₃) 1.9 (8H, s br, THF) 3.9 (8H, s br, THF) 6.7 (5H, s, Cp) NMR data were in agreement with literature values. ³⁷

5.2.2 5-Trimethylsilyl cyclopenta-1,3-diene ⁷⁴

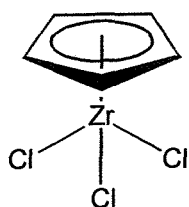


NaH (37.7 g, 0.94 mol, 60% dispersion in mineral oil, unwashed) was dissolved in dry THF (400 mL) under argon. Cyclopentadiene (68 g, 1.03 mol, freshly cracked, diluted to 200 mL with dry THF) was added dropwise so that the temperature stayed below 10° C. H₂ gas was evolved and the red solution was stirred for 30 min after the addition was complete. TMSCl (109.2 mL, 0.86 mol) was added portionwise, the temperature being kept between 15 and 25°C. After the addition was complete the green solution was stirred for 15 min before the addition of water (800 mL) with vigorous stirring. The organic layer was washed with water (5 x 300 mL) and the aqueous phase extracted with pentane (3 x 100 mL). The organic layers were combined, dried (MgSO₄) and concentrated *in vacuo* before the residue was distilled under reduced pressure using a vacuum jacketed Dufton fractionating column to yield the title compound (41.5 g, 35%) as a colourless oil. B.p. = 32-36°C at 11 mmHg (Lit. ⁷⁴ = 35°C at 13 mmHg); δ_H

(300 MHz, CDCl₃) 0.00 (9H, s, Si(CH₃)₃), 3.42 (1H, s br, H-5), 6.62, 6.65 (4H, 2 x s br, H-1, H-2, H-3, H-4).

5.2.3 Cyclopentadienyl zirconium trichloride, tetrahydrofuran complex

(14)³⁹

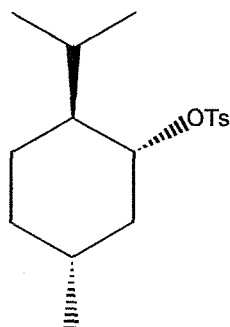


2 THF

ZrCl₄ (17 g, 72.5 mmol handled under inert atmosphere) was suspended in freshly distilled DCM (150 mL) and cooled under argon to 0°C. DMS (10.8 mL, 0.147 mol) was added dropwise and the solution stirred at room temperature for 10 min after which time most of the solid had dissolved. The solution was cooled to 0°C and freshly distilled CpTMS (15 g, 0.11 mol) was added and the resulting yellow solution stirred for 3 h at room temperature with the exclusion of light, during which time a white precipitate formed. The volume was reduced by half and the solution diluted with dry hexane. The supernatant liquid was removed via syringe and the flask cooled to 0°C before cold THF (200 mL) was added and the mixture stirred for 1 h at room temperature. Half the solvent was removed *in vacuo* and the residue diluted with hexane to precipitate solids. The white solid was separated and washed with hexane before drying *in vacuo* to give the title compound (16.65g, 83%) as a white solid. δ_H (300 MHz, CDCl₃) 1.9 (s br, 8H, THF) 3.9 (s br, 8H, THF) 6.7 (s, 5H, Cp).

NMR data were in agreement with literature values.³⁹

5.2.4 (1R,2S,5R)-2-isopropyl-5-methylcyclohexyl 4-methyl-1-benzenesulfonate (17)¹⁶

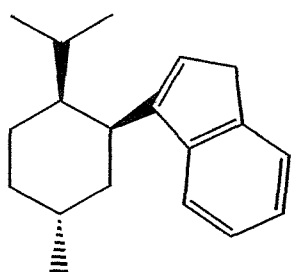


A mixture of (-) menthol (156.3 g, 1 mol) and pyridine (316 mL, 4 mol) was cooled to 10°C and *p*-toluenesulphonic acid chloride was added in 6 portions, the temperature being kept between 10° and 15°C. The mixture was then stirred for 3 h before being added to a mixture of hydrochloric acid (500 mL) and ice (1300 g). The product was collected by filtration before being dissolved in DCM and washed with water (3 x 200 mL), dried (MgSO₄) and concentrated *in*

vacuo to yield a white solid which upon recrystallisation from toluene gave (1*R*,2*S*,5*R*)-2-isopropyl-5-methylcyclohexyl 4-methyl-1-benzenesulfonate (242 g, 78%) as a white crystalline solid. M.p. (toluene) = 62-63°C; δ_{H} 7.79 (2H, d, $J=8.5$), 7.32 (2H, d, $J=7.9$), 4.38 (1H, dt, $J=4.6$ $J=10.8$), 2.43 (3H, s), 2.2-0.9 (9H, m), 0.87 (3H, d, $J=6.6$), 0.82 (3H, d, $J=7.4$), 0.51 (3H, d, $J=6.6$)

NMR data were in agreement with literature values. ¹⁶

5.2.5 3-[(1*S*,2*R*,5*S*)-2-isopropyl-5-methylcyclohexyl]-1*H*-indene (**4**)¹⁶



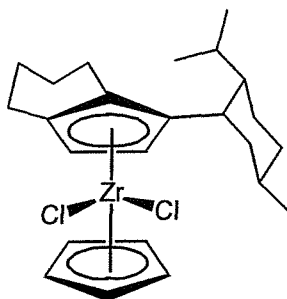
Indene (29.2 mL, 0.2 mol) was dissolved in dry THF (200 mL) and treated with *n*-butyl lithium (2.5M, 80 mL, 0.2 mol) at -78°C before being allowed to warm to room temperature and stirred for 2 h.

The dark red solution was cooled to 0°C before a pre-cooled solution of (1*R*,2*S*,5*R*)-2-isopropyl-5-methylcyclohexyl 4-methyl-1-benzenesulfonate (55.8 g, 0.18 mol in 200 mL THF) was added and the mixture stirred overnight at room temperature. GC analysis showed a yield of 25%. The mixture was then heated to reflux and stirred for a further 24 h after which time GC analysis gave a yield of 46%.

The reaction was quenched with water (200 mL) and ether (150 mL) was added. The organic phase was washed with water (3 x 150 mL) and the aqueous washings extracted with ether (3 x 150 mL). The organic layers were combined, dried (MgSO₄) and concentrated *in vacuo*. Column chromatography of the resulting orange oil afforded a mixed fraction of product and indene. Short path distillation afforded 3-[(1*S*,2*R*,5*S*)-2-isopropyl-5-methylcyclohexyl]-1*H*-indene (16.4 g, 36%) as a pale yellow oil which crystallised on standing. M.p. = 35-37°C.; $[\alpha]_{\text{D}} = -73^{\circ}$ ($c=0.17$, CHCl₃); δ_{H} 7.52 (1H, d, $J=7.4$), 7.43 (1H, d, $J=7.4$), 7.35 (1H, t, $J=7.4$), 7.25 (1H, t, $J=7.4$), 6.42 (1H, s), 3.41 (2H, m), 2.0-1.9 (1H, m), 1.88-1.8 (2H, m), 1.75-1.0 (7H, m), 0.97, (3H, d, $J=6.6$), 0.83 (3H, d, $J=6.6$), 0.77 (3H, d, $J=6.6$).

NMR data were in agreement with literature values. ¹⁶

5.2.6 Cyclopentadienyl(1-neomenthyl-4,5,6,7-tetrahydroindenyl)zirconium dichloride (13)⁷



3-Neomenthylindene (4.0 g, 15.74 mmol) was dissolved in dry THF (100 mL) under an argon atmosphere in the absence of light and cooled to -78°C before *n*-butyl lithium (6.2 mL, 2.5M solution in THF, 15.7 mmol) was added dropwise over 15 min. The red solution was allowed to warm to room

temperature and stir for 2 h to afford a greenish-yellow solution.

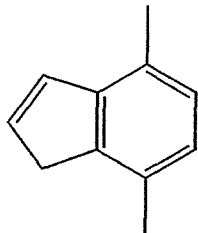
Freshly recrystallised $\text{CpZrCl}_3 \cdot 2\text{THF}$ (7.66 g, 18.8 mmol) was suspended in cold (0°C) THF and stirred for 30 min. The indene solution was added by cannula and the bright yellow solution was stirred overnight at room temperature.

tert-Butyl chloride (6 mL) was added and the solution stirred for 10 min before the solvent was removed *in vacuo* and the bright yellow solid dissolved in dry DCM (80 mL) and PtO_2 (10 mol%) added before the system was purged with hydrogen gas, pressurised to 1 bar and stirred overnight.

The catalyst was removed by filtering over celite to give a colourless solution, which was evaporated to dryness to give a white residue. Recrystallised from hot toluene gave the title compound (4.46 g, 69%) as a white crystalline solid. M.p. (toluene) = $237.5\text{--}239^{\circ}\text{C}$ (Lit. ⁴⁰ = $237\text{--}238^{\circ}\text{C}$); $[\alpha]_{\text{D}} = -130^{\circ}$ ($c=0.12$, CHCl_3); δ_{H} (300MHz, CDCl_3) 6.46 (1H, d, $J=3.0$), 6.44 (5H, s), 5.58 (1H, d, $J=3.0$), 3.22 (1H, m), 3.08 (1H, m), 3.05-2.70 (2H, m), 2.65-2.40 (2H, m), 2.05-1.45 (10H, m), 1.45-1.05 (2H, m), 0.99, 0.74 (2 x 3H, 2 x d, $J=6.6$), 0.38 (3H, d, $J=7.3$); δ_{C} (75 MHz, CDCl_3) 138.2, 137.0, 114.8, 109.9, 102.8, 47.6, 39.4, 36.24, 33.6, 28.75, 24.71, 24.38, 23.96, 22.5, 22.34, 22.00, 21.76, 18.31.

NMR data were in agreement with literature values. ⁴⁰

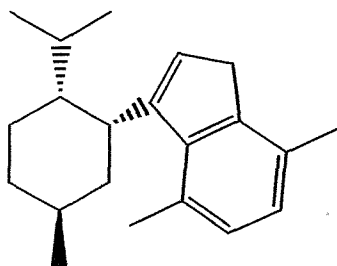
5.2.7 4,7-Dimethyl-1H-indene (27)^{45 46}



Sodium (6 g, washed in pentane, 250 mmol) was dissolved in methanol (62.5 mL) and cooled to 0°C before a mixture of cyclopentadiene (9.9 g, 150 mmol) and 2,5-hexandione (11.7 mL, 100 mmol) was added dropwise over 2 h. The dark brown solution was stirred for 3 h at room temperature before being diluted with water (100 mL) and extracted with ether (4 x 100 mL). The organic layers were combined, dried (MgSO₄) and concentrated *in vacuo* before flash chromatography (petrol) and distillation under reduced pressure (0.1 mbar) to afford the title compound (8.83 g, 61 %) as an orange oil. δ_{H} (300MHz, CDCl₃) 6.98 (2H, m), 6.91 (1H, m), 6.56 (1H, m), 3.28 (2H, s, CH₂), 2.41, 2.33 (2 x 3H, 2 x s, CH₃); ν_{max} = 2921, 1492 (CH)

NMR and IR data were in agreement with literature values.⁴⁶

5.2.8 3-[(1S,2R,5S)-2-isopropyl-5-methylcyclohexyl]-4,7-dimethyl-1H-indene (29)



4,7-Dimethylindene (5.83 g, 40.5 mmol) was dissolved in dry THF (40 mL) and treated with *n*-butyl lithium (2.5M, 16.2 mL, 40.5 mmol) at -78°C before being allowed to warm to room temperature and stir for 2 h.

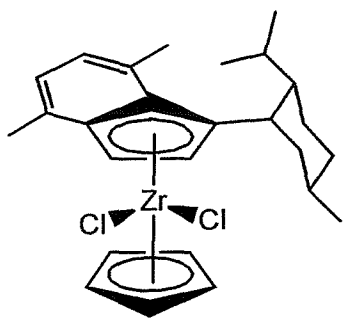
The dark red solution was cooled to 0°C before a pre-cooled solution of (1S,2R,5S)-2-isopropyl-5-methylcyclohexyl 4-methyl-1-benzenesulfonate (11.4 g, 36.8 mmol in 40 mL THF) was added and the mixture was heated to reflux and stirred for 4 days.

The reaction was quenched with water (40 mL) and ether (30 mL) was added. The organic phase was washed with brine (3 x 30 mL) and the aqueous washings extracted with ether (3 x 30 mL). The organic layers were combined, dried (MgSO₄) and concentrated *in vacuo*. Column chromatography of the resulting orange oil afforded a mixed fraction of product and 4,7-dimethylindene. Kugelrohr distillation (120°C at 0.5 mmHg) afforded 3-[(1S,2R,5S)-2-isopropyl-5-methylcyclohexyl]-1H-indene (2.88 g,

28%) as colourless oil and a mixture of isomers. $[\alpha]_D$ (CHCl_3 , $c=1.21$) = +56.198; δ_H (300 MHz, CDCl_3) 7.1-6.8 (4H, m, indenyl CH), 6.8-6.2 (3H, m, alkene CH), 3.8-2.9 (3H, m, vinyl CH/ CH_2), 2.64, 2.48, 2.39, 2.37 (4 x 3H, 4 x s, indenyl CH_3), 2.1-0.6 (20H, m, menthyl CH/ CH_2), 1.22, 1.10, 1.00, 0.85, 0.82, 0.59 (6 x 3H, 6 x d, $J=6.5$, 6 x menthyl CH_3); m/z (APCI +ve) = 282 (100%, M^+), 124 (100%); ν_{max} = 2951, 2921, 2837 (CH) cm^{-1} ; $\text{C}_{21}\text{H}_{30}$ requires C 89.29, H 10.71, found C 88.95, H 10.87%.

As it proved impossible to separate the mixture, the material was used in the next step without further purification.

5.2.9 Cyclopentadienyl (3-[(1*S*,2*R*,5*S*)-2-isopropyl-5-methylcyclohexyl]-4,7-dimethylindenyl) zirconium dichloride (32)



3-[(1*S*,2*R*,5*S*)-2-isopropyl-5-methylcyclohexyl]-4,7-dimethyl-1*H*-indene (846 mg, 3 mmol) was dissolved in dry THF (10 mL) under an argon atmosphere in the absence of light and cooled to -78°C before *n*-butyl lithium (1.2 mL, 2.5M solution in THF, 3 mmol) was

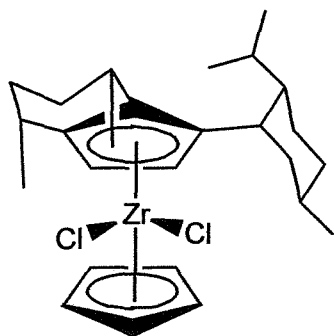
added dropwise over 15 min. The red solution was allowed to warm to room temperature and stir for 2 h to afford a greenish-yellow solution.

Freshly re-crystallised $\text{CpZrCl}_3 \cdot 2\text{THF}$ (1.83 g, 4.5 mmol) was suspended in cold (0°C) THF and stirred for 30 min. The indene solution was added by cannula and the bright yellow solution was stirred overnight at room temperature.

The solvent was removed *in vacuo* and the bright yellow residue was extracted into hot hexane and recrystallized to yield the title compound (593 mg, 38%) as a bright yellow crystalline solid. M.p. (hexane) = $139\text{-}142^\circ\text{C}$; $[\alpha]_D$ (CHCl_3 , $c=0.71$) = -41.1° ; δ_H (270 MHz, CDCl_3) 6.88 (1H, d, $J=7.5$, indenyl CH), 6.95 (1H, d, $J=7.5$, indenyl CH), 6.66 (1H, d, $J=3.0$, indenyl CH), 6.26 (5H, s, cyclopentadienyl CH), 6.21 (1H, d, $J=3.0$, indenyl CH), 4.1-3.9 (1H, m), 2.77, 2.31 (2 x 3H, 2 x s, indenyl CH_3), 2.2-0.7 (9H, m, menthyl CH/ CH_2), 1.13, (3H, d, $J=7$, menthyl CH_3) 0.59, 0.12 (2 x 3H, 2 x d, $J=6$, isopropyl CH_3); δ_C (77.5 MHz, CDCl_3) = 134.9, 134.1, 133.8, 132.4, 127.6, 126.5, 124.6, 117.1, 115.8, 93.8, 46.7, 35.6, 34.2, 29.4, 28.1, 25.9, 24.1, 23.4, 21.1, 20.8, 19.6,

19.2; m/z (APCI +ve) = 471 (17% M+H-Cl); ν_{\max} = 2956, 2924, 2869 (CH) cm^{-1} ; $\text{C}_{26}\text{H}_{34}\text{ZrCl}_2$ requires C 61.40, H 7.14, found C 61.17, H 7.39%.

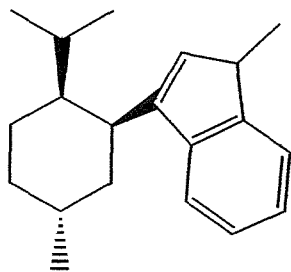
5.2.10 Cyclopentadienyl (3-[(1*S*,2*R*,5*S*)-2-isopropyl-5-methylcyclohexyl]-4,7-dimethylindenylo) zirconium dichloride (33)



Cyclopentadienyl (3-[(1*S*,2*R*,5*S*)-2-isopropyl-5-methylcyclohexyl]-4,7-dimethylindenyl) zirconium dichloride (166 mg, 0.3 mmol) was dissolved in dry DCM (30 mL) in a glass lined pressure vessel. Adam's catalyst (10 mol%) was added before the system was purged with hydrogen gas, pressurised to 2500 psi and stirred at 65°C overnight.

The pressure was vented carefully before the catalyst was removed by filtration through celite to give a colourless solution, which was evaporated to dryness to give a pale yellow residue. Recrystallisation from DCM / hexane gave the title compound (31 mg, 20%) as a white crystalline solid. M.p. (DCM / hexane) = 206°C (dec); δ_{H} (270 MHz, CDCl_3) 6.40 (5H, s, C_5H_5), 6.08 (1H, d, $J=2$, CH), 5.85 (1H, d, $J=2.5$), 3.85-3.5 (1H, m), 3.2-3.0 (1H, m), 2.75-2.4 (1H, m), 2.4-2.15 (1H, m), 2.15-1.4 (12H, m), 1.53 (3H, d, $J=7.5$), 1.18 (3H, d, $J=7$), 1.08 (3H, d, $J=7$), 0.80 (3H, d, $J=7$), 0.27 (3H, d, $J=6.5$); δ_{C} (77.5 MHz, CDCl_3) 146.1, 144.2, 133.4 (3 x Cq), 115.2 (5x C_5H_5), 104.4, 101.8 (2x CH), 42.9, 34.7, 33.6, 32.1, 31.8, 28.4, 28.2, 27.8, 25.9, 25.7, 24.1, 23.9, 21.6, 21.4, 19.0, 18.8; m/z (APCI +ve) = 475 (73%, M - H^+ -Cl), 516 (26% M- H^+ -Cl + MeCN); ν_{\max} = 2955, 2924 (CH) cm^{-1} .

5.2.11 3-[(1*S*,2*R*,5*S*)-2-isopropyl-5-methylcyclohexyl]-1-methyl-1H-indene (34)



3-[(1*S*,2*R*,5*S*)-2-isopropyl-5-methylcyclohexyl]-1H-indene (2 g, 7.9 mmol) was dissolved in THF (20 mL) and cooled to -78°C before dropwise addition of *n*-butyl lithium (3.5 mL, 2.5M solution in hexane, 8.7 mmol) in the absence of light. The yellow solution was allowed to warm to room

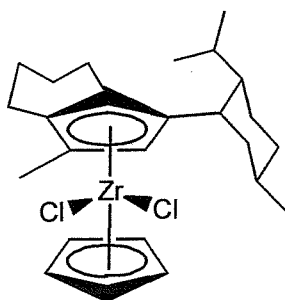
temperature and stir for 2 h before addition of methyl iodide (0.54 mL, 8.7 mmol) and stirring overnight.

The reaction was quenched with saturated ammonium chloride solution (20 mL) and extracted into diethyl ether (3 x 100 mL). The organic layers were combined, dried (MgSO₄) and concentrated *in vacuo* before the residue was distilled under reduced pressure (126°C at 2 mmHg) to afford a mixture of diastereoisomers (1.96 g, 92%). δ_{H} (300 MHz, CDCl₃) 7.6-7.2 (4H, m, indenyl CH), 6.40 (1H, s br, alkene CH), 3.65-3.50 (1H, m, allylic CH), 2.1-1.5 (6H, m), 1.5-1.25 (6H, m), 1.2-1.0, (1H, m), 1.04 (3H, d, $J=6.6$, isopropyl CH₃), 0.90 (3H, d, $J=5.9$, menthyl CH₃), 0.84 (3H, d, $J=6.6$, isopropyl CH₃); δ_{C} (77.5 MHz, CDCl₃) 149.4, 145.9, 142.7 (3 x s, 3 x indenyl quaternary), 137.2 (s, alkene CH), 126.4, 124.7, 122.7, 119.0 (4 x d, 4 x phenyl CH), 47.8, 44.4, 39.7 (t, menthyl CH₂), 35.8 (t, menthyl CH₂), 33.8, 30.2, 27.4 (t, menthyl CH₂), 27.0, 21.8, 21.5, 16.9; ν_{max} = 2948, 2923, 2866, 2841 (CH) cm⁻¹; C₂₀H₂₈ requires C 89.49, H 10.51, found C 89.47, H 10.68.

GCMS analysis showed the compound to be a mixture of 2 peaks RT = 5.66 and 5.70, both with m/z (CI) = 268 (80%, M⁺), 130 (100%).

As it proved impossible to separate these isomers, material was used without further purification.

5.2.12 Cyclopentadienyl(3-[(1*S*,2*R*,5*S*)-2-isopropyl-5-methylcyclohexyl]-1-methyl-4,5,6,7-tetrahydroindenyl)zirconium dichloride (35)



3-[(1*S*,2*R*,5*S*)-2-isopropyl-5-methylcyclohexyl]-1-methyl-1H-indene (804 mg, 3 mmol) was dissolved in dry THF (30 mL) under an argon atmosphere in the absence of light and cooled to -78° C before *n*-butyl lithium (1.2 mL, 2.5M solution in hexane, 3 mmol) was added dropwise. The mixture was

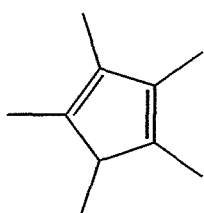
allowed to warm to room temperature and stir for 2 h to afford a yellow solution.

Freshly recrystallised solid CpZrCl₃•2THF (1.46 g, 3.6 mmol) was added in one portion before stirring overnight at room temperature.

The solvent was removed *in vacuo* and the bright yellow solid dissolved in dry DCM (30 mL) and PtO₂ (10 mol%) added before the system was purged with hydrogen gas, pressurised to 1 bar and stirred overnight.

The catalyst was removed by filtering over celite to give a colourless solution that was evaporated to dryness to give a white residue. Soxhlet extraction into hexane followed by recrystallisation from hot toluene gave the title compound (1.48 g, 58%) as a white crystalline solid. M.p. (toluene) = 188-189.5°C; $[\alpha]_D(\text{CHCl}_3, c=0.94) = -30.425$; δ_H (300MHz, CDCl₃) = 6.40 (5H, s, C₅H₅), 6.34 (1H, s, cyclopentadienyl CH), 3.04 (1H, q, $J=5.1$), 2.95-2.80 (2H, m), 2.55 (1H, ddd, $J=5.1, 8.1, 16.17$), 2.37 (1H, dt, $J=5.9, 16.1$), 1.97 (3H, s, cyclopentadienyl CH₃), 2.0-1.85 (3H, m), 1.75-1.40 (7H, m), 1.4-1.2 (2H, m), 1.1-0.95 (1H, m), 0.99 (3H, d, $J=6.6$, menthyl CH₃), 0.77 (3H, d, $J=6.6$, menthyl CH₃), 0.33 (3H, d, $J=6.6$, menthyl CH₃); δ_C (75 MHz, CDCl₃) = 135.4 (s), 133.6 (s), 131.5 (s), 117.0 (s), 115.2 (d), 111.8 (d), 48.3, 40.2 (t), 36.7, 34.2 (t), 29.2, 29.8, 24.8 (t), 24.1, 23.4 (t), 22.4 (t), 22.3, 22.2 (t), 22.0 (t), 18.2, 13.6; m/z (APCI +ve) = 502 (21%, M-Cl+MeCN), 461 (100%, M-Cl); $\nu_{\max} = 2945, 2865$ (CH) cm⁻¹; C₂₅H₃₆ZrCl₂ requires C 60.47, H 7.31, found C 59.48, H 7.20%.

5.2.13 1,2,3,4,5-Pentamethyl-1, 3-cyclopentadiene (22) ⁴³

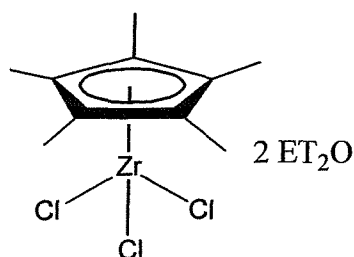


Methyl lithium (54.3 mL, 1.6M in hexanes, 86.8 mmol) was stirred under argon at 0°C and 2,3,4,5-tetramethyl-1, 3-cyclopentenone was added dropwise over 1 h. The solution was allowed to warm to room temperature and stirred overnight.

The yellow solution was quenched with a solution of NH₄Cl (24 g) and HCl (20 mL) in water (100 mL) and washed with this mixture until the aqueous phase was acidic. The aqueous phase was extracted with diethyl ether (3 x 100 mL) and the organic phases combined, dried (MgSO₄) and concentrated *in vacuo* to afford a yellow oil which, upon distillation under reduced pressure (60-62°C at 4 mmHg) gave the title compound (3.03 g, 31%) as a yellow oil. δ_H (300MHz, CDCl₃) 2.4-2.6 (1H, m, CHCH₃), 1.91, 1.86 (2 x 6H, 2 x s, CCH₃), 1.09 (3H, d, $J=7.9$, CHCH₃); $\nu_{\max} = 2955, 2940, 2883, 2870$ (CH), 1442 (CH deformations).

NMR data were in agreement with literature values. ⁴³

5.2.14 1,2,3,4,5-Pentamethyl-1,3-cyclopentadienyl-zirconium trichloride etherate (20)⁴¹



1,2,3,4,5-Pentamethyl-1,3-cyclopentadiene (680 mg, 5 mmol) was dissolved in dry ether under an argon atmosphere and cooled to 0°C before the dropwise addition of *n*-butyl lithium (2 mL, 2.5M in hexanes, 5 mmol). The cloudy colourless solution was allowed to

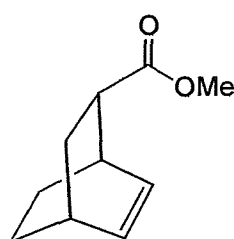
warm to room temperature and stirred for 1 h.

ZrCl₄ (1.165 g, 5 mmol) was added and the mixture stirred for 5 h to give a yellow solution with a white precipitate. The solvent was removed *in vacuo* to give the title compound a white solid contaminated with lithium chloride. (69%, NMR yield based on tetramethylbenzene internal standard). δ_{H} (300MHz, CDCl₃) 2.18 (s, 15H, CH₃), 2.65 (q, $J=7$, ether), 1.24 (t, $J=7$, ether).

NMR data were in agreement with literature values.⁴¹

5.3 Experimental for Chapter 3

5.3.1 Methyl bicyclo[2.2.2]oct-5-ene-2-carboxylate (48)⁵¹

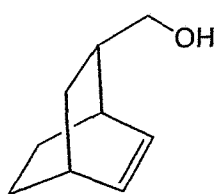


1,3-Cyclohexadiene (47.5g, 594 mmol), methyl acrylate (639.6 g, 457 mmol) and hydroquinone (400 mg) were placed in a Parr pressure reactor and degassed by 3 freeze pump thaw cycles. The vessel was heated to 150°C during which time the pressure rose to 80 psi. After 18 h, the pressure had stabilised at 40 psi. The reactor was

cooled and discharged before the contents were distilled under reduced pressure to give the title compound (63.93g, 84%) as a colourless oil. B.p. = 95-110°C at 19 mmHg (Lit.⁵¹ = 90-94°C at 10 mmHg); δ_{H} (300 MHz, CDCl₃) 6.32, 6.16 (2 x 1H, 2 x t, $J=9$, H-5, H-6), 3.64 (3H, s, OCH₃), 3.0-2.8 (1H, m), 2.7-2.5 (2H, m), 1.9-1.1 (6H, m); ν_{max} = 1682 cm⁻¹ (C=O).

NMR data were in agreement with literature values.⁵¹

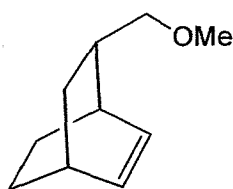
5.3.2 Bicyclo[2.2.2]oct-5-en-2-ylmethanol (49) ⁷⁵



Methyl bicyclo[2.2.2]oct-5-ene-2-carboxylate (96.91 g, 583 mmol) was dissolved in dry diethyl ether (250 mL) before being added dropwise to a slurry of lithium aluminium hydride (33.23 g) in ether (250 mL).

After stirring for 1 h TLC (50% ether/petrol) showed one major product (r.f. 0.4) and no remaining starting material. The mixture was quenched carefully with ethyl acetate and 6M aqueous HCl added to dissolve solids. The aqueous layer was extracted with ethyl acetate (4 x 250 mL) and the organic layers combined, dried (MgSO₄), and concentrated *in vacuo*. The resultant oil was distilled under reduced pressure to give the desired product (71.0 g, 89%) as a colourless oil. B.P. = 109-111 °C at 13 mmHg (Lit. ⁷⁵ = 105 at 9 mmHg); δ_{H} (300 MHz, CDCl₃) 6.29, 6.14 (2 x 1H, 2 x t, $J=7$, H-5, H-6), 3.4-3.1 (2H, m, CH₂OH), 2.62, 2.52 (2 x 1H, 2 x d, $J=4$, H-4, H-1), 2.0-1.0 (7H, m); δ_{C} (75 MHz, CDCl₃) 135.21, 131.87 (2 x CH), 67.69 (CH₂OH), 40.67 (C-1), 31.49 (C-4), 30.33, 29.88 (C-7, C-8), 26.01, 24.87; m/z (APCI +ve) = 139 (18%, M+H), 123 (77%).

5.3.3 5-(Methoxymethyl)bicyclo[2.2.2]oct-2-ene (50)



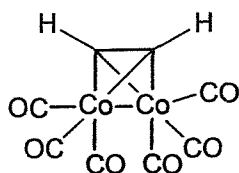
Bicyclo[2.2.2]oct-5-en-2-ylmethanol (40g, 290 mmol) was dissolved in dry ether (150 mL) before being added dropwise to a stirred suspension of NaH (13.9 g, 60% dispersion in mineral oil, washed, 348 mmol) in ether (150 mL). The mixture was stirred at

reflux until the evolution of hydrogen had ceased (5 h).

The mixture was cooled to room temperature before methyl iodide (21.5 mL, 348 mmol) was added and the mixture refluxed overnight after which time GC analysis indicated no remaining starting material. The mixture was diluted with ether (200 mL) and washed with water (3 x 200 mL). The aqueous phase was extracted with ether (3 x 250 mL) and the organic layers combined, dried (MgSO₄), and concentrated *in vacuo* before the resultant oil was purified by flash chromatography (silica, 15% ether/petrol) to give the title compound as a colourless oil (38.8 g, 88%). δ_{H} (300 MHz, CDCl₃) 6.26, 6.12 (2 x 1H, 2 x t, $J=8$, H-2, H-3), 3.30 (3H, s, OCH₃), 3.1-2.8 (2H, m, CH₂OCH₃), 2.65-2.5 (1H, m), 2.5-2.4 (1H, m), 2.1-1.9 (1H, m), 1.67 (1H, ddd, $J=3$, $J=3$, $J=10$),

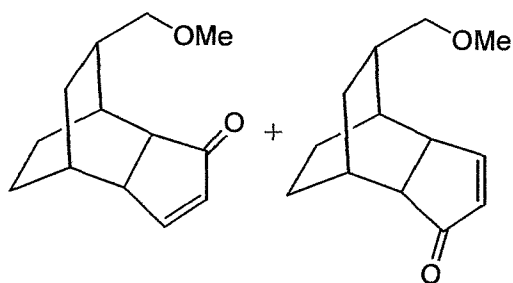
1.6-1.0 (4H, m), 0.8-0.6 (1H m); δ_C (75 MHz, $CDCl_3$) 134.76, 132.10 (2 x CH), 77.85 (OCH₃), 58.80 (CH₂OCH₃), 37.84, 31.53, 30.42, 29.82, 26.00, 24.89; m/z (APCI +ve) = 153 (28%, M+H), 139 (6%, M+H-CH₃); ν_{max} (film) = 3041, 2936, 2862, 2822 (CH) cm^{-1} ; HRMS: Found M^+ , 152.12031, C₁₀H₁₆O requires 152.12012.

5.3.4 Acetylene dicobalt hexacarbonyl (51) ⁷⁶



Dicobalt octacarbonyl (100 g, 292 mmol) was dissolved in petrol (500 mL) in a flask fitted with a dry ice condenser. Purified acetylene was bubbled through the mixture (approx. 1 bubble/sec) for 6 h after which time IR spectroscopy revealed the absence of starting material (by the loss of bridging CO signal). The solvent was removed *in vacuo* to give a black oil which was pre-adsorbed onto neutral alumina before elution through an alumina column (diethyl ether) to give acetylene dicobalt hexacarbonyl (70.1 g, 77%) as a dark red oil. δ_C (75 MHz, $CDCl_3$) = 78.1; ν_{max} (film) = 2958 (CH), 2026 (br, C=O) cm^{-1} .

5.3.5 9-(Methoxymethyl)tricyclo[5.2.2.0^{2,6}]undec-4-en-3-one (52a) and 8-(Methoxymethyl)tricyclo[5.2.2.0^{2,6}]undec-4-en-3-one (52b)



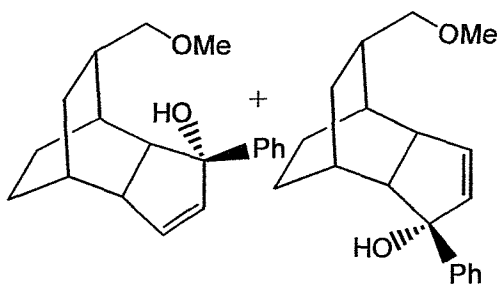
5-(Methoxymethyl)bicyclo[2.2.2]oct-2-ene (14 g, 68.0 mmol) was dissolved in toluene (200 mL) under an argon atmosphere and heated to 80°C before a solution of acetylene-cobalt hexacarbonyl (31.2 g, 74.8 mmol) in toluene (200 mL) was added dropwise over 5 h. GC

analysis showed conversion to be ~50%. After stirring overnight GC analysis still showed conversion to be ~50%. The mixture was preadsorbed onto neutral alumina and flushed through a pad of neutral alumina before the solvent was removed *in vacuo*. The residue was dissolved in 1:1 methanol / water (100 mL) and filtered. Removal of solvents followed by Kugelrohr distillation (135°C at 0.2 mmHg) gave a 1:1 mixture of the title compounds (8.53 g, 45%). δ_H (400 MHz, $CDCl_3$) = 7.64-7.56 (2H, m, enone

CH), 6.25-6.20 (2H, m, enone CH), 3.30 (3H, s, OCH₃), 3.27 (3H, s, OCH₃), 3.35-3.05 (8H, m), 3.05 -2.75 (4H, m), 2.37 (1H, ddd, $J=2.0, 3.8, 6.8$), 2.34-1.45 (6H, m), 1.45-1.08 (4H, m), 1.04-0.93 (2H, m), 0.69-0.61 (1H, m); δ_C (75 MHz, CDCl₃) = 169.3, 168.5 (2 x d, $\underline{\text{C}}\text{H}=\text{CH}=\text{O}$), 135.6, 135.3 (2 x d, $\text{CH}=\underline{\text{C}}\text{H}=\text{O}$), 76.2, 75.8 (2 x $\underline{\text{C}}\text{H}_2\text{OCH}_3$), 59.0 (2 x $\text{CH}_2\text{O}\underline{\text{C}}\text{H}_3$), 48.6, 46.4, 44.0, 41.1, 36.8, 36.2, 31.3, 31.6, 30.2, 29.7, 29.3, 28.9, 22.6, 22.4, 21.3, 21.1; m/z (APCI +ve) = 175 (18% M+H-MeOH), 207 (100%, M+H); ν_{max} = 2935, 2868 (CH), 1737, 1699 (C=O) cm^{-1} ; C₁₃H₁₈O₂ requires C 74.97, H 8.39, found C 74.94, H 8.89%.

Separation of the two isomers was not possible so the mixture was used in the next step without further purification.

5.3.6 (3R)-8-(Methoxymethyl)-3-phenyltricyclo[5.2.2.0^{2,6}]undec-4-en-3-ol (57) and (3R)-9-(methoxymethyl)-3-phenyltricyclo[5.2.2.0^{2,6}]undec-4-en-3-ol (58)



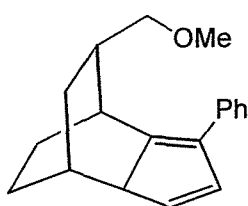
A mixture of 9-(methoxymethyl)tricyclo[5.2.2.0^{2,6}]undec-4-en-3-one and 8-(methoxymethyl)tricyclo[5.2.2.0^{2,6}]undec-4-en-3-one (3.09 g, 15 mmol) was dissolved in THF (40 mL) and cooled to -78°C before dropwise

addition of phenyl lithium (7.5 mL, 2.0M solution in ether, 8.25 mmol). After 5 min TLC (50% ether/hexane) showed no starting material and two products. The reaction was quenched with saturated aqueous sodium bicarbonate solution (30 mL) and diluted with ether (50 mL). The aqueous layer was extracted with ether (3 x 70 mL) and the organic layers combined, dried (MgSO₄) and concentrated *in vacuo*. Column chromatography (silica, 15% ether/petrol) to separate the isomers followed by recrystallisation (ether / petrol) afforded the title compounds as white crystalline solids. R.f. = 0.35, (294 mg, 34%) M.p. (ether / petrol) = 109-110.5 °C; δ_H (300 MHz, CDCl₃) 7.4-7.1 (5H, m, Ph), 6.03 (1H, dd, $J=1.5, 5.5$, H-5), 5.82 (1H, dd, $J=2.5, 5.9$, H-4), 3.33 (3H, s, OCH₃), 3.4-3.15 (2H, m, $\underline{\text{C}}\text{H}_2\text{OCH}_3$), 3.0-2.9 (1H, m CH), 2.97 (1H ddd, $J=2.0, 4.0, 8.9$, Bridgehead CH), 2.23 (1H, d br, ($J=8.9$ Bridgehead CH), 2.1-1.7 (5H, m), 1.6 - 1.2 (3H, m), 0.97 (1H, ddd, $J=3.0, 7.0, 12.6$); δ_C (75 MHz, CDCl₃) 136.8, 136.5 (2 x

alkene CH), 128.3 (2 x phenyl CH), 126.6 (phenyl CH), 124.2 (2 x phenyl CH), 76.4 (CH₂OCH₃), 58.7 (OCH₃), 52.1, 43.6, 35.9, 31.3, 29.1, 26.3, 22.7, 21.4; *m/z* (APCI +ve) = 268 (16%, M+H-OH), 267 (100%, M-OH), 253 (6%, M-OCH₃), 235 (21%, M-OH-OCH₃); ν_{\max} = 3471 (OH), 2970, 2928, 2856 (CH) cm⁻¹; C₁₉H₂₄O₂ requires C 80.24%, H 8.51%, found C 80.05%, H 8.48%.

R.f. = 0.25, (421 mg, 49%) M.p. (ether / petrol) = 98-99.5 °C; δ_{H} (300 MHz, CDCl₃) 7.5-7.2 (5H, m, Ph), 6.03 (1H, dd, *J*=6.4, 8.4, alkene CH), 5.846 (1H, dd, *J*=2.5, 5.9, alkene CH), 3.4-3.35 (1H, m), 3.30 (3H, s, OCH₃), 3.3-3.15 (1H, m, CH₂OCH₃), 2.79 (1H, ddd, *J*= 2.0, 4.0, 8.9, CH), 2.5-2.2 (1H, m), 2.2-1.15 (8H, m), 1.0-0.8 (2H, m); δ_{C} (75 MHz, CDCl₃) 137.727, 135.803 (2 x alkene CH), 128.329 (2 x phenyl CH), 126.613 (phenyl CH), 124.257 (2 x phenyl CH), 75.759 (CH₂OCH₃), 58.733 (OCH₃), 49.139, 46.434, 36.269, 30.538, 28.530, 27.345, 22.910, 21.265; *m/z* (APCI +ve) = 268 (12%, M+H-OH), 267 (100%, M-OH), 235 (24%, M-OH-OCH₃); ν_{\max} = 3394 (OH), 2922, 2858 (CH) cm⁻¹; C₁₉H₂₄O₂ requires C 80.24%, H 8.51%, found C 79.82%, H 8.63%. Single crystal X-ray analysis confirmed this compound to be (3*R*)-9-(Methoxymethyl)-3-phenyltricyclo[5.2.2.0^{2,6}]undec-4-en-3-ol **58**.

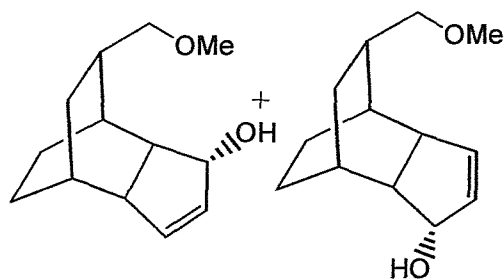
5.3.7 9-(Methoxymethyl)-3-phenyltricyclo[5.2.2.0^{2,6}]undeca-2,5-diene (**59**)



(3*R*)-9-(Methoxymethyl)-3-phenyltricyclo[5.2.2.0^{2,6}]undec-4-en-3-ol (284 mg, 1 mmol) was dissolved in chloroform (30 mL) and solid *p*-toluenesulphonic acid (10 mg) was added. After 5 min the solution was filtered through a pad of basic alumina and the solvents removed *in vacuo* to afford the title compound as a colourless oil (260 mg, 97%). δ_{C} (75 MHz, CDCl₃) = 149.9, 135.9 (2 x s), 128.3 (2 x d, Ph CH), 127.6 (s), 126.4 (2 x d, Ph CH), 125.1, 88.7 (t, CH₂OCH₃), 76.5 (q, CH₂OCH₃), 58.7, 46.8, 42.0, 35.9(4 x d), 30.9(t), 29.4, 27.0(2 x d), 21.3, 20.6 (2 x t); *m/z* (APCI +ve) = 267 (100%, M+H).

The compound was found to be highly unstable in solution and further characterisation proved difficult. The compound was used immediately in subsequent complexation reactions.

5.3.8 (3R)-9-(Methoxymethyl) tricyclo[5.2.2.0^{2,6}]undec-4-en-3-ol (62) and (3R)-8-(methoxymethyl)-tricyclo[5.2.2.0^{2,6}]undec-4-en-3-ol (63)



A mixture of 9-(methoxymethyl)tricyclo[5.2.2.0^{2,6}]undec-4-en-3-one and 8-(methoxymethyl)tricyclo[5.2.2.0^{2,6}]undec-4-en-3-one (2.06 g, 10 mmol) and cerium trichloride (4.47 g, 12 mmol) was dissolved in methanol

(25 mL) and stirred at room temperature before addition of sodium borohydride (453 mg, 12 mmol) in one portion. After 5 min, TLC (50% ether / petrol) showed no starting material and two products. The reaction was quenched with saturated aqueous ammonium chloride solution (25 mL) and diluted with ether (25 mL). The aqueous layer was extracted with ether (3 x 25 mL) and the organic layers combined, dried (MgSO₄) and concentrated *in vacuo*. Column chromatography (silica, 20% ether/petrol) afforded a mixture of the title compounds as a colourless oil. (1.59 g, 76%).

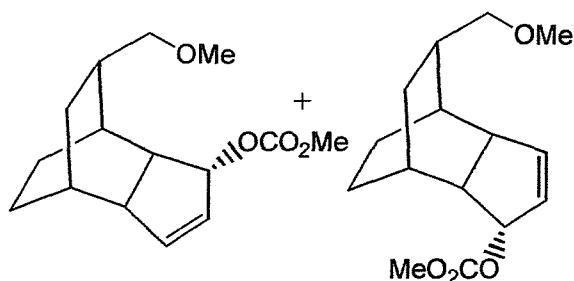
As both of these compounds lead to the same product, subsequent reactions were carried out on the mixture.

Careful column chromatography on a small portion (silica, 20% ether/petrol) afforded the individual compounds.

R.f = 3.0 (major isomer); δ_{H} (300 MHz, CDCl₃) 5.88-5.78 (2H, m, H-4, H-5), 5.02-5.16 (1H, m, CHOH), 3.35 (3H, s, OCH₃), 3.45-3.15 (2H, m, CH_2CH_3), 2.65-2.45 (1H, m), 2.10-1.15 (10H, m), 1.05-0.95 (1H, m); δ_{C} (75 MHz, CDCl₃) 136.1, 134.5 (C-4, C-5), 79.8 (C-3), 75.9 (CH_2OCH_3), 58.9 (OCH₃), 48.8, 36.6, 36.1, 30.5, 28.6, 25.8, 23.0, 21.3; m/z (APCI +ve) = 191 (100% M+H-H₂O).

R.f = 2.5 (minor isomer); δ_{H} (300 MHz, CDCl₃) 5.88-5.77 (2H, m, H-4, H-5), 5.07 (1H, d, $J = 8.5$, CHOH), 3.33 (3H, s, OCH₃), 3.41-3.22 (2H, m, CH_2OCH_3), 2.76 (1H, dd, $J = 1.8$, $J = 9.3$), 2.28 (1H, tt, $J = 2.0$, $J = 9.1$), 2.13-2.00 (1H, m), 1.88-1.54 (5H, m), 1.37-1.17 (2H, m), 1.05-0.95 (1H, m); δ_{C} (75 MHz, CDCl₃) 136.4, 133.7, (C-4, C-5), 80.1 (C-3), 76.7 (CH_2OCH_3), 58.9 (OCH₃), 43.22, 42.5, 36.0, 31.3 (t, CH₂), 29.1, 25.2, 22.7 (t, CH₂), 21.6 (t, CH₂); m/z (APCI +ve) = 191 (100% M+H-H₂O).

5.3.9 (3S)-8-(Methoxymethyl)tricyclo[5.2.2.0^{2,6}]undec-4-en-3-yl methyl carbonate (67a) and (3R)-9-(methoxymethyl)tricyclo[5.2.2.0^{2,6}]undec-4-en-3-yl methyl carbonate (67b)

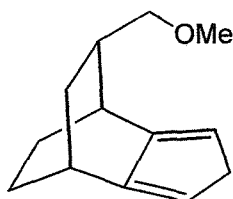


A mixture of (3R)-9-(methoxymethyl)tricyclo[5.2.2.0^{2,6}]undec-4-en-3-ol and (3R)-8-(methoxymethyl)tricyclo[5.2.2.0^{2,6}]undec-4-en-3-ol (1.8 g, 8.6 mmol) and pyridine (816 mg, 10.3 mmol) was dissolved in DCM (40 mL) at

0°C before dropwise addition of methyl chloroformate (0.8 mL, 10.3 mmol). The mixture was allowed to warm to room temperature over 15 min after which time TLC (1:1 ether/hexane) showed no remaining starting material and one product spot (R.f.=0.6). The reaction was quenched with 2M HCl (50 mL) and diluted with ether (50 mL). The organic layer was washed with 2M HCl (2 x 50 mL) and saturated aqueous sodium bicarbonate solution (3 x 50 mL) before being dried and concentrated *in vacuo*. Flash chromatography of the residue (SiO₂, 10% ether in hexane) afforded a mixture of the title compounds (1.81 g, 79%); δ_{H} (300 MHz, CDCl₃) 6.0-5.9 (2H, m, 2 x alkene CH), 5.9-5.75 (2H, m, 2 x alkene CH), 3.77 (6H, s, 2 x OCO₂CH₃), 3.35 (6H, s, CH₂OCH₃), 3.4-3.2 (4H, m, CH₂OCH₃), 2.9-2.4 (4H, m), 2.2-1.15 (14H, m), 1.1-0.9 (6H, m); δ_{C} (75 MHz, CDCl₃) 139.0, 138.5 (2 x d, 2 x alkene CH), 130.0, 129.2 (2 x d, 2 x alkene CH), 86.1, 85.6 (2 x q, 2 x OCO₂CH₃), 76.5, 76.0 (2 x t, 2 x CH₂OCH₃), 58.8, 58.7 (2 x q, 2 x CH₂OCH₃), 54.6, 48.5, 43.0, 41.1, 36.0, 35.9, 35.5, 30.9, 30.6, 28.6, 28.1, 26.6, 26.4, 25.7, 22.4, 22.2, 21.0, 20.6; *m/z* (APCI +ve)= 191 (100% M+H-CO₂CH₃); ν_{max} = 2923 (OH), 1724 (C=O) cm⁻¹.

As the mixture could not be separated and both compounds lead to the same product, subsequent reactions were carried out on the mixture.

5.3.10 8-(Methoxymethyl)tricyclo[5.2.2.0^{2,6}]undeca-2,5-diene (64)



+ isomers

$\text{Pd}(\text{OAc})_2$ (145 mg, 0.65 mmol) was suspended in THF (15 mL) and PBU_3 (202 mg, 0.65 mmol) was added dropwise to give a yellowish solution which was stirred for 10 min. A solution of (3*S*)-8-(methoxymethyl)tricyclo[5.2.2.0^{2,6}]undec-4-en-3-yl methyl carbonate and (3*R*)-9-(methoxymethyl)tricyclo[5.2.2.0^{2,6}]undec-4-en-3-yl methyl carbonate (1.73 g, 6.5 mmol) in THF (45 mL) was added and the mixture heated to reflux. The black mixture was stirred at reflux for 24 h after which time TLC analysis (10% ether / petrol) revealed no remaining starting material. The solvent was removed *in vacuo* and the resultant black oil subjected to column chromatography (SiO_2 , 5% ether / petrol) to give the title compound as a mixture of isomers and as a colourless oil. (933 mg, 73%).

GC analysis (HP5 column, 140°C isothermal) showed a mixture of 2 components, R.T. = 5.08 min (73.2%) and R.T. = 6.04 min (26.9%). GCMS analysis showed both peaks to have identical mass spectra. m/z (EI) = 118 (100%), 190 (70%, M^+).

Proton NMR spectrum was broad and complicated due to a mixture of isomers being present:

δ_{H} (300 MHz, C_6D_6) = 6.21 (1H, s br, cyclopentadienyl CH), 6.12 (1H, s br, cyclopentadienyl CH), 6.07 (1H, s br, cyclopentadienyl CH), 3.50-3.05 (15H, m), 3.36 (1H, s, minor OCH_3), 3.34 (3H, s, major OCH_3), 2.95-2.85 (2H, m), 2.20-1.95 (3H, m), 1.95-1.65 (9H, m), 1.35-1.20 (2H, m).

Carbon data for major isomer:

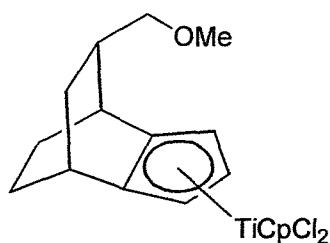
δ_{C} (75 MHz, C_6D_6) = 151.0, 148.8 (2 x s, 2 x alkene Cq), 121.4, 118.2, (2 x d, 2 x alkene CH), 77.3, (t, CH_2OCH_3), 58.6 (q, CH_2OCH_3), 41.4 (t), 37.4 (d), 32.3 (d), 31.7 (t), 30.6 (d), 27.2, (t), 21.1 (t).

Carbon data for minor isomer (some peaks missing):

δ_{C} (75 MHz, C_6D_6) = 152.0, 151.3 (2 x s, 2 x alkene Cq), 118.7, (d, alkene CH), 75.9 (t, CH_2OCH_3), 58.6 (q, CH_2OCH_3), 36.9 (d), 30.5 (d), 31.5 (d), 27.4 (t), 26.5;

ν_{max} = 2936, 2863 (CH) cm^{-1} .

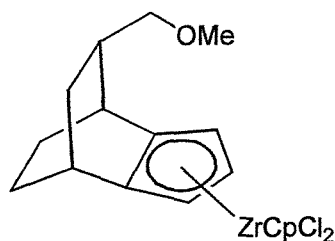
5.3.11 Cyclopentadienyl-(8-(methoxymethyl)tricyclo[5.2.2.0^{2,6}]undeca-2,5-dienyl) titanium dichloride (70)



A solution of 8-(methoxymethyl) tricyclo[5.2.2.0^{2,6}]undeca-2,5-diene (190 mg, 1 mmol) in THF (20 mL) was cooled to -78°C before dropwise addition of *n*-butyl lithium (0.4 mL, 2.5M solution in hexanes, 1 mmol). The solution was allowed to warm to room temperature and stirred for 2 h.

The yellow solution was cooled again to -78°C and solid CpTiCl₃ (241 mg, 1.1mmol) was added *via* a solid addition tube. The solution immediately turned deep red and was stirred overnight. The solvent was removed and the residue extracted into 1:1 toluene / hexane (50 mL) and the extracts cooled to -5°C overnight after which time a deep red precipitate had formed. The supernatant was removed and the solid dried *in vacuo* to afford the title compound as a dark red solid (150 mg, 40%). M.p. (toluene / hexane) = 148°C (dec.); δ_{H} (400 MHz, C₆D₆) = 6.45-6.37 (1H, m, cyclopentadienyl CH), 6.34 (5H, s, C₅H₅), 6.15 (1H, t, *J*=2.0, cyclopentadienyl CH), 6.04 (1H, t, *J*=2.0, cyclopentadienyl CH), 3.25-3.15 (1H, m, CH), 3.12 (3H, s, CH₂OCH₃), 2.84 (1H, q, *J*=2.8, CH), 2.46, (1H, dd, *J*=8.8, 5.7, 1 x CH₂OCH₃), 2.19 (1H, t, 1 x CH₂OCH₃), 2.2-2.05 (1H, m, CH), 1.80 (1H, ddd, *J*=12.1, 8.3, 3.3), 1.68-1.58 (2H, m), 1.45-1.25 (2H, m), 0.29 (1H, ddt, *J*=12.9, 4.7, 4.8, 1 x CH₂); δ_{C} (100 MHz, C₆D₆) = 146.3 (s), 125.0 (d, cyclopentadienyl CH), 119.6 (5 x d, C₅H₅), 113.2, 112.7 (2 x d, 2 x cyclopentadienyl CH), 76.0 (t, CH₂OCH₃), 58.7 (q, CH₂OCH₃), 40.2, 33.7 (2 x d, 2 x CH), 33.5 (t, CH₂), 32.4 (d, CH), 25.9, 25.2 (2 x t, 2 x CH₂); *m/z* (APCI +ve) = 378 (79%, M+H - Cl + MeCN), 337 (100%, M+H - Cl), 234 (66%, CpTiCl₂ + MeCN); ν_{max} (ATR) = 3419 (w), 2936, 2873 (CH) cm⁻¹; HRMS : Found M⁺ 372.05271, C₁₈H₂₂TiOCl₂ requires 372.05272.

5.3.12 Cyclopentadienyl-(8-(methoxymethyl)tricyclo[5.2.2.0^{2,6}]undeca-2,5-dienyl) zirconium dichloride (71)

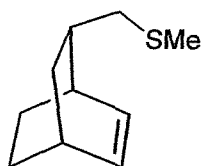


A solution of 8-(methoxymethyl)tricyclo[5.2.2.0^{2,6}]undeca-2,5-diene (190 mg, 1 mmol) in THF (20 mL) was cooled to -78°C before dropwise addition of *n*-butyl lithium (0.4 mL, 2.5M solution in hexanes, 1 mmol). The solution was allowed to warm to room temperature and stirred for 2 h.

The yellow solution was cooled again to -78°C and solid CpZrCl₃•2THF (406 mg, 1.1mmol) was added *via* a solid addition tube. The yellow solution was stirred overnight after which time it had turned a greenish colour. The solvent was removed and the residue taken up in 50% toluene / hexane. Centrifugation gave a yellow solution which was decanted off and the solvent removed *in vacuo* to give the title compound (154 mg, 37%) as a greenish foam.

Analysis of this compound was difficult as it proved to be unstable to air and light. However, comparison of the crude proton and carbon spectra indicated similar structure to the titanium analogue and therefore it was postulated that the metal was on the same face as in the previous case. See Chapter 3 for discussion.

5.3.13 6-((Methylsulphanyl)methyl)bicyclo[2.2.2]oct-2-ene (80)



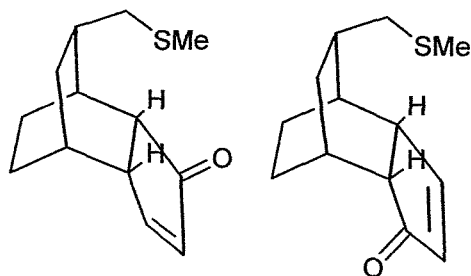
[3-(Hydroxymethyl)bicyclo[2.2.2]oct-5-en-2-yl]methanol (1.38 g, 10 mmol) and pyridine (0.96 mL, 12 mmol) were dissolved in dry DCM (50 mL) and cooled to -78°C before dropwise addition of trifluoromethane sulphonyl anhydride (3.38 g, 12 mmol). The

mixture was allowed to warm to room temperature over 2 h before removal of solvents *in vacuo* to give a blue oil which was dissolved in THF (20 mL) and stirred at -78°C.

Methyl disulphide (1.1 mL, 12 mmol) was dissolved in THF (20 mL) at -78°C before dropwise addition of *n*-butyl lithium (4.8 mL, 2.5M solution in hexanes, 12 mmol). The solution was allowed to warm to room temperature over 2 h before dropwise addition to the first solution.

The mixture was stirred overnight after which time TLC (50% ether / petrol) showed no remaining starting material and one non-polar product (R.f.=0.8). The mixture was diluted with ether (100 mL) and washed with water (3 x 100 mL). The aqueous phase was extracted with ether (3 x 100 mL) and the organic layers combined, dried (MgSO₄), and concentrated *in vacuo*. The resultant oil was flushed through silica (petrol) to give the title compound as a colourless oil (1.3 g, 82%). δ_{H} (300 MHz, CDCl₃) 6.27 (1H, t, $J=7.0$, alkene CH), 6.11 (1H, t, $J=7.0$, alkene CH), 2.65-2.45 (2H, m, bridgehead CH), 2.07 (3H, s, SCH₃), 2.32 (1H, dd, $J=12.4, 7.4$, CH₂SCH₃), 2.18 (1H, dd, $J=12.4, 7.4$, CH₂SCH₃), 1.76 (1H, dt, $J=12.4, 2.5$, CHCH₂SCH₃), 1.55-1.44 (2H, m), 1.35-1.15 (2H, m), 0.95-0.85 (2H, m); δ_{C} (75 MHz, CDCl₃) 135.1, 131.7 (2 x d, 2 x alkene CH), 42.1 (t, CH₂SCH₃), 37.3, 34.2 (t), 33.9, 30.2, 26.2 (t), 24.6 (t), 15.9; m/z (APCI +ve) = 153 (28%, M+H), 139 (6%, M+H-CH₃); ν_{max} (ATR) = 3040 (w, CH str), 2934 (s, CH₂ str), 2861 (m, CH₂ str) cm⁻¹; HRMS: Found M⁺ 168.0972. C₁₀H₁₆S requires 168.0973.

**5.3.14 9-((Methylsulphonyl)methyl)tricyclo[5.2.2.0^{2,6}]undec-4-en-3-one (81a)
and 8-((Methylsulphonyl)methyl)tricyclo[5.2.2.0^{2,6}]undec-4-en-3-one (81b)**

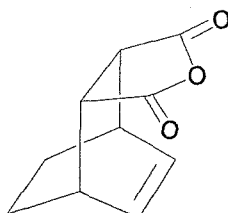


6-((Methylsulphonyl)methyl)bicyclo[2.2.2]oct-2-ene (1.08 g, 6.4 mmol) was dissolved in toluene (20 mL) under an argon atmosphere and heated to 80°C before a solution of acetylene-

dicobalt hexacarbonyl (4.0 g, 12.8 mmol) in toluene (20 mL) was added dropwise over 5 h. After stirring overnight the mixture was preadsorbed onto neutral alumina and flushed through a pad of neutral alumina before the solvent was removed *in vacuo*. The resultant oil was dissolved in ether and ethylene diamine (1 mL) was added before the mixture was flushed through a pad of silica (ether) to give a 1:1 mixture of the title compounds (403 mg, 28%). δ_{H} (300 MHz, CDCl₃) 7.72-7.60 (2H, m, alkene CH), 6.31-6.25 (2H, m, alkene CH), 3.1-2.8 (2H, m), 2.65-2.10 (6H, m), 2.35-1.85 (8H, m), 2.11 (3H, s, SCH₃), 2.10 (3H, s, SCH₃), 1.7-1.55 (1H, m), 1.5-1.1 (9H, m); δ_{C} (75 MHz, CDCl₃) 214.2, 213.3 (2 x s, 2 x C=O), 168.9, 168.3 (2 x d, 2 x CH=CHC=O), 135.5, 135.3 (2 x d, 2 x CH=C=O), 48.3, 43.4, 40.6, 40.3, 40.1 (t), 39.9, 36.0, 35.4, 35.0 (t),

34.1 (t), 33.7, 29.9, 29.1, 22.7 (t), 22.5, 20.8 (t), 20.7 (t), 19.8, 15.9, 15.7; m/z (APCI +ve) = 223 (100%, M+H); ν_{\max} (golden gate) = 2912 (m, CH₂ str), 2867 (w, CH₂ str), 1696 (s, C=O) cm⁻¹.

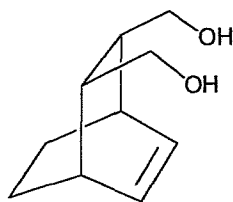
5.3.15 4-Oxatricyclo[5.2.2.0^{2,6}]undec-8-ene-3,5-dione. (72)⁶⁶



A mixture of 1,3-cyclohexadiene (20.8 g, 260 mmol) and maleic anhydride (25.5 g, 260 mmol) was stirred at room temperature for 24 h after which time a white precipitate had formed. The solid was isolated by filtration and recrystallised (ether / petrol) to give the title compound as a white crystalline solid and a single diastereoisomer (30.31 g, 65%). M.p. (ether / petrol) = 157-158°C; δ_{H} (300 MHz, CDCl₃) 6.34, 6.31 (m, 2H, alkene CH), 3.24 (2H t, $J=1.5$, bridgehead CH), 3.14 (2H, d, $J=1.5$, CH), 1.61, 1.41 (2 x 2H, 2 x d, $J=7.3$, 2 x CH₂); δ_{C} (75 MHz, CDCl₃) 172.97, (C=O), 133.19 (alkene CH), 44.91 (bridgehead CH), 31.77 (CH), 23.11 (CH₂); ν_{\max} (DCM) = 2945 (CH), 1837 (C=O), 1779 (C=O)cm⁻¹; m/z (APCI -ve) = 177 (M-H).

Proton NMR data were in agreement with literature values.⁶⁶

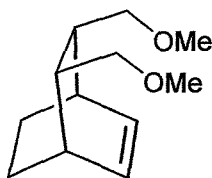
5.3.16 [3-(Hydroxymethyl)bicyclo[2.2.2]oct-5-en-2-yl]methanol (75)⁶⁷



A solution of 4-oxatricyclo[5.2.2.0^{2,6}]undec-8-ene-3,5-dione (30 g, 178 mmol) in THF (100 mL) was added dropwise to a stirred suspension of lithium aluminium hydride (7.75 g, 204 mmol) in THF (100 mL) at room temperature. The mixture was stirred for 18 h after which time TLC (ether) indicated no remaining starting material. The mixture was quenched carefully with water and the inorganic residues dissolved in 6M aqueous HCl. The mixture was extracted with ethyl acetate (5 x 150 mL) and the combined organic extracts washed with brine (3 x 100 mL) before drying over magnesium sulphate. The solvents were removed *in vacuo* to give the title compound (19.5 g, 78%) as a white crystalline solid. M.p. (ether) = 104-106°C; δ_{H} (300 MHz, CDCl₃) = 6.15 (2H, m, 2 x alkene CH), 3.95 (2H, s, 2 x OH), 3.53, 3.50 (2 x 2H, 2x d $J=3.7$, CH₂OH), 2.43 (2H, s br, CH), 2.23 (2H, m), 1.60-1.45 (2H, m, CH₂) 1.30-1.15 (2H, m, CH₂).

Proton NMR data were in agreement with literature values.⁶⁷

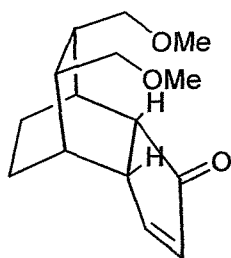
5.3.17 5,6-Di(methoxymethyl)bicyclo[2.2.2]oct-2-ene (73)



[3-(Hydroxymethyl)bicyclo[2.2.2]oct-5-en-2-yl]methanol (8.2 g, 48 mmol) was dissolved in dry THF (50mL) before being added dropwise to a stirred suspension of NaH (5.8 g, 60% dispersion in mineral oil, washed, 145mmol) in ether (50 mL).

The mixture was stirred at reflux until the evolution of hydrogen had ceased (18 h). The mixture was cooled to room temperature before methyl iodide (10.24 g, 72 mmol) was added and the mixture stirred for 5 h before addition of further methyl iodide (10.24 g, 72 mmol). The mixture was stirred overnight after which time TLC (ether) showed no remaining starting material. The mixture was diluted with ether (100 mL) and washed with water (3 x 100 mL). The aqueous phase was extracted with ether (3 x 100 mL) and the organic layers combined, dried (MgSO₄), and concentrated *in vacuo* before the resultant oil was purified by Kugelrohr distillation to give the title compound (8.2 g, 87%) as a colourless oil. δ_{H} (300 MHz, CDCl₃) 6.21 (2H, dd, $J= 2.9, 4.4$, alkene CH), 3.29 (6H, s, OCH₃), 3.26 (2H, dd, $J= 6.6, 8.8$, CH₂OCH₃), 3.05 (2H, t, $J= 8.8$, CH₂OCH₃), 2.7-2.55 (2H, m, CH bridgehead), 2.22-2.09 (2H, m, CH), 1.57-1.48 (2H, m, CH₂), 1.31-1.20 (2H, m, CH₂); δ_{C} (75 MHz, CDCl₃) 133.4 (d, alkene CH), 73.5 (t, CH₂OCH₃), 58.6 (q, CH₂OCH₃), 41.7 (d, bridgehead CH), 32.8 (d, CHCH₂OCH₃), 25.4 (t, alkyl CH₂); ν_{max} (CH₂Cl₂, solution)= 2860 (CH) cm⁻¹; m/z (APCI +ve) = 197 (13%, M+H), 165 (100%, M+H-MeOH), 133 (21%, M+H-2MeOH).

5.3.18 8,9-Di (methoxymethyl)tricyclo[5.2.2.0^{2,6}]undec-4-en-3-one (74)



5,6-Di(methoxymethyl)bicyclo[2.2.2]oct-2-ene (8 g, 40.8 mmol) was dissolved in toluene (100 mL) under an argon atmosphere and heated to 80°C before a solution of acetylene-cobalt hexacarbonyl (29 g, 92 mmol) in toluene (100 mL) was added dropwise over 5 h after which time the mixture was stirred at 80°C for 18 h. The mixture was pre adsorbed onto neutral alumina and flushed through a pad of neutral alumina before the solvent was removed *in vacuo*. Extraction into 50% methanol / water and removal of solvents before Kugelrohr distillation (135°C at 0.2 mmHg) gave the title compound (4.1 g, 25%) as a colourless oil. δ_{H} (300 MHz, CDCl_3) 7.60 (1H, dd, $J=2.2, 5.9$, alkene CH), 6.17 (1H, dd, $J=2.2, 5.9$, alkene CH), 3.50 (1H, dd, $J=5.9, 9.6$, CH_2OCH_3), 3.46-3.35 (2H, m, CH_2OCH_3), 3.28 (1H, dd, $J=5.9, 9.6$, CH_2OCH_3), 3.24 (3H, s, OCH_3), 3.21 (3H, s, OCH_3), 3.02-3.95 (1H, m), 2.35-2.26 (1H, m), 2.25-2.16 (1H, m), 2.14-2.02 (2H, m), 2.01-1.95 (1H, m), 1.4-1.26 (2H, m), 1.25-1.1 (2H, m); δ_{C} (75 MHz, CDCl_3) 214.4 (s, Cq), 169.2, 135.4 (2 x d, 2 x alkene CH), 72.2, 71.5 (2 x t, 2 x CH_2OCH_3), 58.9, 58.8 (2 x q, 2 x OCH_3), 44.1, 41.1, 39.5, 38.8, 32.6, 30.4 (6 x d, 6 x CH), 22.6, 22.3 (2 x t, 2 x CH_2); ν_{max} (ATR) = 2869 (m, CH_2 str), 1693 (s, C=O) cm^{-1} ; m/z (APCI +ve) = 251 (33%, M+H), 218 (100%, M+H-MeOH).

5.4 Propene polymerisation (representative procedure)

A solution of methylalumoxane (2.6 mL, 10% wt solution in toluene, added to 20 mL toluene) was degassed by three freeze pump thaw cycles and saturated with propene by vigorous stirring under a pressure of 2 psi above atmospheric. Injecting a solution of bis neoisomenthyl-indenyl zirconium dichloride (0.8 mg) in toluene (1 mL) started the reaction which was allowed to continue for 1 h before quenching with 5% HCl in methanol. The organic layer was washed with water (3 x 25 mL) and the organic phase dried and concentrated *in vacuo* before the residue was dried under vacuum until constant mass.

6 References

- 1) M. Bochmann. *Organometallics 2 - Complexes with Transition Metal Carbon p-bonds*; Oxford University Press: Oxford, 1994; Vol. 13, pp 43-65.
- 2) C. Elschenbroich and A. Saltzer *Organometallics, A Concise Introduction*; 2nd. ed.; VCH Verlagsgesellschaft mbH: Weinheim, Germany, 1992.
- 3) A.H. Hoveyda and J.P. Morken. *Angew.Chem. Int. Ed. Engl.* **1996**, *35*, 1262-1284.
- 4) R.D. Broene and S.L. Buchwald. *J. Am. Chem. Soc.* **1993**, *115*, 12569-12570.
- 5) C.A. Willoughby and S.L. Buchwald. *J. Org. Chem.* **1993**, *58*, 7626-7629.
- 6) C.A. Willoughby and S.L. Buchwald. *J. Am. Chem. Soc* **1993**, *114*, 7562-7564.
- 7) L. Bell and R.J. Whitby. *Tetrahedron. Lett.* **1996**, *37*, 7139-7142.
- 8) L. Bell, D.C. Brookings, G.J. Dawson, R.J. Whitby, R.V.H. Jones and M.C.H. Standen. *Tetrahedron* **1998**, *54*, 14617-15634.
- 9) G. Dawson, C.A. Durrant, G.G. Kirk and R.J. Whitby. *Tetrahedron. Lett.* **1997**, *38*, 2335-2338.
- 10) *Sigma-Aldrich Prices 1999-2000*: Cp_2TiCl_2 £1.36/g, Cp_2ZrCl_2 £1.41/g, Cp_2HfCl_2 £14.51/g.
- 11) B. Chin and S.L. Buchwald. *J. Org. Chem.* **1997**, *62*, 2267-2268.
- 12) L.A. Paquette, M.L. McLoughlin and J.A. McKinney. *Tetrahedron. Lett.* **1986**, *27*,
- 13) L.A. Paquette, K.J. Moriarty and R.D. Rodger. *Organometallics.* **1989**, *8*,
- 14) L.A. Paquette. *Organometallics* **1989**, *8*, 2159.
- 15) D.C. Brookings *Ph.D. Thesis*; University of Southampton, 1999.
- 16) G. Erker, M. Aulbach, M. Knickermeier, D. Wingbermühle, C. Kruger, M. Nolte and S. Werner. *J. Am. Chem. Soc.* **1993**, *115*, 4590-4601.
- 17) K. Zeigler, E. Holzkamp, H. Breil and H. Martin. *Angew. Chem.* **1955**, *67*, 541.
- 18) K. Zeigler. *Angew. Chem.* **1964**, *76*, 545.
- 19) G. Natta. *Angew. Chem.* **1964**, *76*, 553.
- 20) G. Natta. *Angew. Chem.* **1956**, *68*, 393
- 21) G. Wilkinson, P.L. Pauson, J.M. Birmingham and F.A. Cotton. *J. Am. Chem. Soc.* **1953**, *75* 1011,

- 22) A.A. Anderson, H.G. Cordes, J. Herwig, W. Kaminsky, A. Merck, R. Mottweiler, J. Pein, H. Sinn and H.J. Vollmer. *Angew. Chem.* **1976**, *88*, 689.
- 23) A.A. Anderson, H.G. Cordes, J. Herwig, W. Kaminsky, A. Merck, R. Mottweiler, J. Pein, H. Sinn and H.J. Vollmer. *Angew. Chem. Int. Ed. Engl.* **1976**, *15*, 630.
- 24) M. Bochmann. *J. Chem. Soc., Dalton Trans.* **1996**, 255-270.
- 25) J.A. Ewen. *J. Am. Chem. Soc.* **1984**, *106*, 6335.
- 26) R.M. Waymouth and G.W. Coates. *Science* **1995**, *267*, 222.
- 27) R. Ugo. *Aspects of Homogeneous Catalysis*. **1984**, *Vol 5*, 79-196
- 28) J.B. Jaquith, C.J. Levy, G.V. Bondar, S. Wang and S. Collins. *Organometallics* **1998**, *17*, 914-925.
- 29) C.J. Rousset, D.R. Swanson, F. Lamatay and E.-i. Negishi. *Tetrahedron Lett.* **1989**, *30*, 5105-5108.
- 30) W.A. Nugent and D.F. Taber. *J. Am. Chem. Soc.* **1989**, *111*, 6435-6437.
- 31) K.S. Knight and R.M. Waymouth. *Organometallics* **1994**, *13*, 2575-2577.
- 32) J.P. Morken, M.T. Diduik and A.H. Hoveyda. *J. Am. Chem. Soc.* **1993**, *115*, 6997-6998.
- 33) U.M. Dzhemilev and A.G. Ibragimov. *J. Organomet. Chem* **1994**, *466*, 1-4.
- 34) E.-i. Negishi and D.Y. Kondakov. *J. Am. Chem. Soc.* **1996**, *118*, 1577-1578.
- 35) R.B. Grossman, W.M. Davis and S.L. Buchwald. *J. Am. Chem. Soc.* **1991**, *113*, 2321.
- 36) F.A. Hicks and S.L. Buchwald. *J. Am. Chem. Soc.* **1996**, *118*, 11688-11689.
- 37) G. Erker, K. Berg, L. Treschanke and K. Engel. *Inorg. Chem.* **1982**, *21*, 1277-1278.
- 38) T. Livinghouse and E. Lund. *Organometallics* **1990**, *9*, 2426-2427.
- 39) S. Green *Ph.D. Thesis*. University of Southampton, 1999.
- 40) L. Bell *Ph.D. Thesis*; University of Southampton, 1997.
- 41) J.H. Wengrovius and R.R. Schrock. *J. Organomet. Chem.* **1981**, *205*, 319-327.
- 42) G.H. Llinas, M. Mena, F. Palacios, P. Royo and R. Serrano. *J. Organomet. Chem.* **1988**, *340*, 31-40.
- 43) C.M. Fendrick, L.D. Schertz, E.A. Mintz and T.M. Marks. *Inorganic Synthesis* **1993**, *29*, 193.
- 44) Cp^*ZrCl_3 purchased from Strem.

- 45) G. Erker, M. Nolte, M. Aulbach, A. Weiss, D. Reuschling and J. Rohrmann. German Pat. No. DE 4104931 A1
- 46) J.W. Coe, M.G. Vetelino and D.S. Kemp. *Tetrahedron. Lett.* **1994**, *35*, 6627-6630.
- 47) *G.C. Conditions: HP5 crosslinked column, 220^oC isothermal, octadecane internal standard.*
- 48) J.R. Peterson, J.K. Zjawiony, S.C. Liu, C.D. Hufford, A.M. Clarke and R.D. Rodgers. *J. Med. Chem.* **1992**, *35*, 4069-4077.
- 49) W.G. Brown. *Organic Reactions* **1951**, *6*, 469.
- 50) *G.C. conditions: A-DA column, 80^oC isothermal.*
- 51) R. Furstoss, R. Tadayoni and B. Waegell. *J. Org. Chem* **1977**, *42*, 2848.
- 52) I.U. Khand and P.L. Pauson. *J. Chem. Research* **1978**, 4401-4409.
- 53) T.W. Greene and P.G.M. Wuts *Protective Groups in Organic Synthesis*; 2nd. ed.; Wiley Interscience: New York, 1991.
- 54) A. Merz. *Angew. Chem. Int. Ed. Engl.* **1973**, *12*, 846.
- 55) M.E. Jung and S.M. Kaas. *Tetrahedron. Lett.* **1989**, *30*, 641.
- 56) P. Sykes *A Guidebook to Mechanism in Organic Chemistry*; 6th. ed.; Longman Scientific and Technical; 1986.
- 57) *Modelled by R.J. Whitby using CACHE software, MOPAC parameter set.*
- 58) J.-L. Luche. *J. Am. Chem. Soc.* **1978**, *100*, 2226-2227.
- 59) J.-L. Luche and A.L. Gemal. *J. Am. Chem. Soc.* **1981**, *103*, 5454-5459.
- 60) C.J. Rousset, S. Iyer and E.-i. Negishi. *Tetrahedron Asymmetry* **1997**, *8*, 3921-3926.
- 61) T. Mandai, T. Matsumoto, Y. Nakao, H. Teramoto, M. Kawada and J. Tsuji. *Tetrahedron Lett.* **1992**, *33*, 2549-2552.
- 62) T. Mandai, T. Matsumoto, J. Tsuji and S. Saito. *Tetrahedron Lett.* **1993**, *34*, 2513-2516.
- 63) *GCMS conditions HP5 column, 140^oC isothermal, EI ionisation.*
- 64) *NMR experiments by J.M. Street, University of Southampton.*
- 65) *Modelled using CS Chem3D software, MOPAC PM3 parameter set.*
- 66) H. Stockman. *J. Org. Chem* **1961**, *26*, 2027.
- 67) M. Avenati, O. Pilet, P. Carrupt and P. Vogel. *Helv. Chim. Acta.* **1982**, *1*, 178.
- 68) M. Kraaft. *J. Am. Chem. Soc.* **1991**, *113*, 1693-1703.

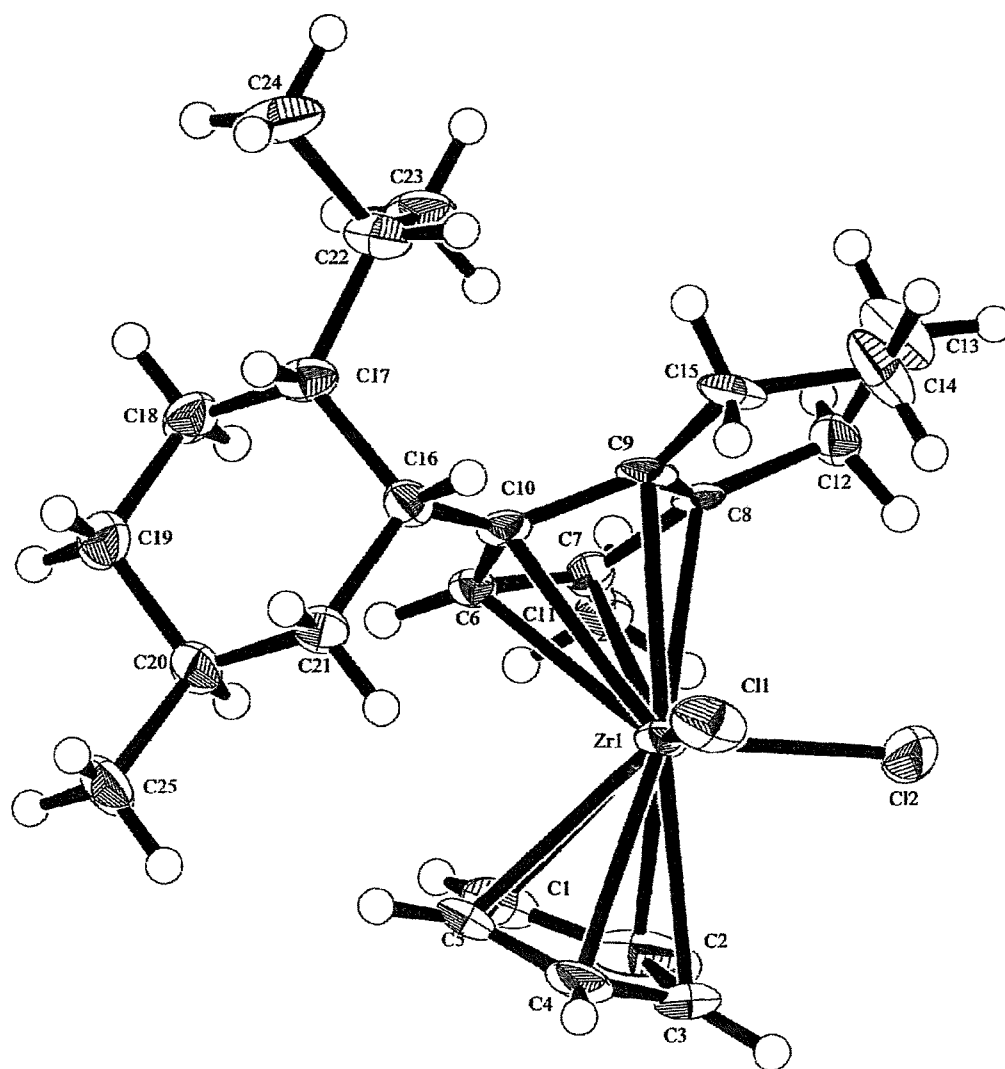


- 69) H. Sinn and W. Kaminsky. *Adv. Organomet. Chem.* **1980**, 18, 99.
- 70) P.C. Mohring and N.J. Coville. *J. Organomet. Chem.* **1994**, 479, 1-29.
- 71) W. Kaminsky, K. Kulper, H.H. Brintzinger and F.R.W.P. Wild. *Angew. Chem. Int. Ed. Engl.* **1985**, 24, 507.
- 72) S. Holding and R.B. Simpson "GPC analysis of polypropylene samples, RAPRA," , 1999.
- 73) W. Kaminsky, K. Kulper, H.H. Brintzinger and F.R.W.P. Wild. *Angew. Chem.* **1985**, 97, 507.
- 74) A.M. Cardoso, R.J.H. Clark and S. Moorhouse. *J. Chem. Soc. Dalton Trans.* **1980**, 1156.
- 75) M. Tichy, A. Orahovats and J. Sicher. *Collect. Czech. Chem. Commun.* **1970**, 35, 459-467.
- 76) S.M. Green, Personal Communication. **1998**

Appendix 1

Crystal structure data for Cyclopentadienyl(1-neomenthyl-3-methyl-4,5,6,7-tetrahydroindenyl)zirconium dichloride

(Absolute stereochemistry was not determined - the opposite enantiomer is shown)



Sample: rjw98 3

X-ray Structure Report
for
Richard Whitby and Cliff Veighey

Organic Chemistry

Fri Mar 27 1998

Introduction

This is the single crystal X-ray structure of RJW98-3 (C₂₅H₃₆ZrCl₂). The structure was solved by the heavy atoms technique using DIRDIF Patty. The structure was refined to convergence using iterative cycles of least squares refinement. All non-hydrogen atoms were refined anisotropically and hydrogen atoms were placed according to their geometrically calculated positions. The Flack parameter was also refined and confirmed the absolute configuration as correct.

Experimental

Data Collection

A colourless block crystal of $C_{25}H_{36}Cl_2Zr$ having approximate dimensions of 0.75 x 0.45 x 0.20 mm was mounted on a glass fiber. All measurements were made on a Rigaku AFC7S diffractometer with graphite monochromated Mo-K α radiation.

Cell constants and an orientation matrix for data collection, obtained from a least-squares refinement using the setting angles of 25 carefully centered reflections in the range $47.14 < 2\theta < 49.97^\circ$ corresponded to a primitive monoclinic cell with dimensions:

$$\begin{aligned}a &= 7.418(10) \text{ \AA} \\b &= 19.026(5) \text{ \AA} \quad \beta = 101.85(7)^\circ \\c &= 8.674(4) \text{ \AA} \\V &= 1198(1) \text{ \AA}^3\end{aligned}$$

For $Z = 2$ and F.W. = 498.69, the calculated density is 1.38 g/cm³. Based on the systematic absences of:

$$0k0: k \neq 2n$$

packing considerations, a statistical analysis of intensity distribution, and the successful solution and refinement of the structure, the space group was determined to be:

$$P2_1 (\#4)$$

The data were collected at a temperature of $-123 \pm 1^\circ\text{C}$ using the ω - 2θ scan technique to a maximum 2θ value of 50.1° . Omega scans of several intense reflections, made prior to data collection, had an average width at half-height of 0.33° with a take-off angle of 6.0° . Scans of $(1.52 + 0.35 \tan \theta)^\circ$ were made at a speed of $16.0^\circ/\text{min}$ (in omega). The weak reflections ($I < 15.0\sigma(I)$) were rescanned (maximum of 4 scans) and the counts were accumulated to ensure good counting statistics. Stationary background counts were recorded on each side of the reflection. The ratio of peak counting time to background counting time was 2:1. The diameter of the incident beam collimator was 1.0 mm and the crystal to detector distance was 400 mm. The computer-controlled slits were set to 9.0 mm (horizontal) and 13.0 mm (vertical).

Data Reduction

Of the 2367 reflections which were collected, 2193 were unique ($R_{int} = 0.033$). The intensities of three representative reflection were measured after every 150 reflections. No decay correction was applied.

The linear absorption coefficient, μ , for Mo-K α radiation is 6.8 cm^{-1} . An empirical absorption correction based on azimuthal scans of several reflections was applied which resulted in transmission factors ranging from 0.91 to 1.00. The data were corrected for Lorentz and polarization effects.

Structure Solution and Refinement

The structure was solved by heavy-atom Patterson methods¹ and expanded using Fourier techniques². The non-hydrogen atoms were refined anisotropically. Hydrogen atoms were included but not refined. The final cycle of full-matrix least-squares refinement³ was based on 2030 observed reflections ($I > 2.00\sigma(I)$) and 253 variable parameters and converged (largest parameter shift was 0.01 times its esd) with unweighted and weighted agreement factors of:

$$R = \Sigma||Fo| - |Fc||/\Sigma|Fo| = 0.046$$

$$R_w = \sqrt{(\Sigma w(|Fo| - |Fc|)^2/\Sigma wFo^2)} = 0.052$$

The standard deviation of an observation of unit weight⁴ was 4.09. The weighting scheme was based on counting statistics and included a factor ($p = 0.008$) to downweight the intense reflections. Plots of $\Sigma w(|Fo| - |Fc|)^2$ versus $|Fo|$, reflection order in data collection, $\sin \theta/\lambda$ and various classes of indices showed no unusual trends. The maximum and minimum peaks on the final difference Fourier map corresponded to 1.41 and $-1.59 e^-/\text{\AA}^3$, respectively.

Neutral atom scattering factors were taken from Cromer and Waber⁵. Anomalous dispersion effects were included in Fcalc⁶; the values for $\Delta f'$ and $\Delta f''$ were those of Creagh and McAuley⁷. The values for the mass attenuation coefficients are those of Creagh and Hubbel⁸. All calculations were performed using the teXsan⁹ crystallographic software package of Molecular Structure Corporation.

References

(1) PATY: Beurskens, P.T., Admiraal, G., Beurskens, G., Bosman, W.P., Garcia-Granda, S., Gould, R.O., Smits, J.M.M. and Smykalla, C. (1992). The DIRDIF program system, Technical Report of the Crystallography Laboratory, University of Nijmegen, The Netherlands.

(2) DIRDIF94: Beurskens, P.T., Admiraal, G., Beurskens, G., Bosman, W.P., de Gelder, R., Israel, R. and Smits, J.M.M. (1994). The DIRDIF-94 program system, Technical Report of the Crystallography Laboratory, University of Nijmegen, The Netherlands.

(3) Least-Squares:

Function minimized: $\Sigma w(|Fo| - |Fc|)^2$

where $w = \frac{1}{\sigma^2(Fo)} = \frac{4Fo^2}{\sigma^2(Fo^2)}$

$$\sigma^2(Fo^2) = \frac{S^2(C+R^2B)+(pFo^2)^2}{Lp^2}$$

S = Scan rate

C = Total integrated peak count

R = Ratio of scan time to background counting time

B = Total background count

Lp = Lorentz-polarization factor

p = p-factor

(4) Standard deviation of an observation of unit weight:

$$\sqrt{\Sigma w(|F_o| - |F_c|)^2 / (N_o - N_v)}$$

where: N_o = number of observations

N_v = number of variables

(5) Cromer, D. T. & Waber, J. T.; "International Tables for X-ray Crystallography", Vol. IV, The Kynoch Press, Birmingham, England, Table 2.2 A (1974).

(6) Ibers, J. A. & Hamilton, W. C.; Acta Crystallogr., 17, 781 (1964).

(7) Creagh, D. C. & McAuley, W.J. ; "International Tables for Crystallography", Vol C, (A.J.C. Wilson, ed.), Kluwer Academic Publishers, Boston, Table 4.2.6.8, pages 219-222 (1992).

(8) Creagh, D. C. & Hubbell, J.H.; "International Tables for Crystallography", Vol C, (A.J.C. Wilson, ed.), Kluwer Academic Publishers, Boston, Table 4.2.4.3, pages 200-206 (1992).

(9) teXsan: Crystal Structure Analysis Package, Molecular Structure Corporation (1985 & 1992).

EXPERIMENTAL DETAILS

A. Crystal Data

Empirical Formula	$C_{25}H_{36}Cl_2Zr$
Formula Weight	498.69
Crystal Color, Habit	colourless block, block
Crystal Dimensions	0.75 X 0.45 X 0.20 mm
Crystal System	monoclinic
Lattice Type	Primitive
No. of Reflections Used for Unit	
Cell Determination (2θ range)	25 (47.1 - 50.0°)
Omega Scan Peak Width at Half-height	0.33°
Lattice Parameters	$a = 7.418(10) \text{ \AA}$ $b = 19.026(5) \text{ \AA}$ $c = 8.674(4) \text{ \AA}$ $\beta = 101.85(7)^\circ$
	$V = 1198(1) \text{ \AA}^3$
Space Group	$P2_1$ (#4)
Z value	2
D_{calc}	1.382 g/cm ³
F_{000}	520.00
$\mu(\text{MoK}\alpha)$	6.84 cm ⁻¹

B. Intensity Measurements

Diffractometer	Rigaku AFC7S
----------------	--------------

Radiation	MoK α ($\lambda = 0.71069 \text{ \AA}$) graphite monochromated
Attenuator	Zr foil (factor = 8.56)
Take-off Angle	6.0°
Detector Aperture	9.0 mm horizontal 13.0 mm vertical
Crystal to Detector Distance	400 mm
Temperature	-123.1°C
Scan Type	ω -2 θ
Scan Rate	16.0°/min (in ω) (up to 4 scans)
Scan Width	(1.52 + 0.35 tan θ)°
$2\theta_{max}$	50.1°
No. of Reflections Measured	Total: 2367 Unique: 2193 ($R_{int} = 0.033$)
Corrections	Lorentz-polarization Absorption (trans. factors: 0.9077 - 1.0000)

C. Structure Solution and Refinement

Structure Solution	Patterson Methods (DIRDIF92 PATTY)
Refinement	Full-matrix least-squares
Function Minimized	$\Sigma w(F_o - F_c)^2$
Least Squares Weights	$\frac{1}{\sigma^2(F_o)} = \frac{4F_o^2}{\sigma^2(F_o^2)}$
p-factor	0.0080
Anomalous Dispersion	All non-hydrogen atoms
No. Observations ($I > 2.00\sigma(I)$)	2030
No. Variables	253
Reflection/Parameter Ratio	8.02
Residuals: R; Rw	0.046 ; 0.052

Goodness of Fit Indicator	4.09
Max Shift/Error in Final Cycle	0.01
Maximum peak in Final Diff. Map	$1.41 e^{-}/\text{\AA}^3$
Minimum peak in Final Diff. Map	$-1.59 e^{-}/\text{\AA}^3$

Table 1. Atomic coordinates and B_{iso}/B_{eq}

atom	x	y	z	B_{eq}
Zr(1)	0.13587(5)	0.5013(4)	0.06918(4)	1.799(7)
Cl(1)	-0.0836(1)	0.4245(4)	0.1605(1)	3.16(3)
Cl(2)	-0.0735(2)	0.6014(4)	0.0070(1)	3.76(3)
C(1)	0.4560(6)	0.5361(5)	0.2026(5)	3.58(10)
C(2)	0.3462(8)	0.5937(5)	0.2192(5)	3.8(1)
C(3)	0.2281(7)	0.5735(5)	0.3182(5)	3.10(10)
C(4)	0.2667(5)	0.5044(6)	0.3619(4)	2.82(8)
C(5)	0.4058(6)	0.4814(5)	0.2889(5)	3.4(1)
C(6)	0.3361(5)	0.4479(5)	-0.0949(4)	1.67(8)
C(7)	0.2671(5)	0.5106(5)	-0.1724(4)	1.83(7)
C(8)	0.0758(5)	0.4984(6)	-0.2341(4)	1.81(6)
C(9)	0.0295(5)	0.4316(5)	-0.1876(4)	1.72(7)
C(10)	0.1927(5)	0.3983(5)	-0.1003(4)	1.77(7)
C(11)	0.3694(6)	0.5755(5)	-0.2029(5)	2.32(9)
C(12)	-0.0539(6)	0.5464(5)	-0.3447(4)	2.39(9)
C(13)	-0.2266(6)	0.5069(6)	-0.4186(5)	4.1(1)
C(14)	-0.2922(6)	0.4590(5)	-0.3108(6)	4.1(1)
C(15)	-0.1591(6)	0.4025(5)	-0.2391(5)	2.50(9)
C(16)	0.2018(5)	0.3216(5)	-0.0515(4)	1.86(7)
C(17)	0.2758(6)	0.2723(5)	-0.1683(5)	2.10(8)
C(18)	0.4809(6)	0.2826(5)	-0.1553(5)	2.38(9)
C(19)	0.5848(6)	0.2643(5)	0.0099(5)	2.75(9)
C(20)	0.5193(6)	0.3089(5)	0.1359(5)	2.26(8)
C(21)	0.3115(6)	0.3053(5)	0.1163(5)	2.20(8)

Table 1. Atomic coordinates and B_{iso}/B_{eq} (continued)

atom	x	y	z	B_{eq}
C(22)	0.1614(6)	0.2727(5)	-0.3405(5)	2.65(9)
C(23)	0.2081(7)	0.3327(5)	-0.4413(5)	3.0(1)
C(24)	0.1894(8)	0.2026(5)	-0.4201(5)	4.0(1)
C(25)	0.6151(6)	0.2849(5)	0.3022(5)	3.4(1)
H(1)	0.5605	0.5367	0.1550	4.2859
H(2)	0.3624	0.6401	0.1841	4.5464
H(3)	0.1494	0.6040	0.3608	3.7123
H(4)	0.2198	0.4796	0.4402	3.3793
H(5)	0.4705	0.4382	0.3106	4.0249
H(6)	0.4631	0.4378	-0.0588	2.0130
H(7)	0.4943	0.5720	-0.1493	2.7804
H(8)	0.3145	0.6156	-0.1659	2.7804
H(9)	0.3640	0.5801	-0.3128	2.7804
H(10)	-0.0852	0.5854	-0.2870	2.8682
H(11)	0.0056	0.5626	-0.4250	2.8682
H(12)	-0.3213	0.5406	-0.4548	4.8416
H(13)	-0.2030	0.4810	-0.5053	4.8416
H(14)	-0.3227	0.4857	-0.2278	4.8943
H(15)	-0.4001	0.4363	-0.3681	4.8943
H(16)	-0.1984	0.3831	-0.1504	3.0302
H(17)	-0.1570	0.3665	-0.3147	3.0302
H(18)	0.0785	0.3075	-0.0537	2.2340
H(19)	0.2631	0.2260	-0.1307	2.5145
H(20)	0.5042	0.3302	-0.1774	2.8547

Table 1. Atomic coordinates and B_{iso}/B_{eq} (continued)

atom	x	y	z	B_{eq}
H(21)	0.5219	0.2530	-0.2294	2.8547
H(22)	0.5654	0.2160	0.0294	3.3073
H(23)	0.7125	0.2724	0.0162	3.3073
H(24)	0.5525	0.3565	0.1229	2.7137
H(25)	0.2757	0.3381	0.1868	2.6465
H(26)	0.2802	0.2592	0.1433	2.6465
H(27)	0.0349	0.2764	-0.3361	3.1736
H(28)	0.3325	0.3286	-0.4520	3.5989
H(29)	0.1916	0.3763	-0.3924	3.5989
H(30)	0.1292	0.3309	-0.5424	3.5989
H(31)	0.1618	0.1649	-0.3572	4.7696
H(32)	0.3137	0.1991	-0.4315	4.7696
H(33)	0.1100	0.2007	-0.5210	4.7696
H(34)	0.5782	0.3144	0.3785	4.1171
H(35)	0.7449	0.2878	0.3122	4.1171
H(36)	0.5815	0.2377	0.3182	4.1171

$$B_{eq} = \frac{8}{3}\pi^2(U_{11}(aa^*)^2 + U_{22}(bb^*)^2 + U_{33}(cc^*)^2 + 2U_{12}aa^*bb^* \cos \gamma + 2U_{13}aa^*cc^* \cos \beta + 2U_{23}bb^*cc^* \cos \alpha)$$

Table 2. Anisotropic Displacement Parameters

atom	U_{11}	U_{22}	U_{33}	U_{12}	U_{13}	U_{23}
Zr(1)	0.0242(2)	0.0329(2)	0.0112(2)	0.0018(2)	0.0034(1)	-0.0019(2)
Cl(1)	0.0321(6)	0.0680(9)	0.0230(5)	-0.0115(6)	0.0128(4)	-0.0017(6)
Cl(2)	0.0588(8)	0.0558(8)	0.0262(6)	0.0287(7)	0.0036(5)	-0.0046(6)
C(1)	0.025(2)	0.088(3)	0.022(2)	-0.012(2)	0.004(2)	-0.010(2)
C(2)	0.078(4)	0.043(3)	0.019(2)	-0.022(2)	0.001(2)	0.000(2)
C(3)	0.048(3)	0.045(2)	0.021(2)	0.004(2)	-0.002(2)	-0.017(2)
C(4)	0.046(2)	0.047(2)	0.009(2)	0.001(3)	-0.005(1)	0.003(3)
C(5)	0.039(2)	0.057(4)	0.022(2)	0.014(2)	-0.017(1)	-0.012(2)
C(6)	0.020(2)	0.030(2)	0.013(2)	0.001(1)	0.003(1)	-0.003(2)
C(7)	0.024(1)	0.035(2)	0.013(1)	0.005(2)	0.009(1)	0.000(2)
C(8)	0.029(1)	0.029(2)	0.011(2)	0.001(2)	0.004(1)	-0.010(2)
C(9)	0.025(2)	0.035(2)	0.006(2)	-0.003(2)	0.004(1)	-0.003(2)
C(10)	0.024(2)	0.033(2)	0.011(2)	-0.001(1)	0.008(1)	-0.005(2)
C(11)	0.034(2)	0.032(2)	0.023(2)	0.002(2)	0.007(2)	0.000(2)
C(12)	0.031(2)	0.044(3)	0.016(2)	0.011(2)	0.005(2)	0.005(2)
C(13)	0.039(2)	0.063(4)	0.043(3)	-0.005(3)	-0.010(2)	0.012(3)
C(14)	0.023(2)	0.082(4)	0.044(3)	0.001(2)	-0.009(2)	0.021(3)
C(15)	0.030(2)	0.047(3)	0.015(2)	-0.010(2)	-0.002(2)	-0.009(2)
C(16)	0.020(2)	0.034(2)	0.018(2)	0.000(2)	0.005(1)	0.001(2)
C(17)	0.039(2)	0.025(2)	0.017(2)	-0.004(2)	0.007(2)	-0.001(2)
C(18)	0.040(2)	0.032(3)	0.021(2)	0.009(2)	0.011(2)	0.000(2)
C(19)	0.042(2)	0.034(3)	0.028(2)	0.014(2)	0.006(2)	0.003(2)
C(20)	0.032(2)	0.034(3)	0.019(2)	0.008(2)	0.002(2)	0.006(2)
C(21)	0.034(2)	0.034(2)	0.016(2)	0.004(2)	0.005(2)	0.002(2)

Table 2. Anisotropic Displacement Parameters (continued)

atom	U_{11}	U_{22}	U_{33}	U_{12}	U_{13}	U_{23}
C(22)	0.041(3)	0.035(2)	0.022(2)	-0.008(2)	-0.001(2)	-0.004(2)
C(23)	0.059(3)	0.040(3)	0.014(2)	0.002(2)	0.005(2)	0.000(2)
C(24)	0.076(4)	0.041(3)	0.033(3)	-0.009(3)	0.011(3)	-0.018(2)
C(25)	0.036(3)	0.069(4)	0.021(2)	0.021(3)	-0.004(2)	0.007(2)

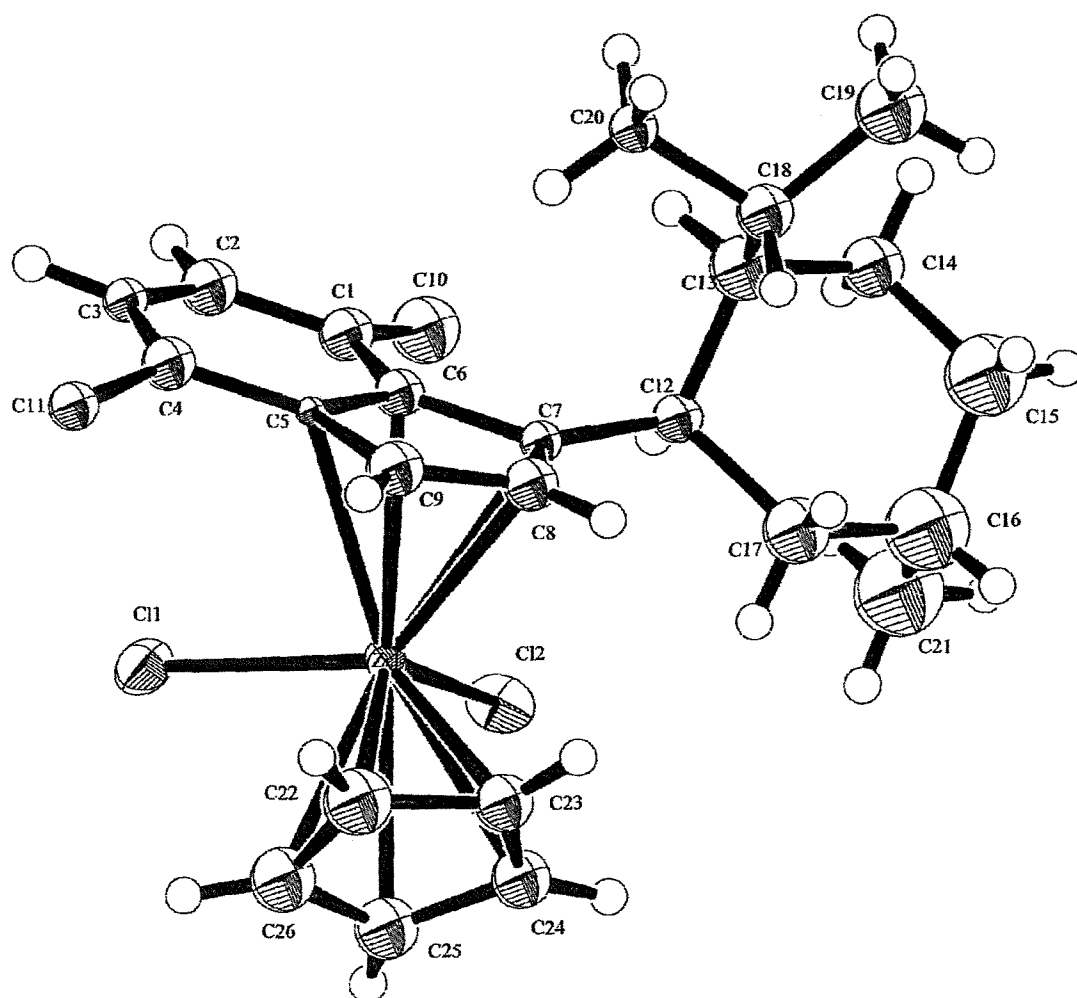
The general temperature factor expression:

$$\exp(-2\pi^2(a^*U_{11}h^2 + b^*U_{22}k^2 + c^*U_{33}l^2 + 2a^*b^*U_{12}hk + 2a^*c^*U_{13}hl + 2b^*c^*U_{23}kl))$$

Appendix 2

Single crystal X-ray structure data for cyclopentadienyl (1-(4,7dimethylneomenthylindenyl) zirconium dichloride

(Absolute stereochemistry was not determined - the opposite enantiomer is shown)



X-ray Structure Report

Mon Oct 2 2000

Introduction

Very weak data from small crystal. Difficulty in finding search peaks (dropped 2θ to 10 deg) to find more. Solved using SHELXS86 to locate Zr, Cl's and 6 C's. Rest of C's by Fourier after least squares. No H's found (with conviction). H's added in calc positions ($d(\text{C-H}) = 0.95 \text{ \AA}$). Remember to reduce Zr radius before adding H's to Cp ring. [Resetting C-H distance with Zr-C bond screws up H's on Cp]. No problem handling the air-sensitive crystals under '3 in 1' oil - stable for hour(s). MW Sept'97

Experimental

Data Collection

A yellow block crystal of $C_{26}H_{34}Cl_2Zr$ having approximate dimensions of 0.25 x 0.20 x 0.07 mm was mounted on a glass fiber. All measurements were made on a Rigaku AFC7S diffractometer with graphite monochromated Mo- $K\alpha$ radiation.

Cell constants and an orientation matrix for data collection, obtained from a least-squares refinement using the setting angles of 11 carefully centered reflections in the range $9.42 < 2\theta < 17.19^\circ$ corresponded to a orthorhombic cell with dimensions:

$$a = 12.922(6) \text{ \AA}$$

$$b = 16.306(7) \text{ \AA}$$

$$c = 11.652(5) \text{ \AA}$$

$$V = 2455(2) \text{ \AA}^3$$

For $Z = 4$ and F.W. = 508.68, the calculated density is 1.38 g/cm^3 . The systematic absences of:

$$h00: h \neq 2n$$

$$0k0: k \neq 2n$$

$$00l: l \neq 2n$$

uniquely determine the space group to be:

$$P2_12_12_1 \text{ (#19)}$$

The data were collected at a temperature of $-123 \pm 1^\circ\text{C}$ using the ω - 2θ scan technique to a maximum 2θ value of 50.0° . Omega scans of several intense reflections, made prior to data collection, had an average width at half-height of 0.19° with a take-off angle of 6.0° . Scans of $(0.89 + 0.35 \tan \theta)^\circ$ were made at a speed of $16.0^\circ/\text{min}$ (in omega). The weak reflections ($I < 15.0\sigma(I)$) were rescanned (maximum of 4 scans) and the counts were accumulated to ensure good counting statistics. Stationary background counts were recorded on each side of the reflection. The ratio of peak counting time to background counting time was 2:1. The diameter of the incident beam collimator was 1.0 mm and the

crystal to detector distance was 400 mm, The computer-controlled slits were set to 9.0 mm (horizontal) and 13.0 mm (vertical).

Data Reduction

A total of 2475 reflections was collected. The intensities of three representative reflection were measured after every 150 reflections. No decay correction was applied.

The linear absorption coefficient, μ , for Mo-K α radiation is 6.7 cm^{-1} . Azimuthal scans of several reflections indicated no need for an absorption correction. The data were corrected for Lorentz and polarization effects.

Structure Solution and Refinement

The structure was solved by direct methods¹ and expanded using Fourier techniques². Some non-hydrogen atoms were refined anisotropically, while the rest were refined isotropically. Hydrogen atoms were included but not refined. The final cycle of full-matrix least-squares refinement³ was based on 807 observed reflections ($I > 2.00\sigma(I)$) and 132 variable parameters and converged (largest parameter shift was 0.01 times its esd) with unweighted and weighted agreement factors of:

$$R = \sum ||F_o| - |F_c|| / \sum |F_o| = 0.058$$

$$R_w = [(\sum w (|F_o| - |F_c|)^2 / \sum w F_o^2)]^{1/2} = 0.054$$

The standard deviation of an observation of unit weight⁴ was 1.36. The weighting scheme was based on counting statistics and included a factor ($p = 0.002$) to downweight the intense reflections. Plots of $\sum w (|F_o| - |F_c|)^2$ versus $|F_o|$, reflection order in data collection,

$\sin \theta/\lambda$ and various classes of indices showed no unusual trends. The maximum and minimum peaks on the final difference Fourier map corresponded to 0.51 and $-0.71 \text{ e}^-/\text{\AA}^3$, respectively.

Neutral atom scattering factors were taken from Cromer and Waber⁵. Anomalous dispersion effects were included in F_{calc} ⁶; the values for $\delta f'$ and $\delta f''$ were those of Creagh and McAuley⁷. The values for the mass attenuation coefficients are those of Creagh and Hubbell⁸. All calculations were performed using the teXsan⁹ crystallographic software package of Molecular Structure Corporation.

References

- (1) SHELXS86: Sheldrick, G.M. (1985). In: "Crystallographic Computing 3" (Eds G.M. Sheldrick, C. Kruger and R. Goddard) Oxford University Press, pp. 175-189.
- (2) DIRDIF94: Beurskens, P.T., Admiraal, G., Beurskens, G., Bosman, W.P., de Gelder, R., Israel, R. and Smits, J.M.M.(1994). The DIRDIF-94 program system, Technical Report of the Crystallography Laboratory, University of Nijmegen, The Netherlands.
- (3) Least-Squares:

Function minimized $\sum w(|F_o| - |F_c|)^2$ where

$$w = 1/[\sigma^2(F_o)] = [\sigma_c^2(F_o) + p^2 F_o^2/4]^{-1}$$

$\sigma_c(F_o)$ = e.s.d. based on counting statistics

p = p-factor

(4) Standard deviation of an observation of unit weight:

$$[\sum w(|F_o| - |F_c|)^2 / (N_o - N_v)]^{1/2}$$

where N_o = number of observations

N_v = number of variables

(5) Cromer, D. T. & Waber, J. T.; "International Tables for X-ray Crystallography", Vol. IV, The Kynoch Press, Birmingham, England, Table 2.2 A (1974).

(6) Ibers, J. A. & Hamilton, W. C.; Acta Crystallogr., 17, 781 (1964).

(7) Creagh, D. C. & McAuley, W.J. ; "International Tables for Crystallography", Vol C, (A.J.C. Wilson, ed.), Kluwer Academic Publishers, Boston, Table 4.2.6.8, pages 219-222 (1992).

(8) Creagh, D. C. & Hubbell, J.H.; "International Tables for Crystallography", Vol C, (A.J.C. Wilson, ed.), Kluwer Academic Publishers, Boston, Table 4.2.4.3, pages 200-206 (1992).

(9) teXsan: Crystal Structure Analysis Package, Molecular Structure Corporation (1985 & 1992).

EXPERIMENTAL DETAILS

A. Crystal Data

Empirical Formula	$C_{26}H_{34}Cl_2Zr$
Formula Weight	508.68
Crystal Color, Habit	yellow, block
Crystal Dimensions	0.25 X 0.20 X 0.07 mm
Crystal System	orthorhombic
Lattice Type	Primitive
No. of Reflections Used for Unit	
Cell Determination (2θ range)	11 (9.4 - 17.2 $^\circ$)
Omega Scan Peak Width	
at Half-height	0.19 $^\circ$
Lattice Parameters	$a = 12.922(6)\text{\AA}$ $b = 16.306(7)\text{\AA}$ $c = 11.652(5)\text{\AA}$ $V = 2455(2)\text{\AA}^3$
Space Group	$P2_12_12_1$ (#19)
Z value	4
D _{calc}	1.376 g/cm ³
F ₀₀₀	1056.00
MU(MoK α)	6.75 cm ⁻¹

B. Intensity Measurements

Diffractometer	Rigaku AFC7S
Radiation	MoK α ($\lambda = 0.71069 \text{ \AA}$) graphite monochromated
Attenuator	Zr foil (factor = 8.58)
Take-off Angle	6.0 $^{\circ}$
Detector Aperture	9.0 mm horizontal 13.0 mm vertical
Crystal to Detector Distance	400 mm
Voltage, Current	0kV, 0mA
Temperature	-123.0 $^{\circ}$ C
Scan Type	ω -2 θ
Scan Rate	16.0 $^{\circ}$ /min (in ω) (up to 4 scans)
Scan Width	(0.89 + 0.35 tan θ) $^{\circ}$
2 θ_{max}	50.0 $^{\circ}$
No. of Reflections Measured	Total: 2475
Corrections	Lorentz-polarization

C. Structure Solution and Refinement

Structure Solution	Direct Methods (SHELXS86)
Refinement	Full-matrix least-squares

Function Minimized	$\Sigma w (F_o - F_c)^2$
Least Squares Weights	$1/\sigma^2(F_o) = 4F_o^2/\sigma^2(F_o^2)$
p-factor	0.0020
Anomalous Dispersion	All non-hydrogen atoms
No. Observations ($I > 2.00\sigma(I)$)	807
No. Variables	132
Reflection/Parameter Ratio	6.11
Residuals: R; Rw	0.058 ; 0.054
Goodness of Fit Indicator	1.36
Max Shift/Error in Final Cycle	0.01
Maximum peak in Final Diff. Map	$0.51 \text{ e}^-/\text{\AA}^3$
Minimum peak in Final Diff. Map	$-0.71 \text{ e}^-/\text{\AA}^3$

Table 1. Atomic coordinates and B_{iso}/B_{eq}

atom	x	y	z	B _{eq}
Zr(1)	0.4236(2)	0.7774(1)	0.0193(2)	1.40(4)
Cl(1)	0.2907(5)	0.8362(4)	0.1437(6)	2.7(2)
Cl(2)	0.3062(5)	0.7467(4)	-0.1398(5)	2.5(2)
C(1)	0.367(2)	0.975(1)	-0.104(2)	2.1(6)
C(2)	0.342(2)	1.031(1)	-0.018(2)	2.4(6)
C(3)	0.388(2)	1.034(2)	0.089(2)	1.5(6)
C(4)	0.466(2)	0.980(1)	0.126(2)	2.2(5)
C(5)	0.497(2)	0.922(1)	0.041(2)	0.6(5)
C(6)	0.450(2)	0.922(1)	-0.072(2)	1.7(6)
C(7)	0.507(2)	0.861(1)	-0.139(2)	1.3(5)
C(8)	0.583(2)	0.829(1)	-0.065(2)	2.2(5)
C(9)	0.577(2)	0.864(1)	0.042(2)	2.4(5)
C(10)	0.305(2)	0.971(2)	-0.213(2)	3.4(7)
C(11)	0.503(2)	0.970(2)	0.248(2)	1.8(5)
C(12)	0.503(2)	0.849(1)	-0.268(2)	1.7(5)
C(13)	0.560(2)	0.915(1)	-0.341(2)	3.3(6)
C(14)	0.535(2)	0.895(1)	-0.469(2)	2.8(6)
C(15)	0.573(2)	0.808(1)	-0.502(2)	5.1(7)
C(16)	0.518(2)	0.739(2)	-0.431(2)	5.2(8)
C(17)	0.541(2)	0.760(2)	-0.303(2)	3.3(7)
C(18)	0.672(2)	0.929(2)	-0.306(2)	2.4(6)
C(19)	0.741(2)	0.954(2)	-0.407(2)	3.6(8)
C(20)	0.679(2)	0.999(1)	-0.221(2)	1.8(5)
C(21)	0.409(2)	0.723(2)	-0.455(2)	5.9(7)

Table 1. Atomic coordinates and $B_{\text{iso}}/B_{\text{eq}}$ (continued)

atom	x	y	z	B_{eq}
C(22)	0.526(2)	0.691(2)	0.162(2)	3.3(7)
C(23)	0.547(2)	0.660(1)	0.051(2)	2.4(6)
C(24)	0.460(2)	0.626(1)	0.007(2)	2.6(6)
C(25)	0.378(2)	0.633(2)	0.087(2)	2.9(6)
C(26)	0.419(2)	0.675(1)	0.184(2)	3.1(6)
H(1)	0.2899	1.0703	-0.0343	2.9384
H(2)	0.3655	1.0749	0.1414	1.7678
H(3)	0.6323	0.7890	-0.0865	2.5986
H(4)	0.6196	0.8506	0.1060	2.8498
H(5)	0.4324	0.8520	-0.2882	2.0809
H(6)	0.5252	0.9657	-0.3255	3.9300
H(7)	0.4626	0.8978	-0.4806	3.4081
H(8)	0.5687	0.9339	-0.5168	3.4081
H(9)	0.5597	0.7986	-0.5811	6.1139
H(10)	0.6458	0.8043	-0.4886	6.1139
H(11)	0.5544	0.6895	-0.4468	6.2342
H(12)	0.6141	0.7562	-0.2904	3.9695
H(13)	0.5072	0.7207	-0.2554	3.9695
H(14)	0.6984	0.8800	-0.2723	2.8616
H(15)	0.8094	0.9642	-0.3800	4.3925
H(16)	0.7423	0.9120	-0.4628	4.3925
H(17)	0.7145	1.0032	-0.4406	4.3925
H(18)	0.7493	1.0071	-0.2005	2.1166
H(19)	0.6523	1.0473	-0.2554	2.1166

Table 1. Atomic coordinates and B_{iso}/B_{eq} (continued)

atom	x	y	z	B_{eq}
H(20)	0.6398	0.9858	-0.1547	2.1166
H(21)	0.3694	0.7710	-0.4422	7.1382
H(22)	0.4012	0.7061	-0.5329	7.1382
H(23)	0.3844	0.6801	-0.4062	7.1382
H(24)	0.5735	0.7173	0.2121	4.0207
H(25)	0.6122	0.6638	0.0131	2.9198
H(26)	0.4550	0.5999	-0.0662	3.0783
H(27)	0.3094	0.6145	0.0773	3.4905
H(28)	0.3819	0.6895	0.2519	3.7703

$$B_{eq} = 8/3 \pi^2 (U_{11}(aa^*)^2 + U_{22}(bb^*)^2 + U_{33}(cc^*)^2 + 2U_{12}(aa^*bb^*)\cos \gamma + 2U_{13}(aa^*cc^*)\cos \beta + 2U_{23}(bb^*cc^*)\cos \alpha)$$

Table 2. Anisotropic Displacement Parameters

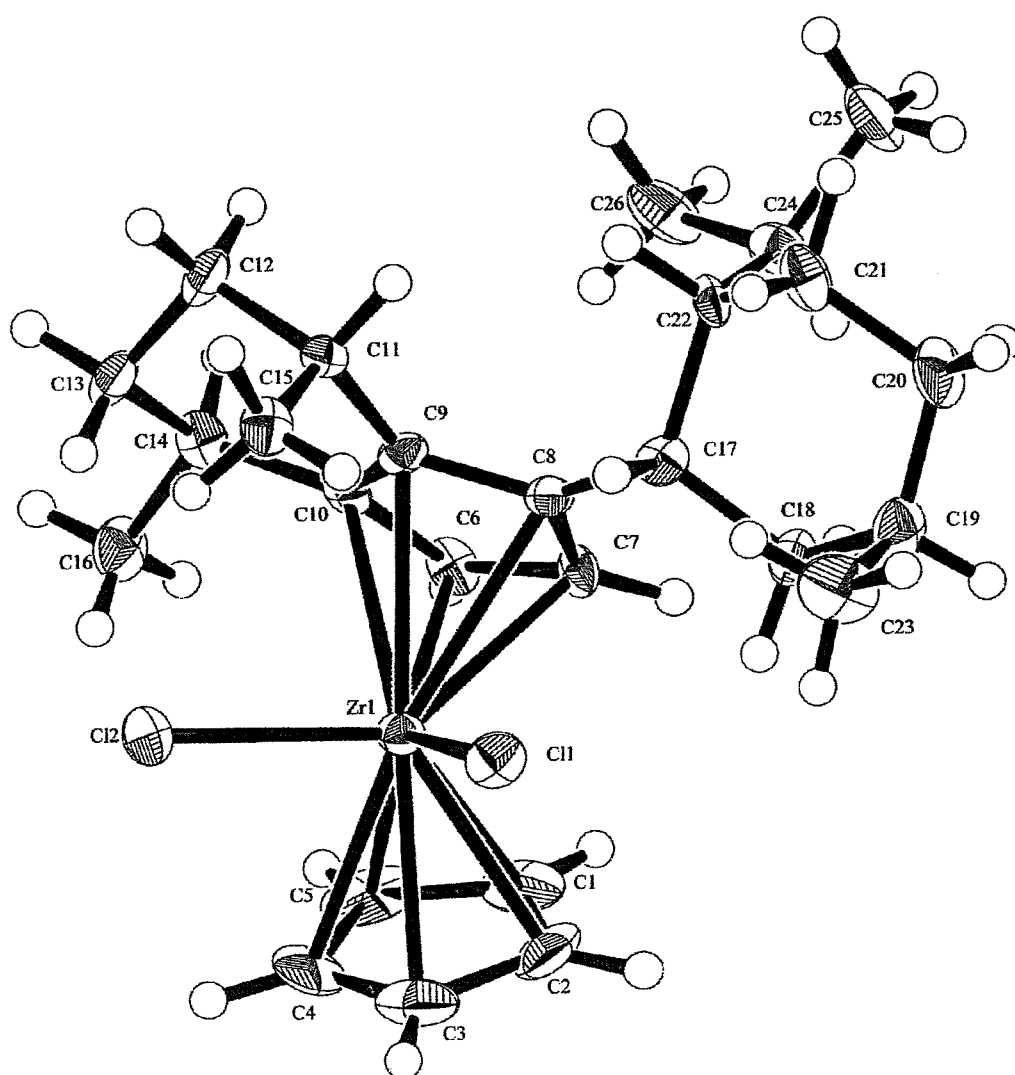
atom	U ₁₁	U ₂₂	U ₃₃	U ₁₂	U ₁₃	U ₂₃
Zr(1)	0.018(1)	0.018(1)	0.018(1)	0.000(2)	0.000(2)	0.000(1)
Cl(1)	0.034(4)	0.034(4)	0.034(5)	0.000(4)	0.000(4)	0.000(4)
Cl(2)	0.031(4)	0.031(5)	0.031(4)	0.000(4)	0.000(3)	0.000(3)

The general temperature factor expression:

$$\exp(-2\pi^2(a^2U_{11}h^2 + b^2U_{22}k^2 + c^2U_{33}l^2 + 2a*b*U_{12}hk + 2a*c*U_{13}hl + 2b*c*U_{23}kl))$$

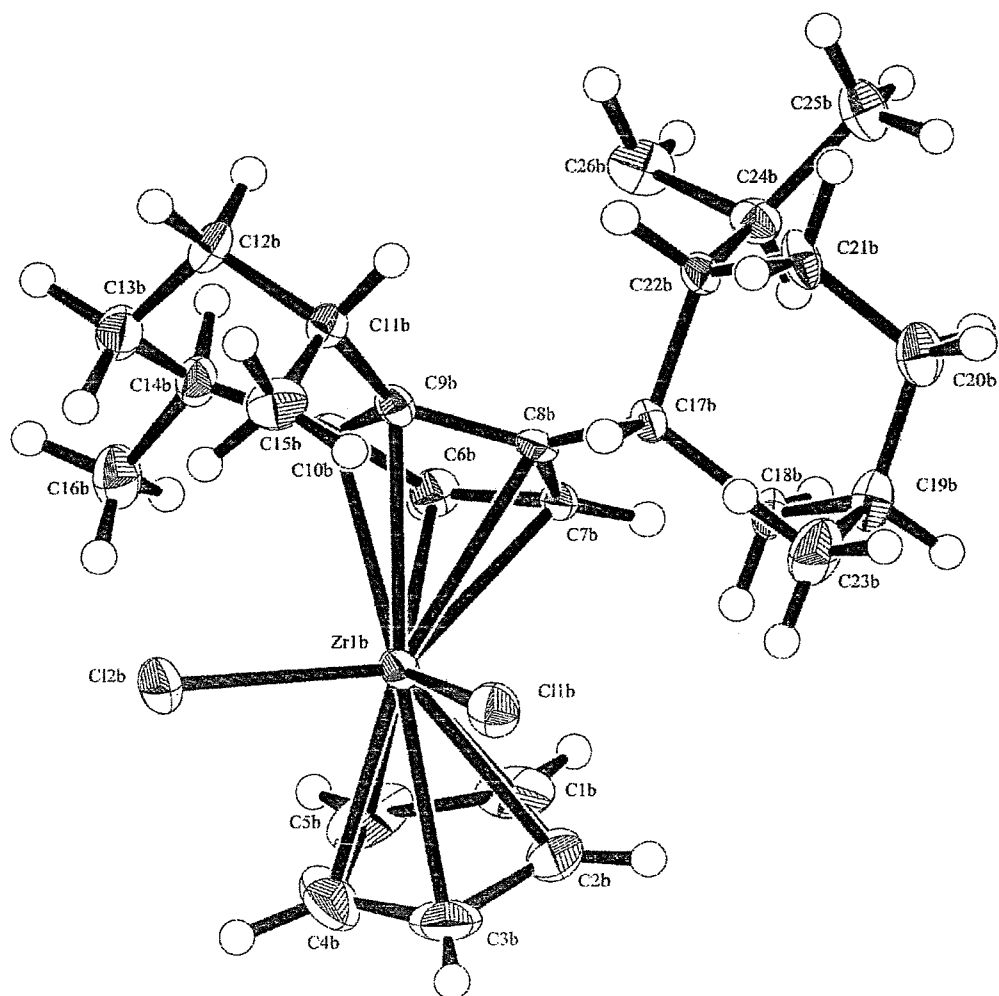
Appendix 3

Single crystal X-ray structure data for Cyclopentadienyl (1-(4,7dimethylneomenthyl-4,5,6,7-tetrahydroindenyl) zirconium dichloride



Single crystal X-ray structure data for Cyclopentadienyl (1-(4,7dimethylneomenthyl-4,5,6,7-tetrahydroindenyl) zirconium dichloride

(2nd molecule in unit cell)



Sample: cvzr1

X-ray Structure Report
for
Cliff Veighy and Richard Whitby

Organic Chemistry

Mon Oct 27 1997

Introduction

This is the structure for CVZr1 (C₂₆H₃₈ZrCl₂). The structure was solved by the Patterson heavy atoms method using the DIRDIF-Patty structure solution package. There are two molecules of the compound in the asymmetric unit cell. The structure was refined using iterative cycles of least squares. All nonhydrogen atoms have been refined anisotropically and hydrogen atoms have been placed according to their geometrically calculated positions. The Flack parameter was refined to check the enantiomorph and gave a value of 0.0479 indicating this is the correct enantiomorph.

Experimental

Data Collection

A colourless block crystal of $C_{26}H_{38}Cl_2Zr$ having approximate dimensions of 0.60 x 0.20 x 0.10 mm was mounted on a glass fiber. All measurements were made on a Rigaku AFC7S diffractometer with graphite monochromated Mo-K α radiation.

Cell constants and an orientation matrix for data collection, obtained from a least-squares refinement using the setting angles of 20 carefully centered reflections in the range $14.04 < 2\theta < 16.91^\circ$ corresponded to a primitive monoclinic cell with dimensions:

$$\begin{aligned}a &= 6.995(4) \text{ \AA} \\b &= 30.426(4) \text{ \AA} \quad \beta = 96.15(5)^\circ \\c &= 11.654(5) \text{ \AA} \\V &= 2466(1) \text{ \AA}^3\end{aligned}$$

For $Z = 4$ and F.W. = 512.71, the calculated density is 1.38 g/cm³. Based on the systematic absences of:

$$0k0: k \neq 2n$$

packing considerations, a statistical analysis of intensity distribution, and the successful solution and refinement of the structure, the space group was determined to be:

$$P2_1 (\#4)$$

The data were collected at a temperature of $-123 \pm 1^\circ\text{C}$ using the ω - 2θ scan technique to a maximum 2θ value of 50.0° . Omega scans of several intense reflections, made prior to data collection, had an average width at half-height of 0.23° with a take-off angle of 6.0° . Scans of $(0.73 + 0.35 \tan \theta)^\circ$ were made at a speed of $16.0^\circ/\text{min}$ (in omega). The weak reflections ($I < 15.0\sigma(I)$) were rescanned (maximum of 4 scans) and the counts were accumulated to ensure good counting statistics. Stationary background counts were recorded on each side of the reflection. The ratio of peak counting time to background counting time was 2:1. The diameter of the incident beam collimator was 1.0 mm and the crystal to detector distance was 400 mm. The computer-controlled slits were set to 9.0 mm (horizontal) and 13.0 mm (vertical).

Data Reduction

Of the 4826 reflections which were collected, 4450 were unique ($R_{int} = 0.043$). The intensities of three representative reflection were measured after every 150 reflections. No decay correction was applied.

The linear absorption coefficient, μ , for Mo-K α radiation is 6.7 cm^{-1} . An empirical absorption correction based on azimuthal scans of several reflections was applied which resulted in transmission factors ranging from 0.81 to 1.00. The data were corrected for Lorentz and polarization effects.

Structure Solution and Refinement

The structure was solved by heavy-atom Patterson methods¹ and expanded using Fourier techniques². The non-hydrogen atoms were refined anisotropically. Hydrogen atoms were included but not refined. The final cycle of full-matrix least-squares refinement³ was based on 3366 observed reflections ($I > 2.50\sigma(I)$) and 523 variable parameters and converged (largest parameter shift was 0.04 times its esd) with unweighted and weighted agreement factors of:

$$R = \Sigma ||F_o| - |F_c|| / \Sigma |F_o| = 0.034$$

$$R_w = \sqrt{(\Sigma w(|F_o| - |F_c|)^2 / \Sigma w F_o^2)} = 0.040$$

The standard deviation of an observation of unit weight⁴ was 1.24. The weighting scheme was based on counting statistics and included a factor ($p = 0.008$) to downweight the intense reflections. Plots of $\Sigma w(|F_o| - |F_c|)^2$ versus $|F_o|$, reflection order in data collection, $\sin \theta/\lambda$ and various classes of indices showed no unusual trends. The maximum and minimum peaks on the final difference Fourier map corresponded to 0.37 and $-0.42 e^-/\text{\AA}^3$, respectively.

Neutral atom scattering factors were taken from Cromer and Waber⁵. Anomalous dispersion effects were included in Fcalc⁶; the values for $\Delta f'$ and $\Delta f''$ were those of Creagh and McAuley⁷. The values for the mass attenuation coefficients are those of Creagh and Hubbel⁸. All calculations were performed using the teXsan⁹ crystallographic software package of Molecular Structure Corporation.

References

(1) PATY: Beurskens, P.T., Admiraal, G., Beurskens, G., Bosman, W.P., Garcia-Granda, S., Gould, R.O., Smits, J.M.M. and Smykalla, C. (1992). The DIRDIF program system, Technical Report of the Crystallography Laboratory, University of Nijmegen, The Netherlands.

(2) DIRDIF94: Beurskens, P.T., Admiraal, G., Beurskens, G., Bosman, W.P., de Gelder, R., Israel, R. and Smits, J.M.M. (1994). The DIRDIF-94 program system, Technical Report of the Crystallography Laboratory, University of Nijmegen, The Netherlands.

(3) Least-Squares:

Function minimized: $\Sigma w(|F_o| - |F_c|)^2$

$$\text{where } w = \frac{1}{\sigma^2(F_o)} = \frac{4F_o^2}{\sigma^2(F_o^2)}$$

$$\sigma^2(F_o^2) = \frac{S^2(C+R^2B)+(pF_o^2)^2}{Lp^2}$$

S = Scan rate

C = Total integrated peak count

R = Ratio of scan time to background counting time

B = Total background count

Lp = Lorentz-polarization factor

p = p-factor

(4) Standard deviation of an observation of unit weight:

$$\sqrt{\Sigma w(|Fo| - |Fc|)^2 / (No - Nv)}$$

where: No = number of observations

Nv = number of variables

(5) Cromer, D. T. & Waber, J. T.; "International Tables for X-ray Crystallography", Vol. IV, The Kynoch Press, Birmingham, England, Table 2.2 A (1974).

(6) Ibers, J. A. & Hamilton, W. C.; Acta Crystallogr., 17, 781 (1964).

(7) Creagh, D. C. & McAuley, W.J. ; "International Tables for Crystallography", Vol C, (A.J.C. Wilson, ed.), Kluwer Academic Publishers, Boston, Table 4.2.6.8, pages 219-222 (1992).

(8) Creagh, D. C. & Hubbell, J.H.; "International Tables for Crystallography", Vol C, (A.J.C. Wilson, ed.), Kluwer Academic Publishers, Boston, Table 4.2.4.3, pages 200-206 (1992).

(9) teXsan: Crystal Structure Analysis Package, Molecular Structure Corporation (1985 & 1992).

EXPERIMENTAL DETAILS

A. Crystal Data

Empirical Formula	$C_{26}H_{38}Cl_2Zr$
Formula Weight	512.71
Crystal Color, Habit	colourless block, block
Crystal Dimensions	0.60 X 0.20 X 0.10 mm
Crystal System	monoclinic
Lattice Type	Primitive
No. of Reflections Used for Unit	
Cell Determination (2θ range)	20 (14.0 - 16.9°)
Omega Scan Peak Width at Half-height	0.23°
Lattice Parameters	$a = 6.995(4) \text{ \AA}$ $b = 30.426(4) \text{ \AA}$ $c = 11.654(5) \text{ \AA}$ $\beta = 96.15(5)^\circ$
	$V = 2466(1) \text{ \AA}^3$
Space Group	$P2_1$ (#4)
Z value	4
D_{calc}	1.381 g/cm ³
F_{000}	1072.00
$\mu(\text{MoK}\alpha)$	6.67 cm ⁻¹

B. Intensity Measurements

Diffractometer	Rigaku AFC7S
----------------	--------------

Radiation	MoK α ($\lambda = 0.71069 \text{ \AA}$) graphite monochromated
Attenuator	Zr foil (factor = 8.58)
Take-off Angle	6.0°
Detector Aperture	9.0 mm horizontal 13.0 mm vertical
Crystal to Detector Distance	400 mm
Temperature	-123.1°C
Scan Type	ω -2 θ
Scan Rate	16.0°/min (in ω) (up to 4 scans)
Scan Width	$(0.73 + 0.35 \tan \theta)^\circ$
$2\theta_{max}$	50.0°
No. of Reflections Measured	Total: 4826 Unique: 4450 ($R_{int} = 0.043$)
Corrections	Lorentz-polarization Absorption (trans. factors: 0.8054 - 1.0000)

C. Structure Solution and Refinement

Structure Solution	Patterson Methods (DIRDIF92 PATTY)
Refinement	Full-matrix least-squares
Function Minimized	$\Sigma w(Fo - Fc)^2$
Least Squares Weights	$\frac{1}{\sigma^2(Fo)} = \frac{4Fo^2}{\sigma^2(Fo^2)}$
p-factor	0.0080
Anomalous Dispersion	All non-hydrogen atoms
No. Observations ($I > 2.50\sigma(I)$)	3366
No. Variables	523
Reflection/Parameter Ratio	6.44
Residuals: R; Rw	0.034 ; 0.040

Goodness of Fit Indicator	1.24
Max Shift/Error in Final Cycle	0.04
Maximum peak in Final Diff. Map	$0.37 e^-/\text{\AA}^3$
Minimum peak in Final Diff. Map	$-0.42 e^-/\text{\AA}^3$

Table 1. Atomic coordinates and B_{iso}/B_{eq}

atom	x	y	z	B_{eq}
Zr(1b)	0.35300(9)	-0.2739(3)	-0.36000(5)	1.56(1)
Cl(2b)	0.1991(3)	-0.3175(3)	-0.2195(2)	2.48(4)
Zr(1)	0.06961(9)	0.5003(3)	0.02709(6)	1.60(1)
Cl(1b)	0.0520(2)	-0.2492(3)	-0.4659(2)	2.31(4)
Cl(1)	-0.2267(2)	0.5081(3)	-0.1023(2)	2.27(4)
Cl(2)	-0.0910(3)	0.4782(3)	0.1944(2)	2.62(4)
C(1)	0.304(1)	0.5612(4)	0.0116(9)	3.4(2)
C(1b)	0.605(1)	-0.2155(4)	-0.3213(9)	3.7(2)
C(2)	0.128(1)	0.5782(4)	-0.0307(8)	3.1(2)
C(2b)	0.438(1)	-0.1938(4)	-0.3514(7)	3.2(2)
C(3)	0.015(1)	0.5810(4)	0.0603(9)	3.3(2)
C(3b)	0.316(1)	-0.1991(4)	-0.2680(8)	3.4(2)
C(4)	0.118(2)	0.5657(4)	0.1591(8)	3.9(2)
C(4b)	0.404(2)	-0.2260(5)	-0.1814(7)	4.1(2)
C(5)	0.300(1)	0.5525(4)	0.1325(9)	4.2(2)
C(5b)	0.585(1)	-0.2372(4)	-0.2137(8)	4.1(2)
C(6)	0.3706(9)	0.4611(4)	0.0118(6)	1.8(1)
C(6b)	0.6449(10)	-0.3098(4)	-0.4157(6)	1.8(1)
C(7)	0.2904(9)	0.4700(4)	-0.1030(6)	1.7(1)
C(7b)	0.5664(9)	-0.2849(4)	-0.5123(6)	1.4(1)
C(8)	0.1267(9)	0.4413(4)	-0.1287(6)	1.6(1)
C(8b)	0.3965(9)	-0.3064(4)	-0.5617(5)	1.3(1)
C(9)	0.1058(10)	0.4168(4)	-0.0266(6)	1.6(1)
C(9b)	0.3696(9)	-0.3445(4)	-0.4921(6)	1.4(1)

Table 1. Atomic coordinates and B_{iso}/B_{eq} (continued)

atom	x	y	z	B_{eq}
C(10)	0.2610(10)	0.4278(4)	0.0569(6)	1.7(1)
C(10b)	0.5251(9)	-0.3469(4)	-0.4046(5)	1.4(1)
C(11)	-0.024(1)	0.3784(4)	-0.0120(6)	1.8(1)
C(11b)	0.227(1)	-0.3811(4)	-0.5175(6)	1.7(1)
C(12)	0.068(1)	0.3479(4)	0.0830(7)	2.3(2)
C(12b)	0.314(1)	-0.4233(4)	-0.4611(6)	2.2(2)
C(13)	0.139(1)	0.3735(4)	0.1923(7)	2.2(2)
C(13b)	0.396(1)	-0.4167(4)	-0.3357(7)	2.3(2)
C(14)	0.3083(10)	0.4025(4)	0.1696(6)	2.0(1)
C(14b)	0.570(1)	-0.3864(4)	-0.3267(6)	2.0(1)
C(15)	-0.233(1)	0.3902(4)	0.0058(6)	2.1(2)
C(15b)	0.025(1)	-0.3725(4)	-0.4844(7)	2.3(2)
C(16)	0.387(1)	0.4314(4)	0.2734(6)	2.6(2)
C(16b)	0.650(1)	-0.3751(4)	-0.2056(7)	2.7(2)
C(17)	0.0141(9)	0.4360(4)	-0.2466(6)	1.7(1)
C(17b)	0.2823(9)	-0.2937(4)	-0.6740(6)	1.3(1)
C(18)	0.031(1)	0.4753(4)	-0.3250(6)	2.1(2)
C(18b)	0.302(1)	-0.2452(4)	-0.7045(6)	1.8(1)
C(19)	-0.100(1)	0.4721(4)	-0.4408(7)	2.8(2)
C(19b)	0.166(1)	-0.2311(4)	-0.8100(7)	2.3(1)
C(20)	-0.068(1)	0.4280(4)	-0.4996(6)	2.9(2)
C(20b)	0.203(1)	-0.2603(4)	-0.9122(6)	2.4(1)
C(21)	-0.081(1)	0.3890(4)	-0.4177(6)	2.4(2)
C(21b)	0.193(1)	-0.3087(4)	-0.8836(6)	2.1(1)

Table 1. Atomic coordinates and B_{iso}/B_{eq} (continued)

atom	x	y	z	B_{eq}
C(22)	0.0618(10)	0.3923(4)	-0.3084(6)	1.7(1)
C(22b)	0.3308(10)	-0.3226(4)	-0.7770(6)	1.6(1)
C(23)	-0.311(1)	0.4798(4)	-0.4236(8)	3.7(2)
C(23b)	-0.045(1)	-0.2310(4)	-0.7884(7)	3.0(2)
C(24)	0.274(1)	0.3869(4)	-0.3291(6)	2.2(1)
C(24b)	0.5470(10)	-0.3229(4)	-0.7979(6)	1.9(1)
C(25)	0.305(1)	0.3551(4)	-0.4275(7)	3.4(2)
C(25b)	0.582(1)	-0.3312(4)	-0.9231(6)	2.5(2)
C(26)	0.401(1)	0.3704(4)	-0.2229(7)	2.9(2)
C(26b)	0.6598(10)	-0.3576(4)	-0.7259(6)	2.2(2)
H(1)	0.4163	0.5582	-0.0318	4.2256
H(1b)	0.7203	-0.2133	-0.3594	4.4058
H(2)	0.0976	0.5902	-0.1072	3.7387
H(2b)	0.4183	-0.1754	-0.4157	3.9274
H(3)	-0.1070	0.5944	0.0584	4.0922
H(3b)	0.1973	-0.1835	-0.2661	4.1453
H(4)	0.0775	0.5663	0.2362	5.0648
H(4b)	0.3634	-0.2340	-0.1064	4.9684
H(5)	0.4138	0.5435	0.1875	5.1871
H(5b)	0.6898	-0.2530	-0.1662	4.8212
H(6)	0.4925	0.4700	0.0445	2.3248
H(6b)	0.7729	-0.3072	-0.3768	2.1670
H(7)	0.3516	0.4863	-0.1577	2.0850
H(7b)	0.6353	-0.2628	-0.5469	1.6988

Table 1. Atomic coordinates and B_{iso}/B_{eq} (continued)

atom	x	y	z	B_{eq}
H(8)	-0.0301	0.3612	-0.0823	2.0634
H(8b)	0.2126	-0.3864	-0.5986	2.1822
H(9)	0.1750	0.3322	0.0574	2.7830
H(9b)	0.4120	-0.4341	-0.5052	3.3034
H(10)	-0.0242	0.3258	0.1021	2.7830
H(10b)	0.2139	-0.4462	-0.4654	3.3034
H(11)	0.0368	0.3910	0.2151	2.6939
H(11b)	0.4347	-0.4459	-0.3004	2.6660
H(12)	0.1750	0.3528	0.2553	2.6939
H(12b)	0.3017	-0.4056	-0.2904	2.6660
H(13)	0.4123	0.3817	0.1583	2.4872
H(13b)	0.6705	-0.4034	-0.3586	2.3008
H(14)	-0.2877	0.4081	-0.0547	2.6846
H(14b)	-0.0262	-0.3467	-0.5196	2.8120
H(15)	-0.2367	0.4043	0.0778	2.6846
H(15b)	-0.0599	-0.3968	-0.5087	2.8120
H(16)	-0.3099	0.3634	0.0065	2.6846
H(16b)	0.0275	-0.3701	-0.4024	2.8120
H(17)	0.4937	0.4479	0.2528	3.3397
H(17b)	0.7658	-0.3592	-0.2054	3.2324
H(18)	0.2879	0.4510	0.2903	3.3397
H(18b)	0.5584	-0.3584	-0.1698	3.2324
H(19)	0.4258	0.4139	0.3389	3.3397
H(19b)	0.6766	-0.4016	-0.1601	3.2324

Table 1. Atomic coordinates and B_{iso}/B_{eq} (continued)

atom	x	y	z	B_{eq}
H(20)	-0.1189	0.4335	-0.2331	2.0215
H(20b)	0.1489	-0.2994	-0.6654	1.4834
H(21)	-0.0056	0.5009	-0.2856	2.5878
H(21b)	0.2741	-0.2281	-0.6399	2.2459
H(22)	0.1615	0.4780	-0.3396	2.5878
H(22b)	0.4312	-0.2399	-0.7191	2.2459
H(23)	-0.0609	0.4948	-0.4925	3.4306
H(23b)	0.1997	-0.2023	-0.8275	2.7400
H(24)	-0.1671	0.4236	-0.5650	3.7542
H(24b)	0.1084	-0.2536	-0.9770	2.8085
H(25)	0.0529	0.4268	-0.5306	3.7542
H(25b)	0.3270	-0.2542	-0.9365	2.8085
H(26)	-0.2077	0.3862	-0.3963	3.3292
H(26b)	0.2198	-0.3267	-0.9494	2.6240
H(27)	-0.0538	0.3614	-0.4577	3.3292
H(27b)	0.0618	-0.3164	-0.8695	2.6240
H(28)	0.0306	0.3677	-0.2593	2.1760
H(28b)	0.2987	-0.3530	-0.7592	1.8745
H(29)	-0.3938	0.4770	-0.4950	4.7560
H(29b)	-0.1243	-0.2204	-0.8548	3.8245
H(30)	-0.3313	0.5074	-0.3909	4.7560
H(30b)	-0.0889	-0.2611	-0.7751	3.8245
H(31)	-0.3533	0.4572	-0.3721	4.7560
H(31b)	-0.0671	-0.2142	-0.7235	3.8245

Table 1. Atomic coordinates and B_{iso}/B_{eq} (continued)

atom	x	y	z	B_{eq}
H(32)	0.3246	0.4139	-0.3452	2.7574
H(32b)	0.5994	-0.2957	-0.7758	2.3135
H(33)	0.2312	0.3640	-0.4964	4.0726
H(33b)	0.5143	-0.3111	-0.9733	2.8685
H(34)	0.4380	0.3537	-0.4409	4.0726
H(34b)	0.7153	-0.3303	-0.9319	2.8685
H(35)	0.2666	0.3253	-0.4098	4.0726
H(35b)	0.5370	-0.3609	-0.9466	2.8685
H(36)	0.5300	0.3686	-0.2375	3.7250
H(36b)	0.7929	-0.3570	-0.7352	2.5532
H(37)	0.3598	0.3400	-0.2057	3.7250
H(37b)	0.6148	-0.3876	-0.7507	2.5532
H(38)	0.3850	0.3876	-0.1586	3.7250
H(38b)	0.6428	-0.3557	-0.6465	2.5532

$$B_{eq} = \frac{8}{3} \pi^2 (U_{11}(aa^*)^2 + U_{22}(bb^*)^2 + U_{33}(cc^*)^2 + 2U_{12}aa^*bb^* \cos \gamma + 2U_{13}aa^*cc^* \cos \beta + 2U_{23}bb^*cc^* \cos \alpha)$$

Table 2. Anisotropic Displacement Parameters

atom	U_{11}	U_{22}	U_{33}	U_{12}	U_{13}	U_{23}
Zr(1b)	0.0240(3)	0.0197(4)	0.0168(3)	-0.0028(3)	0.0065(3)	-0.0012(3)
Cl(2b)	0.038(1)	0.032(1)	0.0257(10)	-0.0053(9)	0.0133(8)	0.0036(8)
Zr(1)	0.0208(3)	0.0180(4)	0.0223(4)	-0.0015(3)	0.0039(3)	-0.0019(3)
Cl(1b)	0.0250(9)	0.033(1)	0.031(1)	0.0043(8)	0.0085(7)	0.0032(9)
Cl(1)	0.0216(9)	0.030(1)	0.035(1)	0.0045(8)	0.0017(7)	0.0030(9)
Cl(2)	0.039(1)	0.034(1)	0.0299(10)	0.0018(9)	0.0154(9)	0.0008(9)
C(1)	0.037(4)	0.022(5)	0.074(5)	-0.019(3)	0.017(4)	-0.014(4)
C(1b)	0.044(4)	0.036(5)	0.063(5)	-0.031(3)	0.018(4)	-0.027(4)
C(2)	0.054(5)	0.019(3)	0.044(5)	-0.008(4)	0.002(3)	0.010(4)
C(2b)	0.062(5)	0.022(2)	0.037(5)	-0.019(4)	0.009(4)	-0.006(4)
C(3)	0.037(5)	0.022(5)	0.069(5)	-0.004(4)	0.016(3)	-0.013(4)
C(3b)	0.054(6)	0.028(5)	0.050(5)	-0.008(4)	0.019(4)	-0.019(4)
C(4)	0.082(6)	0.026(5)	0.044(5)	-0.019(4)	0.018(4)	-0.024(3)
C(4b)	0.080(6)	0.052(6)	0.025(4)	-0.030(5)	0.014(4)	-0.013(4)
C(5)	0.059(5)	0.022(5)	0.068(5)	-0.021(4)	-0.036(4)	-0.008(4)
C(5b)	0.059(5)	0.029(5)	0.058(5)	-0.012(4)	-0.041(4)	-0.013(4)
C(6)	0.014(3)	0.033(4)	0.022(3)	-0.007(2)	-0.001(3)	-0.007(3)
C(6b)	0.021(3)	0.024(4)	0.024(3)	0.003(2)	0.000(3)	0.002(3)
C(7)	0.020(3)	0.026(4)	0.021(3)	-0.006(3)	0.010(2)	-0.001(3)
C(7b)	0.022(3)	0.016(4)	0.018(3)	-0.006(2)	0.009(2)	-0.002(2)
C(8)	0.020(3)	0.016(3)	0.024(3)	0.001(3)	0.004(3)	-0.001(3)
C(8b)	0.018(3)	0.018(3)	0.014(3)	0.003(2)	0.004(2)	-0.004(2)
C(9)	0.018(3)	0.017(4)	0.026(3)	0.005(2)	0.003(3)	0.003(3)
C(9b)	0.016(3)	0.022(3)	0.017(3)	0.001(2)	0.007(2)	0.000(3)

Table 2. Anisotropic Displacement Parameters (continued)

atom	U_{11}	U_{22}	U_{33}	U_{12}	U_{13}	U_{23}
C(10)	0.016(3)	0.026(4)	0.023(3)	0.006(3)	0.009(2)	-0.003(3)
C(10b)	0.020(3)	0.023(3)	0.013(3)	0.005(3)	0.005(2)	-0.002(3)
C(11)	0.030(3)	0.017(4)	0.021(4)	-0.002(2)	0.006(3)	-0.004(3)
C(11b)	0.028(3)	0.018(3)	0.020(4)	-0.004(2)	0.004(3)	0.001(3)
C(12)	0.032(4)	0.027(4)	0.029(4)	0.000(3)	0.007(3)	0.012(3)
C(12b)	0.036(4)	0.016(4)	0.032(3)	-0.004(3)	0.005(3)	0.005(3)
C(13)	0.031(4)	0.023(4)	0.031(4)	0.002(3)	0.008(3)	0.012(3)
C(13b)	0.030(4)	0.026(4)	0.032(3)	0.001(3)	0.007(3)	0.005(4)
C(14)	0.019(4)	0.033(4)	0.023(3)	0.003(3)	0.002(3)	0.000(2)
C(14b)	0.027(4)	0.023(4)	0.027(3)	0.007(3)	0.009(3)	0.009(3)
C(15)	0.026(3)	0.031(5)	0.023(4)	-0.006(3)	0.000(3)	-0.001(3)
C(15b)	0.025(3)	0.029(4)	0.034(4)	-0.005(3)	0.000(3)	-0.005(4)
C(16)	0.038(5)	0.038(5)	0.022(4)	-0.004(4)	-0.005(3)	0.001(3)
C(16b)	0.036(5)	0.040(5)	0.027(4)	0.004(4)	0.001(3)	0.011(4)
C(17)	0.018(4)	0.021(3)	0.023(3)	-0.005(3)	0.000(3)	0.000(2)
C(17b)	0.017(3)	0.020(3)	0.013(3)	-0.003(3)	0.003(2)	0.001(2)
C(18)	0.031(4)	0.026(4)	0.021(3)	-0.005(4)	0.001(3)	0.004(3)
C(18b)	0.028(4)	0.020(3)	0.023(4)	-0.001(3)	0.007(3)	0.007(3)
C(19)	0.042(4)	0.042(4)	0.020(4)	0.002(4)	-0.006(3)	0.006(3)
C(19b)	0.033(3)	0.028(4)	0.028(4)	-0.001(3)	-0.001(3)	0.012(3)
C(20)	0.043(5)	0.048(4)	0.016(4)	-0.006(4)	-0.005(4)	-0.004(3)
C(20b)	0.026(4)	0.040(4)	0.025(4)	0.001(3)	-0.001(3)	0.010(3)
C(21)	0.026(4)	0.046(5)	0.019(4)	0.001(4)	0.001(3)	-0.004(3)
C(21b)	0.031(4)	0.039(4)	0.011(3)	-0.004(4)	-0.001(3)	0.006(3)

Table 2. Anisotropic Displacement Parameters (continued)

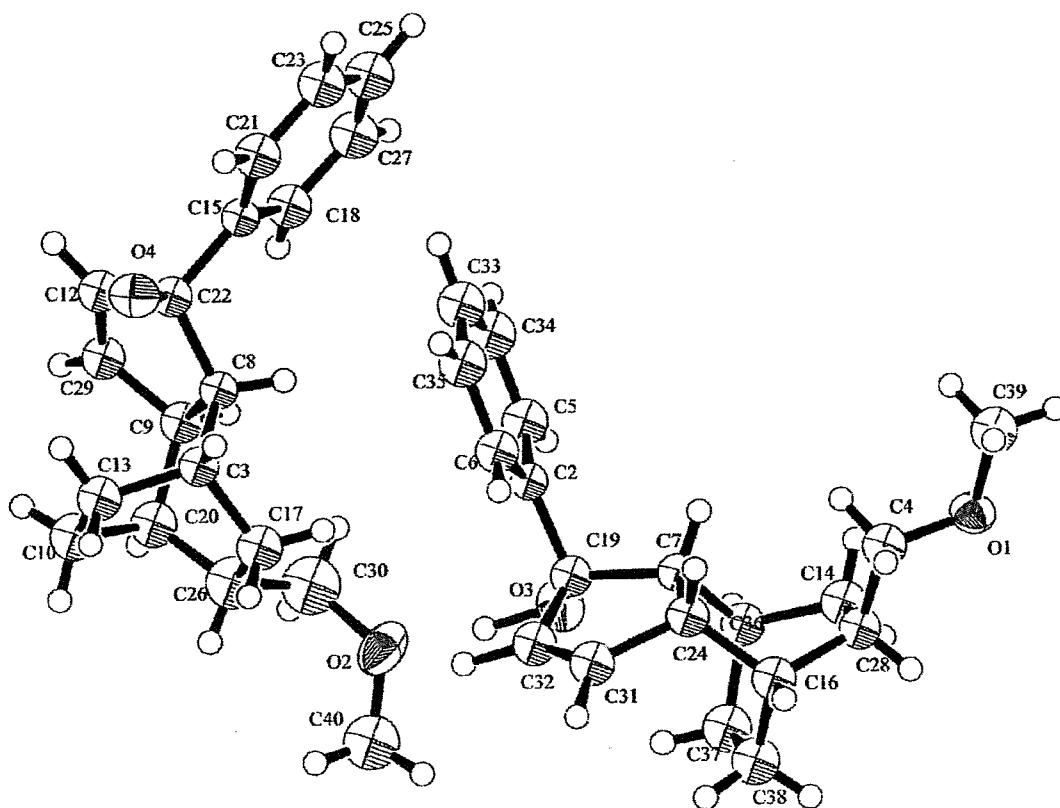
atom	U ₁₁	U ₂₂	U ₃₃	U ₁₂	U ₁₃	U ₂₃
C(22)	0.024(3)	0.026(4)	0.016(3)	-0.010(3)	0.009(2)	-0.004(3)
C(22b)	0.027(3)	0.020(4)	0.012(3)	-0.003(3)	0.000(2)	-0.001(3)
C(23)	0.042(4)	0.051(6)	0.043(5)	0.019(4)	-0.014(4)	-0.004(5)
C(23b)	0.034(4)	0.034(5)	0.046(5)	0.012(4)	0.005(4)	0.015(4)
C(24)	0.023(3)	0.028(4)	0.034(4)	-0.001(3)	0.010(3)	-0.006(3)
C(24b)	0.025(3)	0.027(4)	0.023(3)	-0.004(3)	0.002(3)	-0.005(3)
C(25)	0.052(6)	0.057(6)	0.023(4)	0.014(5)	0.011(4)	-0.011(4)
C(25b)	0.030(4)	0.043(5)	0.020(3)	0.000(4)	0.002(3)	0.005(4)
C(26)	0.025(4)	0.050(6)	0.033(4)	0.007(4)	0.001(3)	-0.016(4)
C(26b)	0.017(4)	0.042(5)	0.025(4)	0.006(3)	-0.002(3)	-0.003(3)

The general temperature factor expression:

$$\exp(-2\pi^2(a^*U_{11}h^2 + b^*U_{22}k^2 + c^*U_{33}l^2 + 2a^*b^*U_{12}hk + 2a^*c^*U_{13}hl + 2b^*c^*U_{23}kl))$$

Appendix 4

Single crystal X-ray structure data for 9-(Methoxymethyl)-3-phenyltricyclo[5.2.2.0^{2,6}]undec-4-en-3-ol.



X-ray Structure Report

Mon Oct 2 2000

Experimental

Data Collection

A colourless crystal of $C_{19}H_{24}O_2$ having approximate dimensions of 0.52 x 0.27 x 0.20 mm was mounted on a glass fiber. All measurements were made on a Rigaku AFC7S diffractometer with graphite monochromated Mo-K α radiation.

Cell constants and an orientation matrix for data collection, obtained from a least-squares refinement using the setting angles of 20 carefully centered reflections in the range $14.01 < 2\theta < 17.93^\circ$ corresponded to a primitive monoclinic cell with dimensions:

$$a = 15.156(4) \text{ \AA}$$

$$b = 6.388(3) \text{ \AA} \quad \beta = 90.39(2)^\circ$$

$$c = 31.934(4) \text{ \AA}$$

$$V = 3092(2) \text{ \AA}^3$$

For $Z = 8$ and F.W. = 284.40, the calculated density is 1.22 g/cm^3 . The systematic absences of:

$$h0l: h+1 \pm 2n$$

$$0k0: k \pm 2n$$

uniquely determine the space group to be:

$$P2_1/n \text{ (#14)}$$

The data were collected at a temperature of $-123 \pm 1^\circ\text{C}$ using the ω - 2θ scan technique to a maximum 2θ value of 50.0° . Omega scans of several intense reflections, made prior to data collection, had an average width at half-height of 0.30° with a take-off angle of 6.0° . Scans of $(0.94 + 0.35 \tan \theta)^\circ$ were made at a speed of $16.0^\circ/\text{min}$ (in omega). The weak reflections ($I < 15.0\sigma(I)$) were rescanned (maximum of 4 scans) and the counts were accumulated to ensure good counting statistics. Stationary background counts were recorded on each side of the reflection. The ratio of peak counting time to background counting time was 2:1. The diameter of the incident beam collimator was 1.0 mm and the crystal to detector distance was 400 mm, The computer-controlled slits were set to 9.0 mm (horizontal) and 13.0 mm (vertical).

Data Reduction

Of the 6227 reflections which were collected, 5989 were unique ($R_{\text{int}} = 0.036$). The intensities of three representative reflection were measured after every 150 reflections. No decay correction was applied.

The linear absorption coefficient, μ , for Mo- $K\alpha$ radiation is 0.8 cm^{-1} . An empirical absorption correction based on azimuthal scans of several reflections was applied which resulted in transmission factors ranging from 0.97 to 1.00. The data were corrected for Lorentz and polarization effects.

Structure Solution and Refinement

The structure was solved by direct methods¹ and expanded using Fourier techniques². Some non-hydrogen atoms were refined anisotropically, while the rest were refined isotropically. Hydrogen atoms were included but not refined. The final cycle of full-matrix least-squares refinement³ was based on 2160 observed reflections ($I > 2.00\sigma(I)$) and 189 variable parameters and converged (largest parameter shift was 0.35 times its esd) with unweighted and weighted agreement factors of:

$$R = \sum ||F_o| - |F_c|| / \sum |F_o| = 0.076$$

$$R_w = [(\sum w (|F_o| - |F_c|)^2 / \sum w F_o^2)]^{1/2} = 0.071$$

The standard deviation of an observation of unit weight⁴ was 2.58. The weighting scheme was based on counting statistics and included a factor ($p = 0.009$) to downweight the intense reflections. Plots of $\sum w (|F_o| - |F_c|)^2$ versus $|F_o|$, reflection order in data collection, $\sin \theta/\lambda$ and various classes of indices showed no unusual trends. The maximum and minimum peaks on the final difference Fourier map corresponded to 0.69 and $-0.33 \text{ e}^-/\text{\AA}^3$, respectively.

Neutral atom scattering factors were taken from Cromer and Waber⁵. Anomalous dispersion effects were included in F_{calc} ⁶; the values for $\delta f'$ and $\delta f''$ were those of Creagh

and McAuley⁷. The values for the mass attenuation coefficients are those of Creagh and Hubbell⁸. All calculations were performed using the teXsan⁹ crystallographic software package of Molecular Structure Corporation.

References

(1) SIR88: Burla, M.C., Camalli, M., Cascarano, G., Giacovazzo, C., Polidori, G., Spagna, R. & Viterbo, D. (1989), *J. Appl. Cryst.*, **22**, 389-303.

(2) DIRDIF94: Beurskens, P.T., Admiraal, G., Beurskens, G., Bosman, W.P., de Gelder, R., Israel, R. and Smits, J.M.M. (1994). The DIRDIF-94 program system, Technical Report of the Crystallography Laboratory, University of Nijmegen, The Netherlands.

(3) Least-Squares:

Function minimized $\sum w(|F_o| - |F_c|)^2$ where

$$w = 1/[\sigma^2(F_o)] = [\sigma_c^2(F_o) + p^2 F_o^2/4]^{-1}$$

$\sigma_c(F_o)$ = e.s.d. based on counting statistics

p = p-factor

(4) Standard deviation of an observation of unit weight:

$$[\sum w(|F_o| - |F_c|)^2 / (N_o - N_v)]^{1/2}$$

where N_o = number of observations

N_v = number of variables

(5) Cromer, D. T. & Waber, J. T.; "International Tables for X-ray Crystallography", Vol. IV, The Kynoch Press, Birmingham, England, Table 2.2 A (1974).

(6) Ibers, J. A. & Hamilton, W. C.; *Acta Crystallogr.*, **17**, 781 (1964).

(7) Creagh, D. C. & McAuley, W.J. ; "International Tables for Crystallography", Vol C, (A.J.C. Wilson, ed.), Kluwer Academic Publishers, Boston, Table 4.2.6.8, pages 219-222 (1992).

(8) Creagh, D. C. & Hubbell, J.H. ; "International Tables for Crystallography", Vol C, (A.J.C. Wilson, ed.), Kluwer Academic Publishers, Boston, Table 4.2.4.3, pages 200-206 (1992).

(9) teXsan: Crystal Structure Analysis Package, Molecular Structure Corporation (1985 & 1992).

EXPERIMENTAL DETAILS

A. Crystal Data

Empirical Formula	$C_{19}H_{24}O_2$
Formula Weight	284.40
Crystal Color, Habit	colourless,
Crystal Dimensions	0.52 X 0.27 X 0.20 mm
Crystal System	monoclinic
Lattice Type	Primitive
No. of Reflections Used for Unit	
Cell Determination (2θ range)	20 (14.0 - 17.9 $^\circ$)
Omega Scan Peak Width at Half-height	0.30 $^\circ$
Lattice Parameters	$a = 15.156(4)\text{\AA}$ $b = 6.388(3)\text{\AA}$ $c = 31.934(4)\text{\AA}$ $\beta = 90.39(2)^\circ$ $V = 3092(2)\text{\AA}^3$
Space Group	$P2_1/n$ (#14)
Z value	8
D _{calc}	1.222 g/cm ³
F ₀₀₀	1232.00
MU(MoK α)	0.77 cm ⁻¹

B. Intensity Measurements

Diffractometer	Rigaku AFC7S
Radiation	MoK α ($\lambda = 0.71069 \text{ \AA}$) graphite monochromated
Attenuator	Zr foil (factor = 8.56)
Take-off Angle	6.0 $^{\circ}$
Detector Aperture	9.0 mm horizontal 13.0 mm vertical
Crystal to Detector Distance	400 mm
Voltage, Current	0kV, 0mA
Temperature	-123.0 $^{\circ}$ C
Scan Type	ω -2 θ
Scan Rate	16.0 $^{\circ}$ /min (in ω) (up to 4 scans)
Scan Width	(0.94 + 0.35 tan θ) $^{\circ}$
2 θ_{max}	50.0 $^{\circ}$
No. of Reflections Measured ($R_{\text{int}} = 0.036$)	Total: 6227 Unique: 5989
Corrections	Lorentz-polarization Absorption (trans. factors: 0.9688 - 1.0000)

C. Structure Solution and Refinement

Structure Solution	Direct Methods (SIR88)
Refinement	Full-matrix least-squares
Function Minimized	$\Sigma w (F_o - F_c)^2$
Least Squares Weights	$1/\sigma^2(F_o) = 4F_o^2/\sigma^2(F_o^2)$
p-factor	0.0090
Anomalous Dispersion	All non-hydrogen atoms
No. Observations ($I > 2.00\sigma(I)$)	2160

No. Variables	189
Reflection/Parameter Ratio	11.43
Residuals: R; Rw	0.076 ; 0.071
Goodness of Fit Indicator	2.58
Max Shift/Error in Final Cycle	0.35
Maximum peak in Final Diff. Map	0.69 e ⁻ /Å ³
Minimum peak in Final Diff. Map	-0.33 e ⁻ /Å ³

Table 1. Atomic coordinates and B_{iso}/B_{eq}

atom	x	y	z	B_{eq}
O(1)	0.7390(3)	-0.2157(7)	0.1845(1)	3.4(1)
O(2)	0.2405(3)	0.3962(8)	0.0511(2)	4.9(1)
O(3)	0.3903(3)	0.2901(7)	0.0944(1)	3.9(1)
O(4)	-0.0900(3)	-0.1476(7)	0.1534(1)	3.3(1)
C(2)	0.3254(4)	0.014(1)	0.1367(2)	2.5(1)
C(3)	0.0224(4)	0.000(1)	0.0926(2)	2.7(1)
C(4)	0.6703(4)	-0.267(1)	0.1555(2)	3.4(2)
C(5)	0.2990(5)	0.164(1)	0.1656(2)	3.7(2)
C(6)	0.2899(4)	-0.185(1)	0.1398(2)	3.3(1)
C(7)	0.4885(4)	0.015(1)	0.1195(2)	2.6(1)
C(8)	0.0125(4)	0.134(1)	0.1321(2)	2.5(1)
C(9)	-0.0150(4)	0.361(1)	0.1180(2)	3.0(1)
C(10)	-0.0729(5)	0.240(1)	0.0486(2)	4.0(2)
C(12)	-0.1308(4)	0.220(1)	0.1589(2)	3.1(1)
C(13)	-0.0582(4)	0.013(1)	0.0637(2)	3.5(2)
C(14)	0.6444(4)	0.110(1)	0.1338(2)	3.6(2)
C(15)	-0.0237(4)	0.062(1)	0.2088(2)	2.5(1)
C(16)	0.6125(4)	-0.180(1)	0.0832(2)	3.3(1)
C(17)	0.1027(5)	0.084(1)	0.0685(2)	3.6(2)
C(18)	0.0129(4)	0.245(1)	0.2256(2)	3.4(2)
C(19)	0.3944(4)	0.071(1)	0.1035(2)	3.0(1)
C(20)	-0.0066(5)	0.381(1)	0.0699(2)	3.8(2)
C(21)	-0.0255(4)	-0.114(1)	0.2338(2)	3.6(2)
C(22)	-0.0592(4)	0.058(1)	0.1638(2)	2.9(1)

Table 1. Atomic coordinates and B_{iso}/B_{eq} (continued)

atom	x	y	z	B _{eq}
C(23)	0.0084(5)	-0.108(1)	0.2749(2)	3.8(2)
C(24)	0.5154(4)	-0.191(1)	0.0969(2)	3.0(1)
C(25)	0.0444(5)	0.072(1)	0.2902(2)	4.0(2)
C(26)	0.0852(5)	0.315(1)	0.0548(2)	4.9(2)
C(27)	0.0473(5)	0.248(1)	0.2663(2)	4.0(2)
C(28)	0.6721(4)	-0.111(1)	0.1197(2)	3.0(1)
C(29)	-0.1079(4)	0.378(1)	0.1345(2)	3.3(1)
C(30)	0.1543(6)	0.453(1)	0.0689(3)	6.0(2)
C(31)	0.4480(4)	-0.206(1)	0.0618(2)	3.5(2)
C(32)	0.3858(5)	-0.067(1)	0.0649(2)	3.4(2)
C(33)	0.2066(5)	-0.084(1)	0.2004(2)	4.0(2)
C(34)	0.2402(5)	0.114(1)	0.1970(2)	4.2(2)
C(35)	0.2301(5)	-0.234(1)	0.1716(2)	4.0(2)
C(36)	0.5599(4)	0.179(1)	0.1109(2)	3.2(1)
C(37)	0.5800(5)	0.198(1)	0.0638(2)	4.0(2)
C(38)	0.6204(5)	-0.012(1)	0.0488(2)	3.9(2)
C(39)	0.7344(5)	-0.347(1)	0.2205(2)	3.9(2)
C(40)	0.2602(5)	0.459(1)	0.0103(3)	5.3(2)
H(1)	0.3221	0.3010	0.1641	4.4628
H(2)	0.3065	-0.2906	0.1204	4.0146
H(3)	0.1667	-0.1159	0.2226	5.2415
H(4)	0.2245	0.2192	0.2169	5.3117
H(5)	0.2062	-0.3709	0.1733	4.7179
H(6)	0.0138	0.3692	0.2093	4.0891

Table 1. Atomic coordinates and B_{iso}/B_{eq} (continued)

atom	x	y	z	B_{eq}
H(7)	-0.0510	-0.2410	0.2232	4.3206
H(8)	0.0073	-0.2318	0.2914	4.7753
H(9)	0.0662	0.0754	0.3187	5.0964
H(10)	0.0742	0.3713	0.2766	4.9932
H(11)	0.6787	-0.3281	0.2340	4.6799
H(12)	0.7398	-0.4902	0.2126	4.6799
H(13)	0.7803	-0.3132	0.2399	4.6799
H(14)	0.3174	0.4084	0.0030	6.7202
H(15)	0.2179	0.4035	-0.0085	6.7202
H(16)	0.2601	0.6073	0.0088	6.7202
H(17)	0.0678	0.1405	0.1463	2.9923
H(18)	0.0220	0.4602	0.1317	3.6310
H(19)	-0.0650	0.2456	0.0189	5.0042
H(20)	-0.1312	0.2826	0.0550	5.0042
H(21)	-0.0495	-0.0759	0.0402	4.3800
H(22)	-0.1090	-0.0327	0.0785	4.3800
H(23)	0.1536	0.0758	0.0854	4.3146
H(24)	0.1106	0.0019	0.0437	4.3146
H(25)	-0.0170	0.5229	0.0622	4.7016
H(26)	0.0847	0.3179	0.0257	5.8051
H(27)	0.1585	0.4505	0.0978	7.7689
H(28)	0.1400	0.5897	0.0589	7.7689
H(29)	0.0326	-0.1421	0.1002	3.3859
H(30)	0.4869	-0.0106	0.1488	3.1241

Table 1. Atomic coordinates and B_{iso}/B_{eq} (continued)

atom	x	y	z	B_{eq}
H(31)	0.6310	-0.3108	0.0726	3.8834
H(32)	0.5080	-0.3063	0.1156	3.6262
H(33)	0.7312	-0.1025	0.1099	3.7806
H(34)	0.5414	0.3116	0.1209	3.9036
H(35)	0.6795	-0.4040	0.1451	4.0573
H(36)	0.6152	-0.2601	0.1693	4.0573
H(37)	0.6339	0.1118	0.1631	4.3610
H(38)	0.6904	0.2078	0.1276	4.3610
H(39)	0.5280	0.2253	0.0488	4.9651
H(40)	0.6220	0.3059	0.0595	4.9651
H(41)	0.6805	0.0080	0.0421	5.2238
H(42)	0.5889	-0.0573	0.0244	5.2238
H(43)	0.3272	0.3384	0.0739	5.7212
H(44)	0.4537	-0.3148	0.0338	5.7212
H(45)	0.3265	-0.0121	0.0466	5.7212
H(46)	-0.1885	0.2094	0.1725	3.7782
H(47)	-0.1471	0.4965	0.1278	4.1147

$$B_{eq} = 8/3 \text{PI}^2(U_{11}(aa^*)^2 + U_{22}(bb^*)^2 + U_{33}(cc^*)^2 + 2U_{12}(aa^*bb^*)\cos \gamma + 2U_{13}(aa^*cc^*)\cos \beta + 2U_{23}(bb^*cc^*)\cos \alpha)$$

Table 2. Anisotropic Displacement Parameters

atom	U ₁₁	U ₂₂	U ₃₃	U ₁₂	U ₁₃	U ₂₃
O(1)	0.050(3)	0.039(3)	0.039(3)	-0.004(3)	-0.001(2)	0.011(2)
O(2)	0.041(3)	0.060(4)	0.084(4)	0.010(3)	0.012(3)	0.033(3)
O(3)	0.057(3)	0.030(3)	0.062(3)	-0.001(3)	-0.009(3)	0.017(3)
O(4)	0.059(3)	0.025(3)	0.041(3)	-0.012(3)	0.002(2)	-
	0.010(2)					

The general temperature factor expression:

$$\exp(-2\pi^2(a^2U_{11}h^2 + b^2U_{22}k^2 + c^2U_{33}l^2 + 2a*b*U_{12}hk + 2a*c*U_{13}hl + 2b*c*U_{23}kl))$$